Investigation of Performance Characteristics for the Powder Mixed Electric Discharge Machining of Tungsten Carbide

A Thesis report

SUBMITTED IN PARTIAL FULLFILMENT OF THE REQUIREMENT FOR THE AWARD OF THE DEGREE OF

MASTER OF ENGINEERING

(PRODUCTION AND INDUSTRIAL ENGINEERING)

UNDER THE GUIDANCE OF

Dr.V.K.SINGLA

Associate Professor

Mechanical Engineering Department, Thapar University Patiala

SUBMITTED BY

JAGDEEP SINGH

(801082012)

DEPARTMENT OF MECHANICAL ENGINEERING

THAPAR UNIVERSITY

PATIALA – 147004

July-2012

CERTIFICATE

This is to certify that the thesis report entitled **"Investigation of Performance characteristics for the Powder Mixed Electric Discharge Machining of Tungsten-Carbide"** is an authentic record of my study carried out as requirements for the award of **MASTER OF ENGINEERING (PRODUCTION AND INDUSTRIAL ENGINEERING)** Degree to Thapar University, Patiala, under the guidance of Dr. VINOD KUMAR SINGLA, Associate Professor, Department of Mechanical Engineering, Thapar University Patiala.

This report or the matter involved in this thesis is of desired standard and has not been submitted in any other University or Institute for the award of any degree.

11/07/2011

Dr.V.K.SINGLA
Associate Professor
Mechanical Engineering Department
Thapar University, Patiala
Punjab-147004

Countersigned by

Dr. AJAY BATISH
Professor and Head,
Department of Mechanical Engineering,
Thapar University, Patiala-147004

Dr. S.K.MOHAPATRA
Dean of Academic Affairs,
Thapar University, Patiala- 147004

ACKNOWLEDGEMENT

I am highly grateful to the authorities of Thapar University, Patiala for providing this opportunity to carry out the Thesis work.

I would like to express a deep sense of gratitude and thanks profusely to my thesis guide **Dr.V.K.Singla,** Associate Professor, Department of Mechanical Engineering, Thapar University, Patiala and for his sincere and invaluable guidance, suggestion and sympathetic attitude which inspired me to submit this Thesis report in the present form. I am highly thankful to the **Dr. Ajay Batish,** Professor and Head of Mechanical Engineering Department and **Dr. S.K.Mohapatra,** Dean of Academic Affairs Thapar University, Patiala for his great support and encouragement for my thesis work. I am also thankful to other faculty members of Mechanical Engineering Department, Thapar University, Patiala for their intellectual support.

I would like also thanks to Department of Material Science for providing the equipment and other sources for my thesis work.

My special thanks to my all family members specially my parents who loved me a lot and friends who constantly encouraged me to complete this study.

JAGDEEP SINGH

ROLL NO: 801082012

Abstract

Now a days we know that product and process technology is a very advance, many types of new materials are being developed which have very high strength, high thermal and electrical conductivity which are very difficult to machine by traditional machining methods. So Non conventional machining methods are used to machine such type of materials, EDM is also one of the Non conventional machining method which is used to machine such advance hard and brittle materials to satisfy the present day product needs like aerospace, mould, dies and other applications.EDM has recently employed to alter the properties or raw materials by using appropriate electrodes and various types of powders and additives in the effects of various input parameters. The Objective of this work is mainly to study the effect of various input parameters like Pulse-On, Pulse-Off, Current, Powder and Tool on the various output parameters like MRR, TWR, Micro hardness and Surface roughness. In this study, these output parameters are studied by using the ANOVAs through Minitab software. By using this software, study the Means and S/N ratios for all these output parameters. Micro structure was also observed by using SEM machine and composition of the workpiece is also investigated that what are the effects before and after machining by different machining conditions by using EDS machine.

ABBREVATIONS

ANOVA	Analysis of Variance
DC	Direct Current
DOF	Degree of Freedom
EDM	Electric Discharge Machining
RC	Relaxation Circuit
MRR	Material Removal Rate
TWR	Tool Wear Rate
SR	Surface Roughness
SEM	Scanning Electron Microscope
XRD	X-Ray diffraction
S/N Ratio	Signal to Noise Ratio
EDS	Energy Dispersion Spectroscopy

NOTATIONS

OA	Orthogonal Array
A	Pulse-On
B	Pulse-Off
C	Current
D	Powder
E	Tool
Gr	Graphite Powder
Al_2O_3	Aluminium Oxide
Mix	Graphite Powder + Aluminium Oxide
CI	Confidence Interval
SS	Sum of Squares
v	Variance
V	Degree of freedom
Cu	Copper Tool
Al	Aluminium Tool
Br	Brass Tool
WC	Tungsten Carbide

CONTENTS

TITLE **PAGE NO.**

LIST OF FIGURES

LIST OF TABLES

Chapter 1

Introduction

1.1 Introduction to Non-Traditional Machining Process

Non Traditional Machining Processes (NTM), one needs to understand and analyse the differences and similar characteristics between conventional machining processes and NTM processes.

Conventional Machining Processes mostly remove material in the form of chips by applying forces on the work material with a wedge shaped cutting tool that is harder than the work material under machining condition. Such forces induce plastic deformation within the work piece leading to shear deformation along the shear plane and chip formation. Fig [1.1] below depicts such chip formation by shear deformation in conventional machining.

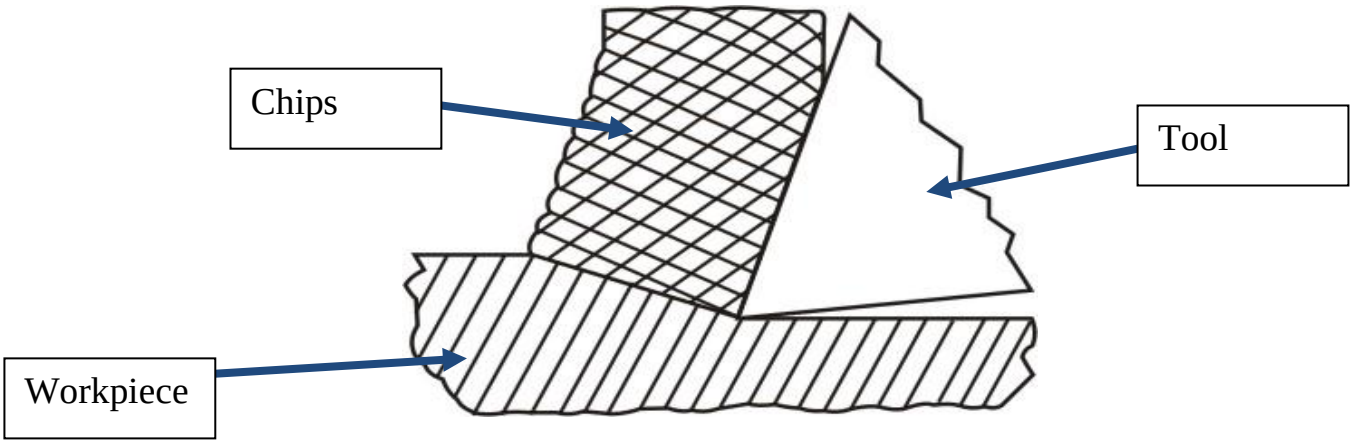

Fig.1.1 Shear deformation in conventional machining leading to chip formation [37]

Thus the major characteristics of conventional machining are:

• Generally macroscopic chip formation by shear deformation

• Material removal takes place due to application of cutting forces – energy domain can be classified as mechanical

• Cutting tool is harder than work piece at room temperature as well as under machining conditions.

Non Traditional Machining (NTM) Processes on the other hand are characterised as follows:

• Material removal may occur with chip formation or even no chip formation may take place. For example in AJM, chips are of microscopic size and in case of Electrochemical machining material removal occurs due to electrochemical dissolution at atomic level

- In NTM, there may not be a physical tool present. For example in laser jet machining, machining is carried out by laser beam. However in Electrochemical Machining there is a physical tool that is very much required for machining
- In NTM, the tool need not be harder than the work piece material. For example, in EDM, copper is used as the tool material to machine hardened steels.
- Mostly NTM processes do not necessarily use mechanical energy to provide material removal. They use different energy domains to provide machining. For example, in USM, AJM, WJM mechanical energy is used to machine material, whereas in ECM electrochemical dissolution constitutes material removal.

In unconventional machining methods, there is no direct contact between the too, and work piece; hence the tool need not to be harder than work piece. Further, in spite of the recent technical advancement, the conventional machining processes are inadequate to produce complex geometries shapes in hard and temperature resistant alloy and die steels. Keeping these requirements in mind, a number of non conventional methods have been developed. Below give classification of machining process based on type of energy used, the mechanism of metal removal, the source of energy requirement.

- **Mechanical Energy (Mechanical Processes) :** in mechanical processes metal removal takes place either by a mechanism of simple shear or by erosion mechanism where high velocity particles are used as a transfer media and pneumatic/hydraulic pressure acts as source of energy. It includes ultrasonic machining, water jet machining and abrasive jet machining etc.
- **Thermal Energy (Thermal process):** Thermal processes involve the application of the application of very thin intense local heat. Here melting and vaporization from the small areas at the surface of the work piece removes material. The source of energy used is amplified light, ionized material and high voltage. Examples are laser beam machining, ion beam machining, plasma arc machining and electrical discharge machining.
- **Electrical Energy (Electro chemical Processes):** Electrochemical processes involve removal of metal by mechanism of ion displacement. High current is required as the source of energy, and electrolyte acts as transfer media. It includes electro-chemical machining, electro chemical grinding etc.

- **Chemical Energy (chemical processes):** Chemical processes involve the application of resistant material (acidic or alkaline in nature) to certain portion of the work piece. The desired amount of material is removed from the remaining area of the work piece by subsequent application of an etching that converts the work piece material into a dissolve metallic salt. it includes chemical machining and photochemical machining.

1.2 History of EDM

In 1770, English physicist Joseph Priestley studied the erosive effect of electrical discharges. Furthering Priestley's research, the EDM process was invented by two Russian scientists, Dr. B. R. Lazarenko and Dr. N. I. Lazarenko, in 1943. In their efforts to exploit the destructive effects of an electrical discharge, they developed a controlled process for machining of metals. Their initial process used a spark machining process, named after the succession of sparks (electrical discharges) that took place between two electrical conductors immersed in a dielectric fluid. The discharge generator effect used by this machine, known as the Lazarenko circuit, was used for many years in the construction of generators for electrical discharge. Additional researchers entered the field and contributed many fundamental characteristics of the machining method we know today. In 1952, the manufacturer Charmilles created the first machine using the spark machining process and was presented for the first time at the European Machine Tool Exhibition in 1955.

1.3 Working Principle and Mechanism of material removal in EDM

In EDM, the removal of material is based upon the electro discharge erosion (EDE) effect of electric sparks occurring between two electrodes that are separated by a dielectric liquid. Metal removal takes place as a result of the generation of extremely high temperatures generated by the high-intensity discharges that melt and evaporate the two electrodes. A series of voltage pulses of magnitude about 20 to 120 V and frequency on the order of 5 kHz is applied between the two electrodes, which are separated by a small gap, typically 0.01 to 0.5 mm. When using RC generators, the voltage pulses are responsible for material removal. Schematic diagram of EDM is shown in fig.1.2

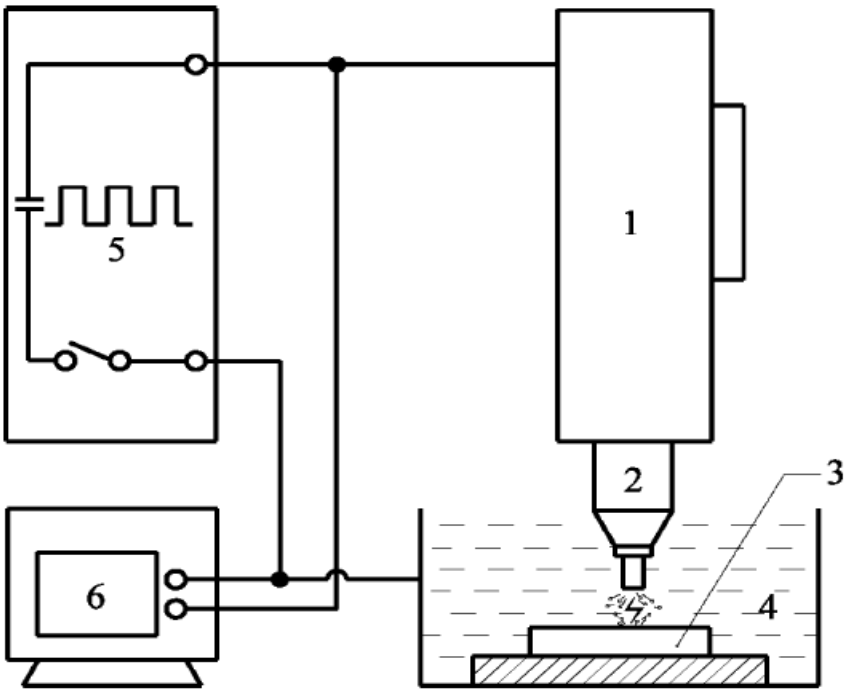

Figure 1.2 Schematic diagram of the EDM process: 1) servo-control, 2) electrode, 3) workpiece, 4) dielectric fluid, 5) pulse generator, 6) oscilloscope [22]

According to McGeough (1988), the application of voltage pulses, as shown in Fig. 1.3, causes electrical breakdown to the dielectric in a channel of radius 10 μm. The breakdown arises from the acceleration toward the anode of both electrons emitted from the cathode by the applied field and the stray electrons present in the gap. These electrons collide with neutral atoms of the dielectric, thereby creating positive ions and further electrons, which in turn are accelerated respectively toward the cathode and anode.

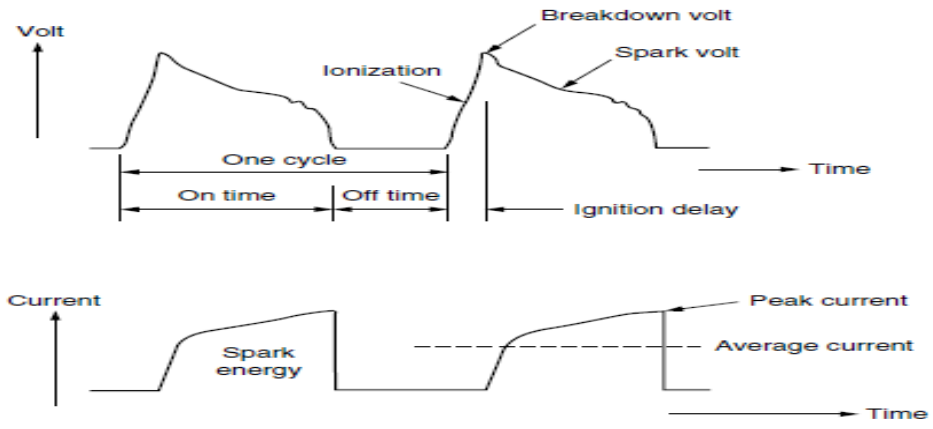

Figure-1.3 Voltage and Current Waveforms during EDM [36]

When the electrons and the positive ions reach the anode and cathode, they give up their kinetic energy in the form of heat. Temperatures of about 8000 to 12,000°C and heat fluxes up to 1017 W/m2 are attained. With a very short duration spark of typically between 0.1 to 2000μs the temperature of the electrodes can be raised locally to more than their normal boiling points. Owing to the evaporation of the dielectric, the pressure on the plasma channel rises rapidly to values as high as 200 atmospheres. Such great pressures prevent the evaporation of the superheated metal.

At the end of the pulse, the pressure drops suddenly and the superheated metal evaporates explosively. Metal is thus removed from the electrodes as shown in Fig. 1.4

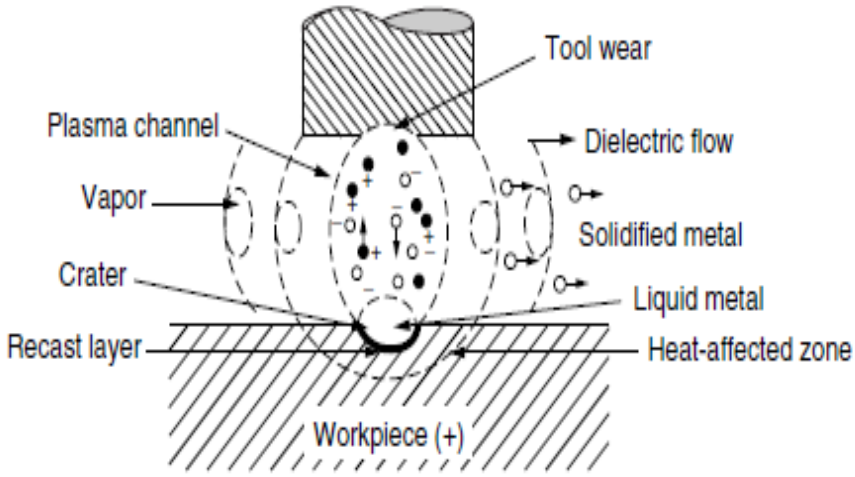

Figure-1.4 EDM Spark description [36]

Fresh dielectric fluid rushes in, flushing the debris away and quenching the surface of the work piece. Unexpelled molten metal solidifies to form what is known as the recast layer. The expelled metal solidifies into tiny spheres dispersed in the dielectric liquid along with bits from the electrode. The remaining vapour rises to the surface. Without a sufficient off time, debris would collect making the spark unstable. This situation creates an arc, which damages the electrode and the work piece. The relation between the amount of material removed from the anode and cathode depends on the respective contribution of the electrons and positive ions to the total current flow. The electron current predominates in the early stages of the discharge. Since the positive ions are roughly 104 times more massive than electrons, they are less easily mobilized than the electrons. Consequently the erosion of the anode work piece should be greater than that of the cathode. At the end of the EDM action,

the plasma channel increases in width, and the current density across the inter electrode gap decreases. With the fraction of the current due to the electrons diminishing, the contributions from the positive ions rise, and proportionally more metal is then eroded from the cathode. The high frequency of voltage pulses supplied, together with the forward servo-controlled tool motion, toward the work piece, enables sparking to be achieved along the entire length of the electrodes.

The frequency of discharges or sparks usually varies between 500 and 500,000 sparks per second. With such high sparking frequencies, the combined effects of individual sparks provide a substantial material removal rate. The position of the tool electrode is controlled by the servomechanism, which maintains a constant gap width (200–500 μm) between the electrodes in order to increase the machining efficiency through active discharges. EDM performance measures such as material removal rate, electrode tool wear, and surface finish, for the same energy, depends on the shape of the current pulses. Based upon the situation in the inter electrode gap, four different electrical pulses are distinguished, namely, open circuit pulses, sparks, arcs, and short circuits. They are usually defined on the basis of time evolution of discharge voltage and/or discharge current. Their effect upon material removal and tool wear differs quite significantly.

1.4 EDM Process parameters

1.4.1 Discharge Voltage

Discharge voltage in EDM is related to the spark gap and breakdown strength of the dielectric. Before current can flow, the open gap voltage increases until it creates an ionization path through the dielectric. Once the current starts to flow, voltage drops and stabilizes at the working gap level. The present voltage determines the width of the spark gap between the leading edge of the electrode and work piece. Higher voltage settings increase the gap, which improves the flushing conditions and helps to stabilize the cut. MRR < TWR and surface roughness increases with increasing open circuit voltage because electric field strength increases.

1.4.2 Peak Current

This is the amount of power used in discharge machining, measured in units of amperage and is the most important machining parameter in EDM. During each on-time pulse, the current increases until it reaches a preset level, which is expressed as the peak current. Higher currents will improve MRR but at the cost of TWR and surface finish, fig.1.5 shows the effect of current on surface

Figure-1.5 Effect of pulse current on removal rate and surface roughness [36]

1.4.3 Pulse On-time and Off-time

Each cycle has an on-time and off-time that is expressed in units of microseconds. Since all the work is done during on-time, the duration of these pulses and the number of cycles per second are important. Metal removal is directly proportional to the amount of energy applied during the on-time. The resulting crater will be deep and broader than a crater produced by a shorter on-time. Excessive on-times can be counter productive when the optimum on-time for each electrode-work material combination is exceeded, material rate starts to decreases.

The cycle is completed when sufficient when sufficient off-time is allowed before the start of the next cycle. Off-time will affect the speed and stability of the cut. Shorter the off-time, the faster will be the machining operation. However, if the off-time is too short, the ejected work piece material will not be swept away by the flow of the dielectric and the fluid will not be de-ionized. This will cause the next spark to be unstable. Unstable conditions cause erratic cycling and retraction of the advancing servo. This slows down cutting more than long, stable off-times. Off-time must be greater than the de-ionized time to prevent continued sparking at one point.

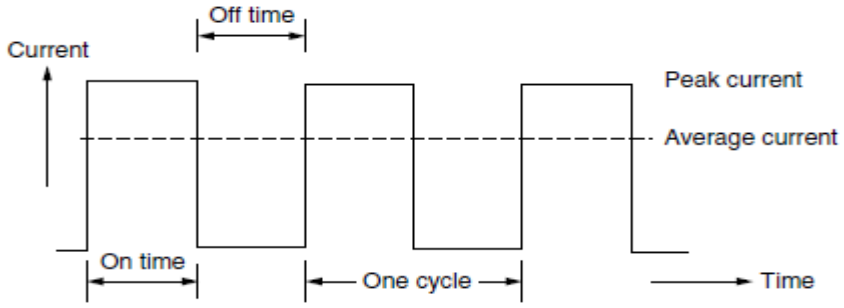

Figure-1.6 shows the pulse duration in EDM [19]

1.4.4 Polarity

The polarity of the electrode can be either positive or negative. The current passing the gap creates high temperatures causing material evaporation at both electrode spots. As the electron processes show quicker reaction, the anode material is worn out predominantly. This causes minimum wear to the tool electrodes and becomes of importance under finishing operations with shorter on-times. However while longer discharges, the early electron process predominance changes to positron process, resulting in high tool wear.

1.4.5 Frequency

This is a measure of the number of times the current is turned on and off. During roughing, the 'on time' is increased significantly for high removal rates and fewer cycles per second. Frequency is distinct from the duty cycle, as this is a measure of efficiency.

1.4.6 Type of flushing

It is basic requirement of dielectric that it should maintain its dielectric strength (insulating properties) during its whole operation. There is no problem at the start of EDM, but after discharge the debris are produced in the gap reduce the dielectric strength, which cause unwanted discharges which can damage to both tool and workpiece. Hence effective flushing is required to remove unwanted debris from the gap [3]. TWR and MRR are affected by the type of dielectric and the method of its flushing. In EDM, flushing can be achieved by following methods:

1.4.6.1 Suction flushing

In this, dielectric may be sucked through either the workpiece or the electrode. This technique is employed to avoid any tapering effect due to sparking between machining debris and the side walls of the electrodes. Suction flushing through the tool rather than through the workpiece is more effective.

1.4.6.2 Injection flushing

In this technique, dielectric is fed through either the workpiece or the tool which are predrilled to accommodate the flow. With the injection method, tapering of components arises due to the lateral discharge action occurring as a result of particles being flushed up the sides of electrodes.

1.4.6.3 Side flushing

When the flushing holes cannot be drilled either in the workpiece or the tool, side flushing is employed. If there is need of flushing of entire working area, special precautions have to taken for the pumping of dielectric.

1.4.6.4 Flushing by dielectric pumping

This method has been found particularly suitable in deep hole drilling. Flushing is obtained by using the electrode pulsation movement. When the electrode is raised, clean dielectric is sucked into mix with contaminated fluid, and as the electrode is lowered the particles are flushed out. [1].

1.4.7 **Dielectric fluids.**

The main functions of the dielectric fluid are to

1. Flush the eroded particles from the machining gap
2. Provide insulation between the electrode and the workpiece
3. Cool the section that was heated by the discharging effect

The main requirements of the EDM dielectric fluids are adequate viscosity, high flash point, good oxidation stability, minimum odor, low cost, and good electrical discharge efficiency. For most EDM operations kerosene is used with certain additives that prevent gas bubbles and de-odoring. Silicon fluids and a mixture of these fluids with petroleum oils have given excellent results. Other dielectric fluids with a varying degree of success include aqueous solutions of ethylene glycol, water in emulsions, and distilled water. Flushing of the dielectric plays a major role in the maintenance of stable machining and the achievement of close tolerance and high surface quality. Inadequate flushing can result in arcing, decreased electrode life, and increased production time.

1.4.8 **Material used for EDM electrodes**

Metals with a high melting point and good electrical conductivity are usually chosen as tool materials for EDM. Graphite is the most common electrode material since it has fair wear characteristics and is easily machinable and small flush holes can be drilled into graphite

electrodes. Copper has good EDM wear and better conductivity. It is generally used for better finishes in the range of 0.5μm *Ra*. Copper tungsten and silver tungsten are used for making deep slots under poor flushing conditions especially in tungsten carbides. It offers high machining rates as well as low electrode wear. Copper graphite is good for cross-sectional electrodes. It has better electrical conductivity than graphite while the corner wear is higher. Brass ensures stable sparking conditions and is normally used for specialized applications such as drilling of small holes where the high electrode wear is acceptable.

1.5 **ORGANIZATION OF THESIS**

Chapter 1 covers brief introduction to non-conventional machining, principle of electric discharge machining, mechanism of material removal and process parameters of EDM.

Chapter 2 presents an available literature of EDM process on EDM and for surface modification.

Chapter 3 presents the aim of this work and show what is the objective of this study and to design the experiments and pattern on which this work has been done.

Chapter 4 presents the analysis and results of the MRR. Results after the Analysis of Variance (ANOVA) and Taguchi Signal-to-Noise ratio are shown in this chapter. Effect of various factors and effect of interactions shown in this chapter, optimal design for MRR has been discussed in this chapter.

Chapter 5 presents the analysis and results of the TWR. Results after the Analysis of Variance (ANOVA) and Taguchi Signal-to-Noise ratio are shown in this chapter. Effect of various factors and effect of interactions, optimal design for TWR is also discussed in this chapter.

Chapter 6 presents the analysis and results of the Micro hardness. Results after the Analysis of Variance (ANOVA) and Taguchi Signal-to-Noise ratio are shown in this chapter. Effect of various factors and effect of interactions shown in this chapter. Optimal design conditions have also been discussed.

Chapter 7 presents the analysis and results of the Surface roughness. Results after the Analysis of Variance (ANOVA) and Taguchi Signal-to-Noise ratio are shown in this chapter. Effect of various factors and effect of interactions shown in this chapter, optimal design for Surface roughness is also obtained in this chapter.

Chapter 8 presents the regression of analysis for MRR, TWR, Micro hardness and surface roughness.

Chapter 9 presents the analysis of microstructure by SEM and analysis of composition by EDS.

Chapter 10 presents the results and conclusions from the experimental work.

Chapter 2

Literature Review

2.1 Introduction

Large amount of work has been done on the EDM so the effects have been made cover the maximum literature on the EDM process parameters and on the surface improvement of

various materials through EDM and Powder EDM. Literature is divided into main two portions:

1. Effect of various machine parameters of EDM on different materials.
2. Effect of various powders on the EDM for the surface modification.

2.1.1 Effect of various machine parameters of EDM on different materials.

H. Hocheng et al. [**3**] studied Metal matrix composite (MMC) materials have increasingly widened their use due to the merits of possessing high specific strength and modulus of elasticity while carrying good deformability and conductivity comparable to metals in addition to its use structural and functional components for high-performance applications, such as aerospace vehicles and racing automobiles, MMC also has potential for molds. Especially for the large and mid-size molds in precision manufacturing, where handling is difficult due to the heavy weight, MMC can improve the productivity by saving the cost of loading, positioning and stocking. MMC is difficult to machine due to serious tool wear caused by the hard reinforcement. To exploit the potential industrial applications and investigate proper manufacturing processes, the machinability of electrical discharge machining (EDM) of MMC needs to be studied for reliable and economical production. The fundamental analysis starts from the material removal of MMC by a single spark. This paper presents the correlation between the major machining parameters, electrical current and on-time, and the crater size produced by a single spark for the representative material SiC/Al. The experimental results not only show the predicted proportionality based on heat conduction model, but are also compared with common steels regarding the material removal rate. Though the crater size of SiC/Al is larger than steel, the SiC particles can interfere the discharges. For effective EDM, large electrical current and short on-time is recommended. Based on the obtained knowledge, one can proceed to the study of machinability of MMC by EDM for optimal production cycle

H. T. Lee, T. Y. Tai [4] presented a study of the relationship between EDM parameters and surface cracks by using a full factorial design, based upon discharge current and pulse-on time parameters. The study analyzes the EDM machining of D2 and H13 tool steels as materials. The formation of surface cracks is explored by considering surface roughness, white layer thickness, and the stress induced by the EDM process. When the pulse voltage is

maintained at a constant value of 120 V, it is possible to avoid the formation of cracks if machining is carried out with a pulse current in the range of 12–16 A together with a pulse-on duration of 6–9 μs. Based upon the experimental results, this study establishes a crack prediction map, and indicates whether or not cracks are likely to form for a given pulse-on and pulse current combination. Its use will provide a valuable aid in improving the quality of the EDM process.

Kanagarajan et al. [5] studied that Tungsten carbide/cobalt (WC/Co) cemented carbide is one of the important composite materials that are used in the manufacture of cutting tools, dies, and other special tools. It has high hardness and excellent resistance to shock and wear, and is not possible to machine easily using conventional techniques. WC/Co cemented carbide produced through powder metallurgy is subjected to electro discharge machining (EDM). In this study four design factors: electrode rotation (S), pulse on time (T), current (A), and flushing pressure (P) of EDM, were chosen as variables in order to study the process performance in terms of material removal rate (MRR) and surface roughness (Ra). The experiments were performed on a newly designed experimental set-up developed in the laboratory. The response surface methodology is used to identify the most influential parameters for maximizing metal removal rate and for minimizing the surface roughness. The recommended optimal process conditions have been verified by conducting confirmation experiments. The experimental results are used to develop the statistical models based on the second-order polynomial equations for the different process characteristics.

D. Bhaduri et al. [6] showed that Titanium nitride-aluminium oxide (TiN–Al_2O_3) is a new generation ceramic composite material having potential for many industrial applications as it possesses high resistance to thermal degradation, anti-wear and anti-abrasion properties. But conventional machining of such ceramic composite is difficult to perform for some of its peculiar properties like anisotropy, low thermal conductivity, and abrasive nature of the reinforcing phases. In the present investigation, non-conventional machining like electro discharge machining (EDM) has been carried out to machine the material. Energy dispersive X-ray spectroscopy and X-ray diffraction analysis have also been carried out on the composite matrix to verify the presence of two distinguishable phases of TiN and Al_2O_3. The present article reports the effects of EDM process parameters on material removal rate,

electrode wear rate, radial overcut, and taper angle while machining TiN–Al_2O_3 composite. The characteristic features of the EDM process are explored through Taguchi L_9 orthogonal array design–based experimental studies with various process parametric combinations. Finally, optimum parameter settings for each response factor are obtained and tested through verification experiments. The whole experimental study indicates that EDM has a very good potential in machining of TiN–Al_2O_3 ceramic composite in some particular ranges of process parameters.

Abdulkareem et al. [7] investigated that in electrical discharge machining (EDM), material is removed by a series of electrical sparks that develops a temperature in the range 8, 000°C-12, 000°C between the electrode and the work piece. Due to the high temperature of the sparks, the work piece is melted and vaporized. At the same time, the electrode material is also eroded by melting and vaporization. This erosion of the electrode is termed as electrode wear (EW). The EW process is similar to the material removal mechanism as the electrode and the work piece are considered as a set of electrodes in EDM. Due to EW, electrodes lose their dimensions resulting in inaccuracy of the cavity formed by EDM. This paper reports on the study of the effect of electrode cooling during the EDM of titanium alloy (Ti-6Al-4 V). Investigation on the effect of electrode cooling on electrode wear was carried out. Current, pulse on-time, pause off-time, and gap voltage were considered as the machining parameters while EW is the response. Analysis of the influence of electrode cooling on the response has been carried out, and it was possible to reduce EW by 27% using this method.

Yan-Cherng Linycline et al. [8] investigated cemented tungsten carbides graded K10 and P10 were machined by electrical discharge machining (EDM) using an electrolytic copper electrode. The machining parameters of EDM were varied to explore the effects of electrical discharge energy on the machining characteristics, such as material removal rate (MRR), electrode wear rate (EWR), and surface roughness. Moreover, the effects of the electrical discharge energy on heat-affected layers, surface cracks and machining debris were also determined. The experimental results show that the MRR increased with the density of the electrical discharge energy; the EWR and diameter of the machining debris were also related to the density of the electrical discharge energy. When the amount of electrical discharge energy was set to a high level, serious surface cracks on the machined surface of the cemented tungsten carbides caused by EDM were evident.

Bhattacharyya et al. [9] studied that to determine possible correlations between the EDM machining parameters (pulse on, current) and the machine ability components (stock removal, electrode wear, overcut, surface finish and surface integrity). The surface finish and the metallurgical sub surface characteristics. The present work indicates a correlation between the overcut (gap B) and the total thickness of the damaged surface layer (white layer and heat, affected zone).

Puertas et al. [10] studied the correct selection of manufacturing conditions is one of the most important aspects to take into consideration in the majority of manufacturing processes and, particularly, in processes related to electrical discharge machining (EDM) of conductive ceramic materials. It is these conditions that determine such important characteristics as surface roughness, electrode wear, and material removal rate. In this article, a review of the state of art of the die-sinking EDM processes for conductive ceramic materials, as well as a description of the equipment used for carrying out the experiments, are presented. Also, a series of mathematical models will be devised using design of experiments techniques combined with multiple linear regression, which will allow us, while only performing a small number of experiments, to select the optimal machining conditions for the finishing stage of the EDM process. To that end, in this piece of work, a study will be made of the influence of the most important factors in the process of die-sinking EDM of a boron carbide conductive ceramic, namely the intensity supplied by the generator (I), the pulse time (ti), and the duty cycle (η) over some of the most important technological characteristics, such as surface roughness (Ra and Rt), the volumetric electrode wear, and the material removal rate.

Lin, Yan-Cherngycline [11] showed the effects of the machining parameters in electrical-discharge machining (EDM) on the machining characteristics of SKH 57 high-speed steel were investigated. A well-designed experimental scheme was used to reduce the total number of experiments. Parts of the experiment were conducted with the L18 orthogonal array based on the Taguchi method. Moreover, the signal-to-noise ratios associated with the observed values in the experiments were determined by ANOVA and F-test. The significant parameters that critically influenced the machining characteristics were examined, and the optimal combination levels of machining parameters for material removal rate, electrode wear rate, and surface roughness were determined.

Gokhan Kucukturk & Can Cogun [12] studied a new method for machining of nonconductive ceramic work pieces in electric discharge machining (EDM) was developed. Machining surfaces of nonconductive work pieces were coated with a conductive layer (CL) and graphite powder was added to dielectric fluid for machining. Al_2O_3, ZrO_2, SiC, B_4C and glass work piece samples were machined by using the method. Different machining conditions were tested for each sample and optimum machining parameters were determined. Effect of electrical conductivity, thermal conductivity and melting point of work pieces on material removal rate (MRR) was investigated. Optical microscope and SEM (Scanning Electron Microscope) surface photographs of work pieces taken after machining are presented and discussed.

P. Narender Singh et al. [13] studied that Optimization of process parameters is the key step in the Taguchi methods to achieve high quality without cost inflation. Optimization of multiple response characteristics is more complex compared to optimization of single performance characteristics. The multi-response optimization of the process parameters viz., metal removal rate (MRR), tool wear rate (TWR), taper (T), radial overcut (ROC), and surface roughness (SR) on electric discharge machining (EDM) of Al–10%SiCP as cast metal matrix composites using orthogonal array (OA) with Grey relational analysis is reported. The optimization of the process was performed in the following steps:

(a) Normalizing the experimental results of MRR, TWR, T, ROC, and SR for all the trials.

(b) Performing the Grey relational generating and to calculate the Grey relational coefficient.

(c) Calculating the Grey relational grade by averaging the Grey relational coefficient.

(d) Performing statistical analysis of variance (ANOVA) for the input parameters with the Grey relational grade and to find which parameter significantly affects the process.

(e) Selecting the optimal levels of process parameters.

(e) Conduct confirmation experiment and verify the optimal process parameters setting.

P.M. George et al. [14] studied to determine the optimal setting of the process parameters on the electro-discharge machining (EDM) machine while machining carbon–carbon composites. The parameters considered are pulse current, gap voltage and pulse-on-time; whereas the responses are electrode wear rate (EWR) and material removal rate (MRR). The optimal setting of the parameters are determined through experiments planned, conducted and

analysed using the Taguchi method. It is found that the electrode wear rate reduces substantially, within the region of experimentation, if the parameters are set at their lowest values, while the parameters set at their highest values increase the MRR drastically

Yan-Cherng Lin et al. [15] was investigated machining performance of conductive ceramics (Al2O3 + 30vol% TiC) using electrical discharge machining (EDM) is the aim of this work. The EDM machining parameters such as machining polarity, peak current, auxiliary current with high voltage, pulse duration, no load voltage, and servo reference voltage were chosen to explore the effects on material removal rate (MRR), electrode wear rate (EWR), and surface roughness (SR). The L18 orthogonal array based on the Taguchi experimental method was adopted to determine EDM machining characteristics systemically, and the experimental data were statistically analyzed by analysis of variance (ANOVA). Experimental results showed EDM is a feasible process to shape conductive ceramics, and relationships between machining characteristics and parameters were examined. Moreover, machining parameter optimal combination levels in machining conductive ceramics via EDM were also determined.

Harminder Singh, D.K. Shukla [16] studied the energy distribution in the Electrical Discharge Machining (EDM) process influences the material removal rate, and other machining characteristics like crater geometry, relative wear ratio and surface roughness. During this process the electrical energy is converted into heat energy and this energy is distributed among the electrode, workpiece and the dielectric fluid. The fraction of the energy which is transferred to the workpiece is the useful energy and this energy should be maximum, for optimum utilization of energy. This fraction of energy is one of the important parameters used in the existing thermo-physical models of EDM process. Due to apparent incongruities and conflicting data early researchers conjectured the same value of fraction of energy transferred to electrodes for all machining parameters in their models for numerically calculating the volume and geometry of the crater formed. This assumption is one of the reasons of error in the models from the experimental data. So this study is planned to experimentally study the variation of this fraction of input discharge energy with the help of thermo-mathematical models during EDM of Tungsten-Carbide by varying the machining parameters current and pulse duration. The data calculated in this study can be further used in

the existing thermo physical models, expecting to bring the models preciously more close to the real conditions. This data will also be helpful for numerically calculating the optimum parameters using optimum value of the fraction of energy transferred to the electrodes especially workpiece. The results obtained showed that the energy effectively transferred to the workpiece varies with the discharge current and pulse duration from 6.5% to 17.7%, which proves that the fixed value assumed in the models is not in line with real EDM process.

Shankar Singh et al. [17] studied that EDM, a 'non-traditional machining processes has been replacing drilling, milling, grinding and other traditional machining operations and is now a well-established machining option in many manufacturing industries throughout the world. Modern machinery is capable of machining geometrically complex or hard material components, that are precise and difficult-to-machine such as heat treated tool steels, composites, super alloys, ceramics, etc. This paper reports the results of an experimental investigation carried out to study the effects of machining parameters such as pulsed current on material removal rate, diameteral overcut, electrode wear, and surface roughness in electric discharge machining of En-31 tool steel (IS designation: T105 Cr 1 Mn 60) hardened and tempered to 55 HRc. The work material was ED machined with copper, copper tungsten, brass and aluminium electrodes by varying the pulsed current at reverse polarity. Investigations indicate that the output parameters of EDM increase with the increase in pulsed current and the best machining rates are achieved with copper and aluminium electrodes.

M.P. Jahan et al. [18] studied that the capability of machining intricate features with high dimensional accuracy in hard and difficult-to- cut material has made electro discharge machining (EDM) process as an inevitable and one of the most popular non-conventional machining processes. In recent years, both EDM and micro-EDM processes are being used extensively in the field of mould making, production of dies, cavities and complex 3D structures using difficult-to-cut tungsten carbide and its composites. The objective of this paper is to provide a state of the art in the field of EDM and micro-EDM of tungsten carbide and its composites. The review begins with a brief introduction on the EDM and micro-EDM processes. The research and developments in electro discharge machining of tungsten carbide are grouped broadly into conventional EDM of tungsten carbide, micro-EDM of tungsten

carbide and current research trends in EDM and micro-EDM of tungsten carbide. The problems and challenges in the area of conventional and micro- EDM of tungsten carbide and the importance of compound and hybrid machining processes are discussed. A summary of the future research directions based on the review is presented at the final section.

C.J. Luis et al. [19] studied the die-sinking electrical discharge machining (EDM) of siliconised or reaction-bonded silicon carbide (SiSiC) has been carried out. The selection of the above-mentioned conductive ceramic was made taking into account its wide range of applications in the industrial field: high-temperature gas turbines, bearings, seals and lining of industrial furnaces. This study was made only for the finish stages and has been carried out on the influence of five design factors: intensity supplied by the generator of the EDM machine (I), pulse time (ti), duty cycle (η), open-circuit voltage (U) and dielectric flushing pressure (P), over the two previously mentioned response variables. This has been done by means of the technique of design of experiments (DOE), which allows us to carry out the above-mentioned analysis performing a relatively small number of experiments. In this case, a $25-1$ fractional factorial design, whose resolution is V, has been selected considering the number of factors considered in the present study. The resolution of this fractional design allows us to estimate all the main effects, two-factor interactions and pure quadratic effects of the five design factors selected to perform this study.

Yih-fong Tzeng et al. [20] described the application of the fuzzy logic analysis coupled with Taguchi methods to optimise the precision and accuracy of the high-speed electrical discharge machining (EDM) process. A fuzzy logic system is used to investigate relationships between the machining precision and accuracy for determining the efficiency of each parameter design of the Taguchi dynamic experiments. From the fuzzy inference process, the optimal process conditions for the high-speed EDM process can be easily determined as A1B1C3D1E3F3G1H3. In addition, the analysis of variance (ANOVA) is also employed to identify factor B (pulse time), C (duty cycle), and D (peak value of discharge current) as the most important parameters, which account for about 81.5% of the variance. The factors E (powder concentration) and H (powder size) are found to have relatively weaker impacts on the process design of the high-speed EDM. Furthermore, a confirmation experiment of the optimal process shows that the targeted multiple performance characteristics are significantly improved to achieve more desirable levels.

Bu¨lent Ekmekci [21] studied the effect of dielectric liquid and electrode type on white layer structure in electric discharge machined surfaces has been studied in terms of retained austenite and residual stresses using X-ray diffraction method. The machining tests were conducted by using two different tool electrodes (copper and graphite) and dielectric liquid (kerosene and de-ionized water) under same operational conditions. The present work suggests that the surface is saturated with carbon irrespective of the tool electrode material when machining with kerosene dielectric liquid. But, retained austenite is formed on the surface due to carbon uptake from graphite tool electrode when machining with de-ionized water dielectric liquid. On the other hand, even though surface residual stresses increase with structural non-homogeneities in the white layer, no clear consequences have been observed in residual stress distribution beneath the white layer.

Y. H. Guu et al. [22] investigated the electrical discharge machining (EDM) of a Fe-Mn- Al alloy. The surface phenomena caused by EDM were studied in terms of machining parameters. An empirical model of the Fe-Mn-Al alloy was also proposed based on the experimental data. Experimental results indicate that the higher the discharge energy, the faster the machining time. This treatment introduces machining damage in the resolidified surface layer and worsens the surface roughness. The optimum pulse-on duration on the basis of the electrode wear ratio for the copper electrode was about 200 μs. The increase of crater depth with the applied pulsed current and pulse-on duration appears minimal under a small input energy.

Dhananjay pardhan et al. [23] studied that Electrical discharge machining (EDM) has been recognized as an efficient production method for precision machining of electrically conducting hardened materials. Copper and aluminium are used as electrode materials in this process with Kerosene oil as the dielectric medium. In this work, the behavior of copper and aluminium electrodes on electric discharge machining of EN-8 alloy steel had been studied. Keeping all other machining parameters same, the hardened work material was machined with the two electrodes at different values of peak current, pulse-on time & duty factor according to 23 full factorial design. It has been found that copper shows better results than

aluminium in term of surface finish (μm) in same dielectric media. Therefore, copper is recommended as a good electrode material.

2.1.2 Effect of various powders on the EDM for the surface modification

Y. S. Wong et al. [24] presented a study of the near-mirror-finish phenomenon in electrical discharge machining (EDM) when fine powder is introduced into the dielectric fluid as a suspension at the tool–workpiece or inter-electrode gap during machining. For this study, the dielectric flushing system of a conventional die-sinking EDM machine was specially modified to inject and distribute the powder into the dielectric fluid, especially at the gap between the tool and the workpiece. Machining was performed on various types of steel with different types of powder suspensions at a peak current of around 1 A. Particular combinations of powder-mixed dielectric and workpiece have been found to produce mirror-finish or glossy machined surfaces. Close scrutiny of the mirror-finish surfaces reveals shallow overlapping re-solidified discs with smooth rims, unlike typical EDMed surfaces, which are typically covered with deep craters, pock marks and globules. The various factors affecting the generation of the mirror-like surfaces are discussed. The appropriate settings of electrode polarity and pulse parameters and the correct combination of work piece material and powder characteristics have a significant influence on the mirror-finish condition. The use of negative electrode polarity (i.e. with the tool as the negative electrode, which is a condition normally used for finishing EDM) is necessary to achieve the mirror-finish condition. Other features of the powder-mixed dielectric EDM are shorter machining time, more uniform dispersion of the electrical discharges, and stable machining. Based on the results of the experimental investigation, the types of material composition, powder properties and machine setting in bringing about near-mirror conditions are discussed

Y.-F. Tzeng et al. [25] presented the effects of various powder characteristics on the efficiency of electro discharge machining (EDM) SKD-11. The additives examined include aluminium (Al), chromium (Cr), copper (Cu), and silicon carbide (SiC) powders that have significant differences in their thermo physical properties. The machining mechanism with the addition of the foreign particles, the tool wear rate (TWR), and the material removal rate (MRR) have been investigated. It was found experimentally that the particle concentration, the particle size, the particle density, the electrical resistivity, and the thermal conductivity of

powders were important characteristics that significantly affected the machining performance in the EDM process. Proper addition of powders to the dielectric fluid increased the MRR and, thus, decreased the TWR. Under the same particle concentration experiments, the smallest suspended particle size led to the greatest MRR and, thus, the lowest TWR. Of the additives investigated, chromium powder produced the greatest MRR and the lowest TWR, whereas the process without foreign particles has the converse effects. The addition of copper powder to the dielectric fluid was found to make almost no difference to the pure kerosene EDM system.

H.K. Kansal et al. [26] studied that how to optimize the process parameters of powder mixed electrical discharge machining (PMEDM). Response surface methodology has been used to plan and analyze the experiments. Pulse on time, duty cycle, peak current and concentration of the silicon powder added into the dielectric fluid of EDM were chosen as variables to study the process performance in terms of material removal rate and surface roughness. Experiments are performed on a newly designed experimental setup developed in the laboratory. The results identify the most important parameters to maximize material removal rate and minimize surface roughness. The recommended optimal process conditions have been verified by conducting confirmation experiments.

C ¸Cogun et al. [27] study, the variations of machining performance outputs, namely workpiece surface roughness, surface profile power spectral density, workpiece removal rate, electrode wear rate, relative wear, workpiece surface hardness, and workpiece surface microstructure were experimentally investigated with the varying machining parameters for metal powder mixed dielectric liquid in electrical discharge machining (EDM). The machining tests were conducted by using a prismatic steel workpiece and copper electrodes with graphite and boric acid powders (H3BO3) mixed kerosene dielectric at different powder concentrations and pulse time settings. The experiments have shown that the type and concentration of the powders mixed into the dielectric and the pulse time were effective on machining performance outputs in EDM.

Anil Kumar [28] studied a technique for optimization of abrasive mixed electrical discharge machining (AEDM) process with multiple performance characteristics based on the

orthogonal array with grey relational analysis has been studied. The process input parameters, i.e., concentration of silicon abrasive powder in dielectric fluid, peak current, pulse-on time, and duty factor, were chosen to study process performance in the form of MRR and surface roughness. The research outcome identifies significant parameters and their effect on process performance on EN-24 tool steel using copper electrode with silicon powder (2 g/l) suspended in kerosene dielectric. The optimum process conditions have been verified by conducting the confirmation experiments.

H.K. Kansal et al. [29] studied that Powder mixed electric discharge machining (PMEDM) is one of the recent innovations for the enhancement of capabilities of EDM process. In PMEDM, the electrically conductive powder is mixed in the dielectric of EDM, which reduces the insulating strength of the dielectric fluid and increases the spark gap between the tool and workpiece. As a result, the process becomes more stable, thereby, improving the material removal rate (MRR) and surface finish. Moreover, the surface develops high resistance to corrosion and abrasion. This paper presents a tutorial introduction, comprehensive history and review of research work carried out in the area of PMEDM. The machining mechanism, current issues, applications and observations are also discussed.

Sanjeev Kumar et al. [30] investigated that Surface modification by material transfer during electrical discharge machining (EDM) has emerged as a key research area in the last decade. Material may be provided to the machined surface of the workpiece by the eroding tool electrode or by using powder-mixed dielectric. Breakdown of the hydrocarbon dielectric contributes carbon to the plasma channel which may also cause surface modification. The present work has investigated the response of three die steel materials to surface modification by EDM method with tungsten powder mixed in the dielectric medium. Taguchi experimental design technique was used to conduct the experiments on each work material independently. Peak current, pulse on-time and pulse off time were taken as variable factors and micro-hardness of the machined surface was taken as the response parameter. X-ray diffraction (XRD) and spectrometric analysis show substantial transfer of tungsten and carbon to the workpiece surface and an improvement of more than 100% in micro-hardness for all the three die steels. Presence of tungsten carbide (WC and W2C) indicates that its

formation is taking place in the plasma channel. Machining parameters for the best value of micro-hardness for each work material were found to be the same.

H.K. Kansal [31] studied the effect of silicon powder mixing into the dielectric fluid of EDM on machining characteristics of AISI D2 (a variant of high carbon high chrome) die steel has been studied. Six process parameters, namely peak current, pulse on time, pulse-off time, concentration of powder, gain, and nozzle flushing have been considered. The process performance is measured in terms of machining rate (MR). The research outcome will identify the important parameters and their effect on MR of AISI D2 in the presence of suspended silicon powder in a kerosene dielectric of EDM. The study indicated that all the selected parameters except nozzle flushing have a significant effect on the mean and variation in MR (S/N ratio). Optimization to maximize MR has also been undertaken using the Taguchi method. The ANOVA analysis indicates that the percentage contribution of peak current and powder concentration toward MR is maximum among all the parameters. The confirmation runs showed that the setting of peak current at a high level (16 A), pulse-on time at a medium level (100μs), pulse-off time at a low level (15μs), powder concentration at a high level (4 g/l), and gain at a low level (0.83 mm/s) produced optimum MR from AISI D2 surfaces when machined by silicon powder mixed EDM.

P. Pecas, E. Henriques [32] studied that Electrical discharge machining (EDM) is one of the most widely disseminated manufacturing technologies, in particular as regards the generation of accurate and complex geometrical shapes on hard metallic components. Nevertheless current EDM technologies have major limitations when dealing with fine surface finish over large process area. Indeed this is one reason that explains the need of final manual polishing of mould cavities performed by EDM. Recently EDM with powder-mixed dielectric (PMD-EDM) has been a focus of an intense research work in order to overcome these technological performance barriers. This paper presents a research work within the objective to acquire deep knowledge on EDM technology with powder mixed dielectric and to compare its performance to the conventional EDM when dealing with the generation of high-quality surfaces. In particular the analysis of the effect of the electrode area in the surface quality measured by the surface roughness and craters morphology was carried out for both technologies. The results achieved evidenced a linear relationship between the electrode area

and the surface quality measures as well as a significant performance improvement when the powder mixed dielectric is used.

F. Klocke et al. [33] investigated that EDM is used to machine every electrically conductive material by removing material through electrical discharges in a dielectric fluid. During machining the heat intensity from the spark melts a part of the work piece. This liquid phase of the material re-solidifies rapidly and builds the recast layer. A lot of work has been done before to explain the physical principles governing the process and the thermal influenced zone. Effects on the recast layer by using micro Joule-range discharge energies in combination with powder suspended working fluids are examined in this paper. The effects of a capacitor connected parallel to the gap were investigated in relation to the recast layer formation. In addition, transverse section pictures show the morphology and the depth of the thermal influenced zone. The aim was to investigate the influence of the powder particles in micro-sinking-EDM and especially in the gap, on the thermal spread in the dielectric and on the influenced zone. Pictures were taken during the spark generation in different suspended dielectrics with a high speed framing camera. Furthermore, a complete qualitative and quantitative analysis of an EDX spectrum has been performed in order to examine the changes of the recast layer composition by using powder suspended dielectrics at the work piece surface.

Min-Seop Han et al. [34] showed that a new method has been investigated to improve the surface integrity of electro-chemical discharge machining (ECDM) process by use of conductive particles in the electrolyte. In conventional ECDM processes the generation of fine sparks with uniform energy has been most desired technique to improve the machining efficiency and the surface quality. However, precise control of the spark generations in ECDM process has been a challenging problem. In electrical discharge machining (EDM) processes, which is thermal erosion machining process using spark energy similar to the ECDM, powder-mixed EDM (PM-EDM) fluids have been used to improve machining quality. Although the exact role of the conductive particles in the EDM process could not be clearly explained yet, it has been reported that the powder stabilizes discharge current as a result of discharge energy dispersion. Considering the similarity of the ECDM process compared to EDM where electrical sparks are utilized, powder-mixed electrolyte was

introduced to create similar effects. In this paper fine graphite powder (which has good thermal and electrical conductivity) mixed with electrolyte has been applied to the ECDM process. Borosilicate glass, which is frequently used as a material for micro structures, was used as a work piece. To investigate effectiveness of the proposed method experiments were conducted. The experiment results demonstrated that the break down voltage was reduced and the peak current during the process was decreased by ten percents. Discharging pattern was modified such that a single discharge pulse was branched into two or three. As a result, the surface quality was improved compared to that from the conventional process. Various experiment results of product quality with respect to powders volume ratio are also presented.

Kun Ling Wu et al [35] studied that Electrical discharge machining (EDM) process is widely used to process hard materials in the industry. Electrical discharge distribution effects can be achieved by the addition of Al powder in the dielectric. A fine surface roughness value of the work piece is thus obtained. However, the electrostatic force among fine Al particles is found to agglomerate the Al powders in the dielectric. A surfactant can be adopted to separate the Al powder in the dielectric homogenously. A better surface evens the mirror-like quality of the EDM work piece is thus desired. In the study, the effect of surfactant and Al powders added in the dielectric on the surface status of the work piece after EDM is investigated. It is observed the best distribution effect is found when the concentrations of the Al powder and surfactant in the dielectric are 0.1 and 0.25 g/L, respectively. An optimal surface roughness (Ra) value of 0.172 mm is achieved under the following parameter—positive polarity, discharge current 0.3 A, pulse duration time 1.5 ms, open circuit potential 140 V, gap voltage 90 V and surfactant concentration 0.25 g/L. The surface roughness status of the work piece has been improved up to 60% as compared to that EDM under pure dielectric with high surface roughness Ra of 0.434 mm.

2.1 EXHAUSTIVE SUMMARY OF LITERATURE REVIEW

From literature review, it was concluded that a lot of work has been done in surface modification with EDM. In the literature survey, Researcher [24] get near mirror finish by using powder mixed EDM. Researcher [30], [25] add powders in kerosene and use as a dielectric medium in EDM. Researcher [31], [28] shows the effect of addition of Si powder in dielectric and improvement in surface finish. In [30], shows the effect of Tungsten powder

mixed in dielectric on the EDM performance. [33] Shows the effect of powder on thermal influenced zone in EDM. [23], [32] shows the effect of different electrodes in the EDM. Researchers [37], show the analysis of rapidly re-solidified re-cast layer formed on the surface of metal. [36], shows the improvement of surface finish on steel by using aluminium and surfactant added in the dielectric. From the literature survey, it is observed that the field of surface modification using Powder EDM process is still at experimental stage.

2.2 GAPS IN LITERATURE REVIEW

The field of surface modification using EDM process is still in at the experimental stage. In the present study more experimental work has been done and obtained many significant results. From the literature review, it is observed that a little research work has been carried out on surface modification using graphite and aluminium oxide powder in kerosene oil dielectric fluid along copper, aluminium and brass electrodes. Also little work has been done on Tungsten Carbide by using Al_2O_3 and Gr as a powders in dielectric medium and Al, Br and Cu as an electrode.

Chapter 3

DESIGN OF EXPERIMENT

3.1 Methodology

The Taguchi method involves reducing the variation in a process through robust design of experiments. The overall objective of the method is to produce high quality product at low cost to the manufacturer. Taguchi developed a method for designing experiments to investigate how different parameters affect the mean and variance of a process performance characteristic that defines how well the process is functioning. The experimental design

proposed by Taguchi involves using orthogonal arrays to organize the parameters affecting the process and the levels at which they should be varies. Instead of having to test all possible combinations like the factorial design, the Taguchi method tests pairs of combinations. This allows for the collection of the necessary data to determine which factors most affect product quality with a minimum amount of experimentation, thus saving time and resources. The Taguchi method is best used when there are an intermediate number of variables (3 to 50), few interactions between variables, and when only a few variables contribute significantly. The arrays are selected by the number of parameters (variables) and the number of levels (states). The Taguchi method has been proposed to overcome these limitations by simplifying and standardizing the fractional factorial design. The methodology involves identification of controllable and uncontrollable parameters (electrode, pulse on time, pulse off time, current and powder) and the establishment of a series of experiments to find out the optimum combination of the parameters which has greatest influence on the performance and the least variation from the target of the design [37].

3.2 Taguchi Design of Experiments

The general steps involved in the Taguchi method are as follows:

1. Define the objective of study.

2. Determine the design parameters affecting the study.

3. Design the orthogonal arrays for the parameter design indicating the number of and conditions for each experiment. The selection of orthogonal arrays is based on the number of parameters and the levels of variation for each parameter.

4. Conduct the experiments indicated in the completed array to collect data on the effect on the performance measure.

5. Complete data analysis to determine the effect of the different parameters on the performance measure.

6. Analyze the results.

7. Confirmation of the results.

3.3 ESTABLISHMENT OF OBJECTIVE FUNCTION

The main objective of this study is to investigate the Performance characteristics of parameters electrode, pulse off, pulse on time, current and powder on the MRR, TWR, surface roughness and micro hardness .The SEM and EDS study was performed to analyse the micro-structure and composition of the material.

3.4 SELECTION OF FACTORS AND INTERACTION

The factors are selected according to the availability of the materials extensively used in the industries and then according to factors to be selected decide the main interactions that which factor is more affective and in which main factors we are interested. The lists of factors studied with their levels are shown in the Table 3.1.

Table 3.1 Factors interested and their levels

FACTORS	**LEVELS**		
	Level-1	**Level-2**	**Level-3**
Pulse on (µs), A	15	50	100
Pulse off (µs), B	10	50	75
Current (Amp), C	3	6	9
Powder, D	Gr	Al_2O_3	Mix
Electrode, E	Cu	Al	Br

Some of interactions between the main factors were believed to be of interest. The interaction identified for detailed statistical analysis is as under:

- **Current × Powder, C × D**
- **Current × Electrode, C × E**
- **Powder × Electrode, D × E**

3.4.1 DEGREE OF FREEDOM (DOF)

The number of factors and their interactions and level for factors determine the total degree of freedom required for the entire experiment. The degree of freedom for each factor is given by the number of levels minus one.

DOF for each factor : k-1

Where k is the number of level for each factor

DOF for interactions between factors : (kA-1) × (kB-1)

Where kA and kB are number of level for factor A and B

The minimum DOF required in the experiment are the sum of all the degrees of freedom of factors and interactions. In the present experiment set up there are 5 factors and 3 levels. The no. of degree of freedoms of above mentioned parameters A, B, C, D, and E are two. The most suitable orthogonal array that can be used for this experiment is L27, which has 26 dof assigned to its various columns. The total DOF for the experiment including the interaction is given in Table 3.2

Table 3.2 Degree of freedom

Factor	**A**	**B**	**C**	**D**	**E**	**C × D**	**C × E**	**D × E**	**Total**
Degree of freedom	2	2	2	2	2	**2 × 2 = 4**	**2 × 2 = 4**	**2 × 2 = 4**	22

3.5 ORTHOGONAL ARRAY

A lot of factors are often taken up at the same time at the early stage of the problem solving. The experiment frequency increases in the factorial experiment on which it experiments by all the level combinations when the number of factors taken up in the experiment increases. Then, the obtaining necessary information can be done by an experiment frequency that is less than the factorial experiment by providing experimental conditions by using the table that is called an orthogonal array. The effect of many different parameters on the performance characteristic in a condensed set of experiments can be examined by using the orthogonal array experimental design proposed by Taguchi. Once the parameters affecting a process that can be controlled have been determined, the levels at which these parameters should be varied must be determined. Determining what levels of a variable to test requires an in-depth understanding of the process, including the minimum, maximum, and current value of the parameter. If the difference between the minimum and maximum value of a parameter is large, the values being tested can be further apart or more values can be tested. If the range of a parameter is small, then less value can be tested or the values tested can be closer together. The algorithms ensure that the OA to be constructed in a statistically independent manner that each level has an equal number of occurrences within each column; and for each level within one column, each level within any other column will occur an equal number of times as well. Then, the columns are called orthogonal to each other. OA's are available with a variety of factors and levels in the Taguchi method. Since each column is orthogonal to the others, if the results associated with one level of a specific factor are much different at another level, it is because changing that factor from one level to the next has strong impact on the quality characteristic being measured.

Taguchi's orthogonal arrays are experimental designs that usually require only a fraction of the full factorial combinations. The arrays are designed to handle as many factors as possible in a certain number of runs compared to those dictated by full factorial design. The columns of the arrays are balanced and orthogonal. This means that in each pair of columns, all factor combinations occur same number of times. Orthogonal designs allow estimating the effect of each factor on the response independently of all other factors. Once the degrees of freedom are known, the next step, selecting the orthogonal array (OA) is easy. The number of treatment conditions is equal to the number of rows in the orthogonal array and it must be equal to or greater than the degrees of freedom. The interactions to be evaluated will require an even larger orthogonal array. Once the appropriate orthogonal array has been selected, the

factors and interactions can be assigned to the various columns. The linear graph used for assignment of factors in L27 array is shown in Figure 3.1.

The L27 array has 13 columns and each column has two DOF associated with it. In the linear graph, each vertex of the triangle represents a column in L27 array

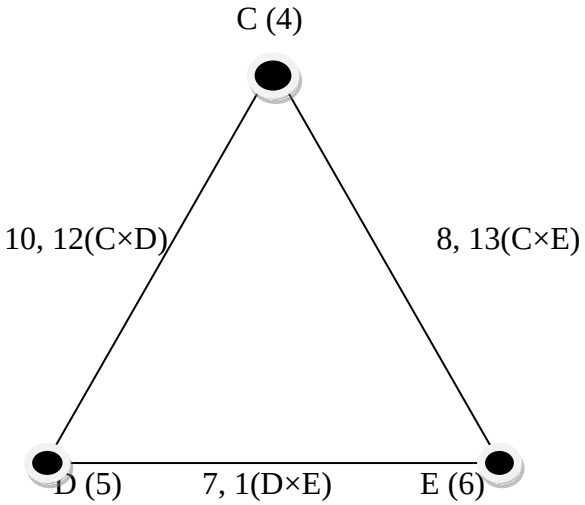

Figure 3.1: L27 Linear Graph [2]

Factor C has been assigned to column 4, Factor D has been assigned to column 5 and Factor E has been assigned to column 6. Each connecting line of the triangle represents interaction and also the column merged for the purpose. Column 9 and 11 merged to measure the interaction of C × D, Column 7 and 1 merged to measure the interaction of D × E and Column 8 and 13 merged to measure the interaction of C × E.

The 27 trial conditions represented by Taguchi's L27 are given in Table 3.3.

Table 3.3: L27 Experimental design

Sr. no.	Workpiece	Dielectric fluid	Pulse-on Time(μs)	Pulse-off Time(μs)	Current Amps	Powder	Tool Material
1.	Tungsten Carbide	Kerosene oil	15	10	3	Gr	Cu
2.	Tungsten Carbide	Kerosene oil	15	10	3	Al_2O_3	Al

3.	Tungsten Carbide	Kerosene oil	15	10	3	Mix	Br
4.	Tungsten Carbide	Kerosene oil	50	50	6	Gr	Cu
5.	Tungsten Carbide	Kerosene oil	50	50	6	Al_2O_3	Al
6.	Tungsten Carbide	Kerosene oil	50	50	6	Mix	Br
7.	Tungsten Carbide	Kerosene oil	100	75	9	Gr	Cu
8.	Tungsten Carbide	Kerosene oil	100	75	9	Al_2O_3	Al
9.	Tungsten Carbide	Kerosene oil	100	75	9	Mix	Br
10.	Tungsten Carbide	Kerosene oil	15	50	9	Gr	Al
11.	Tungsten Carbide	Kerosene oil	15	50	9	Al_2O_3	Br
12.	Tungsten Carbide	Kerosene oil	15	50	9	Mix	Cu
13.	Tungsten Carbide	Kerosene oil	50	75	3	Gr	Al
14.	Tungsten Carbide	Kerosene oil	50	75	3	Al_2O_3	Br
15.	Tungsten Carbide	Kerosene oil	50	75	3	Mix	Cu
16.	Tungsten Carbide	Kerosene oil	100	10	6	Gr	Al
17.	Tungsten Carbide	Kerosene oil	100	10	6	Al_2O_3	Br
18.	Tungsten	Kerosene	100	10	6	Mix	Cu

	Carbide	oil					
19.	Tungsten Carbide	Kerosene oil	15	75	6	Gr	Br
20.	Tungsten Carbide	Kerosene oil	15	75	6	Al_2O_3	Cu
21.	Tungsten Carbide	Kerosene oil	15	75	6	Mix	Al
22.	Tungsten Carbide	Kerosene oil	50	10	9	Gr	Br
23.	Tungsten Carbide	Kerosene oil	50	10	9	Al_2O_3	Cu
24.	Tungsten Carbide	Kerosene oil	50	10	9	Mix	Al
25.	Tungsten Carbide	Kerosene oil	100	50	3	Gr	Br
26.	Tungsten Carbide	Kerosene oil	100	50	3	Al_2O_3	Cu
27.	Tungsten Carbide	Kerosene oil	100	50	3	Mix	Al

3.6 EXPERIMENTAL SET UP

The experiments have been conducted on the Electrical Discharge Machine model T-3822of Victory Electromech available at Thapar University, Patiala in Machine Tool lab. I had selected Pulse-on, Pulse-off, Current, Powder and Tool as 5 parameters in my experiments and they had varied during the whole EDM experiments. Pulse-on, pulse-off and Current are the parameters of the machine and they are varied from the machine to get output. We get output from these parameters in several forms like MRR, TWR, surface finish and hardness.

Constant Input parameters shown in table 3.4

Table 3.4: Constant input parameters

S.No	Parameter	Value
1.	Open circuit voltage	135+/-5%
2.	Polarity	Positive
3.	Machining time	10 minutes
4.	Spark energy	Low
5.	Powder concentration	15 gm/l

To avoid the powder to get mixed into the filtering system I bought a plastic tank of 10 litres capacity was taken whose Length is 284.31mm, Width is 211.48mm and Height is 132.3mm.The thickness of plastic sheet is 12mm. A stirrer is also used to shake the powder continuously in the box whose rpm is controlled by a heavy duty regulator.

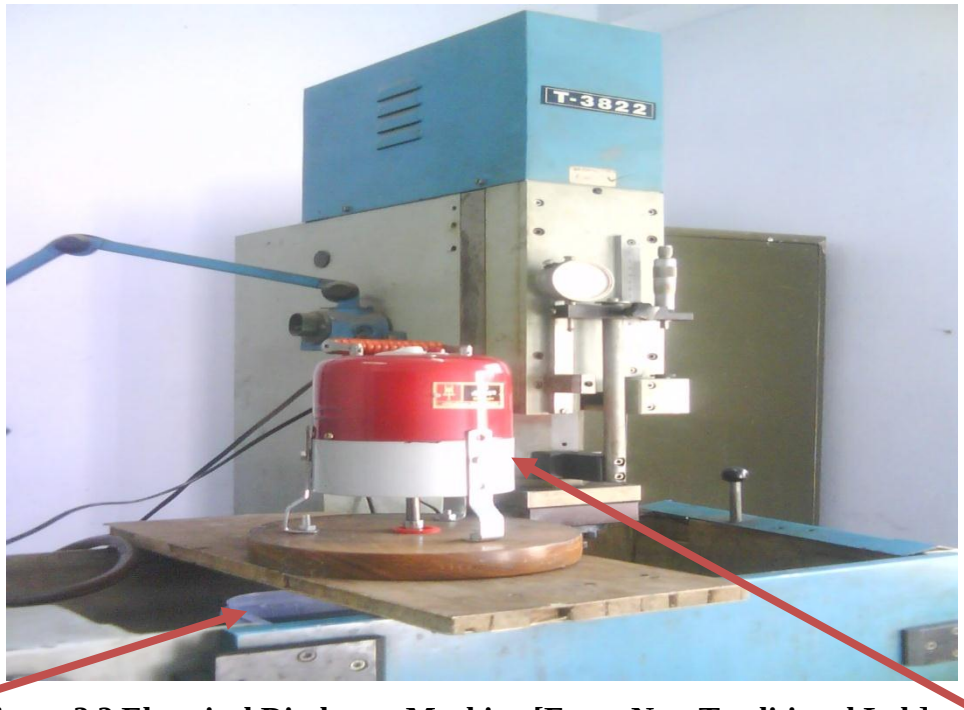

Figure 3.2 Electrical Discharge Machine [From-Non-Traditional Lab]

3.7 MEASURING AND TESTING EQUIPMENT USED

Micro hardness and surface roughness tests were conducted on all the samples, produced after each of the 27 trials. Also, MRR and TWR were measured using a weighing machine. The details of important test equipment used in experimental study are given below:

3.7.1 Surface Roughness Tester

Surface roughness was measured using the Perthometer; model SJ-400 of Mitutoyo, Japan available in the Metrology lab of Thapar University, Patiala. The equipment uses the stylus method of measurement, has profile resolution of 12 nm and measure roughness up to 100µm. A tracing length of 0.24 mm was used for analysis. Surface roughness of each sample was measured at the centre of each machined sample.

3.7.2 Micro Hardness Tester

Micro hardness was measured on a computer interfaced Micro Hardness Tester, (model MVH-2) Meta tech industries, Pune, India, available at Thapar University, Patiala. The micro hardness measurement is dependent on the diameter of indentation on the samples. The indents formed in the pyramid shaped indenter were measured with Quantimet software using a load of 1 kg for 25 seconds.

3.7.3 Energy Dispersion Spectroscopy (EDS)

Composition was taken out of some selected samples on Energy Dispersion Spectroscopy, model of OXFORD Company, USA, available in Material Testing lab of Thapar University, Patiala.

3.7.4 Scanning Electron Microscope (SEM) Machine

Microstructure was carried out of some selected samples on Scanning Electron Microscope, (model JSM-840A) of Joel, Japan, available in Material Testing lab of Thapar University, Patiala. The range of magnification from 10× to 3, 00,000×. SEM of samples was carried out on three ranges, namely, 50,100, 250×and 500×.

3.8. **ANALYSIS OF RESULTS**

3.8.1 Signal-to-noise ratio

The parameters that influence the output can be categorized into two classes, namely controllable (or design) factors and uncontrollable (or noise) factors. Controllable factors are those factors whose values can be set and easily adjusted by the designer. Uncontrollable factors are the sources of variation often associated with operational environment. The best settings of control factors as they influence the output parameters are determined through experiments. From the analysis point of view, there are three possible categories of the response characteristics explained below. *r* is the number of tests in a trial (noise of repetitions regardless of noise levels)

1. **Higher is Best**. The S/N for higher the better is given by:
   "Higher is better" type response which is given by:

   $$(S/N)HB = -10 \log (MSDHB) \qquad \text{(Equation ....3.1)}$$

   Where $MSD_{HB} = \frac{1}{r} \sum_{j=1}^{r} \frac{1}{y_j^2}$ (Equation ....3.2)

2. **Nominal is Best**. The S/N for nominal is best is:
   "Nominal is best" type response which is given by:
   $$(S/N)NB = -10 \log (MSDNB) \qquad \text{(Equation....3.3)}$$

Where $MSD_{LB} = \frac{1}{r} \sum_{i=1}^{r} (y_j - y_0)2$ (Equation....3.4)

3. **Lower is Best**

'Lower is better' type response which is given by:

S/N_{LB} = -10 log (MSD) = -10 log $[(\frac{1}{r} \sum_{i=1}^{r} y^2 i)$ (Equation 3.5)

Where $MSD_{LB} = \frac{1}{r} \sum_{i=1}^{r} (y_j^2)$ (Equation 3.6)

3.8.2 Signal to noise ratio for response characteristics

The parameters that influence the output can be categorized in two categories, controllable factors and uncontrollable factors. The control factors that may contribute to reduced variation can be quickly identified by looking at the amount of variation present in response. The uncontrollable factors are the sources of variation often associated with operational environment. For this experimental work, response characteristics have given in the Table 3.5.

Table 3.5: Response Characteristics

Response name	Response type	Units
Material Removal Rate (MRR)	Higher the better	mm^3/min
Tool Wear Rate (TWR)	Lower the better	mm^3/min
Micro Hardness	Higher the better	HVN
Surface Roughness	Lower the better	Microns

3.8.3 Measurement of F-value of Fisher's F ratio

The principle of the *F* test is that the larger the *F* value for a particular parameter, the greater the effect on the performance characteristic due to the change in that process parameter. *F* value is defined as:

$$F = \frac{\text{MS for a term}}{\text{MS for the error term}} \qquad \text{(Equation....3.7)}$$

3.9 TEST RESULTS FOR WORKPIECE MATERIAL BEFORE MACHINING

Workpiece material as Tungsten carbide has been used. Before the start of experimentation, the chemical composition of workpiece material was measured on Niton XLT Portable XRF (Material Sorter σ + - 10%) in the Indian Auto Parts & Hand Tool Technology, phase-5, focal point, Ludhiana. The percentage composition of the workpiece material is provided in Table 3.6.

Table 3.6 Chemical composition of workpiece materials

Sr. no.	% composition				
	W	**Cu**	**Nb**	**Co**	**Ti**
1.	65.50	3.66	4.69	10.07	15.47

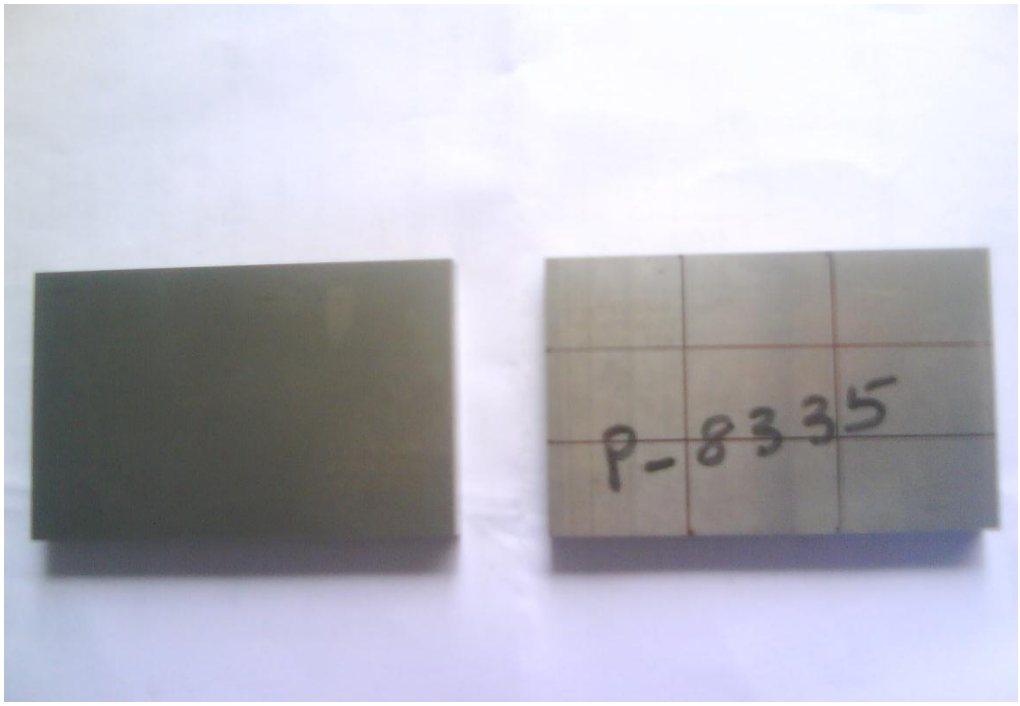

Figure 3.4 Workpiece materials a) Before Machining

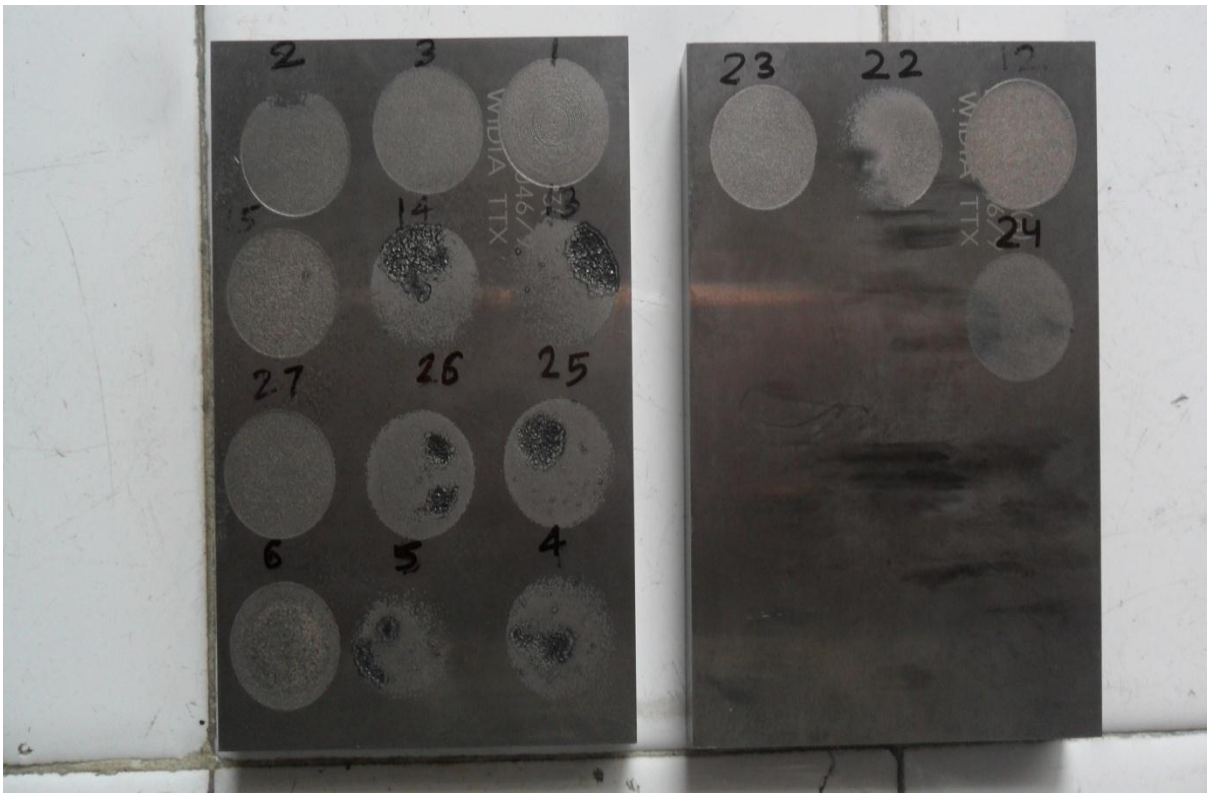

1.

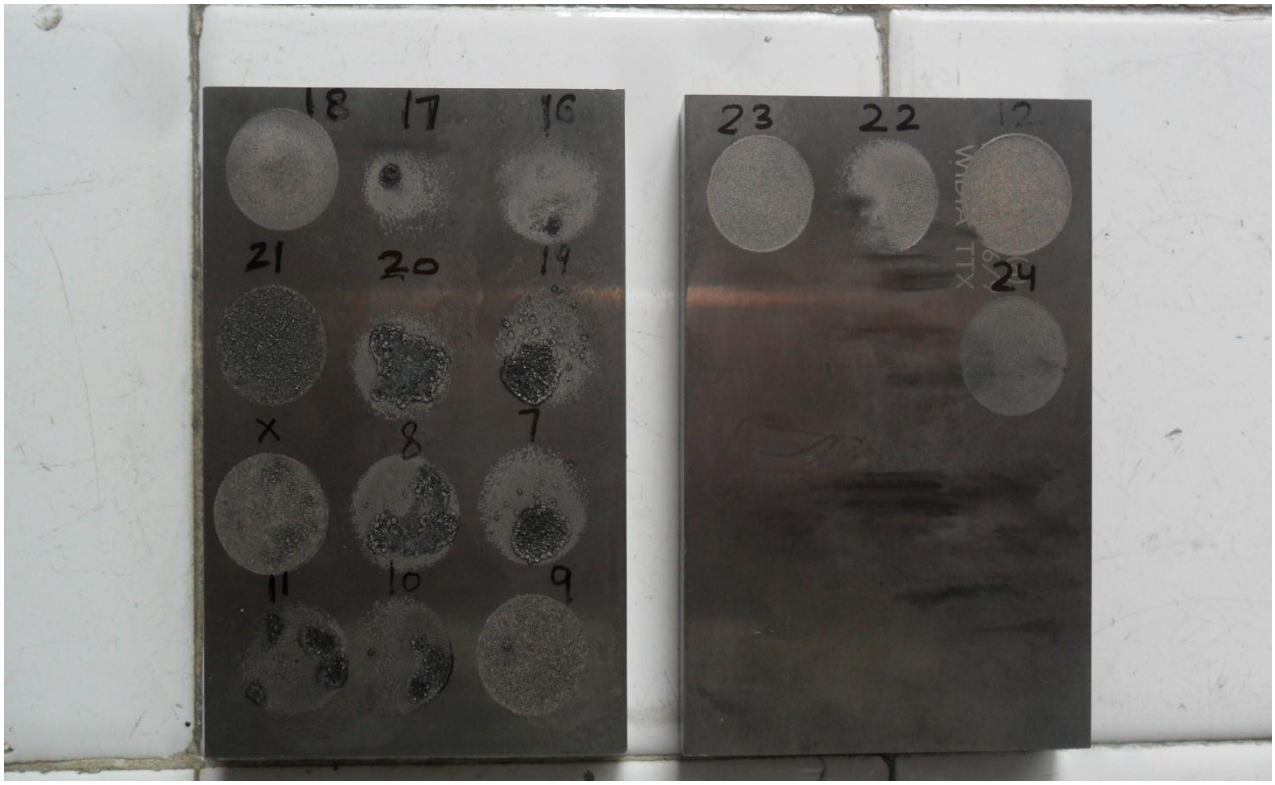

2.

Figure 3.5 Workpiece materials b) After Machining

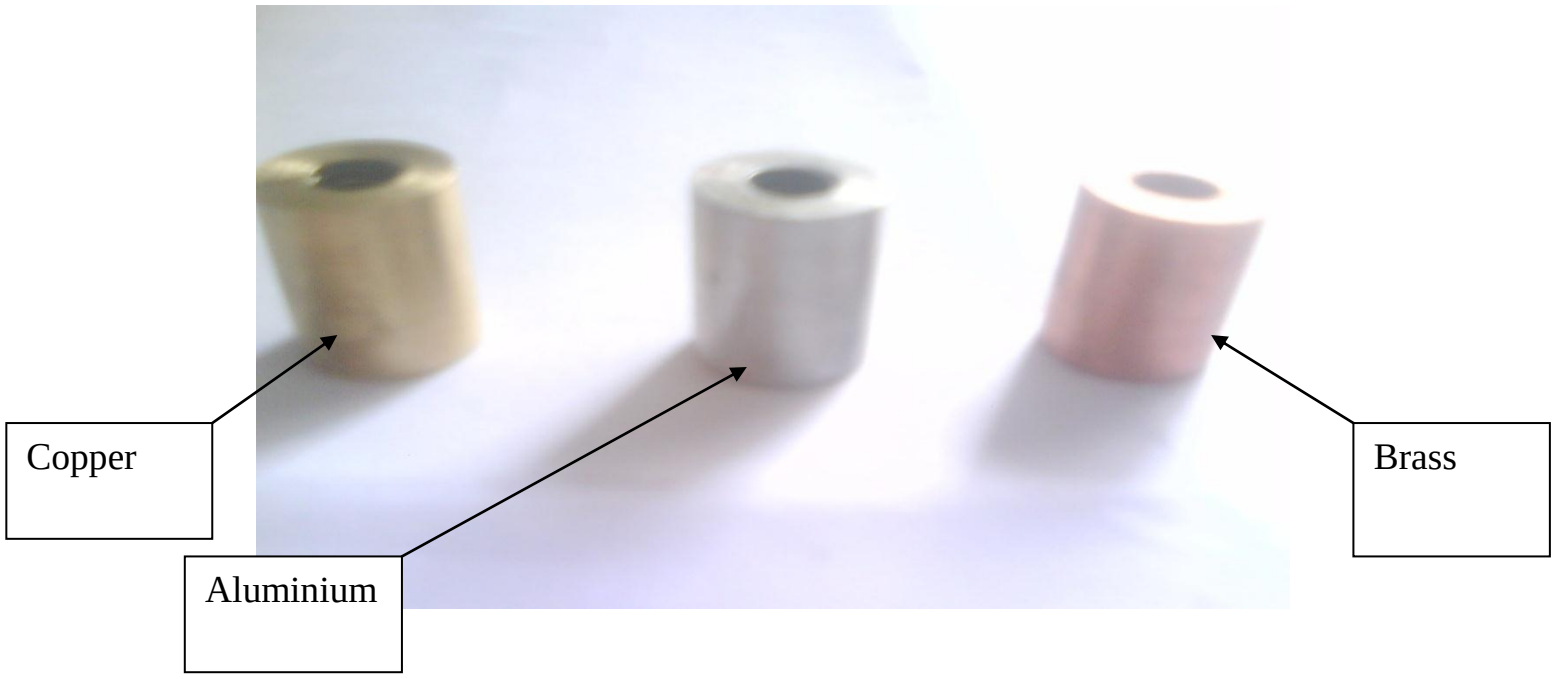

Figure 3.6 Electrodes used [16 mm diameter and 22 mm length]

Chapter 4

RESULTS AND ANALYSIS OF MRR

4.1 INTRODUCTION

The effects of parameters i.e. electrode, pulse on time, pulse off time, current and powder was evaluated using ANOVA and factorial design analysis. A confidence interval of 95% has been used for the analysis. Total 27 experiments were performed and each experiment performs only at once. During the time of machining there is rise in temperature between tool and workpiece which is more than 4000˚C.

4.2 RESULTS FOR MRR

The results for MRR for each of the 27 treatment conditions are given in Table 4.1. MRR of each sample is calculated from weight difference of work piece before and after the performance trial, which is given by:

$$MRR = \frac{(Wi - Wf)}{\rho \times t} \times 1000 \text{ mm}^3/\text{min} \qquad \text{(Equation ....4.1)}$$

Where, W_i = Initial weight of workpiece material (gm)

W_f= Final weight of workpiece material (gm)

t = Time period of trails in minutes

ρ = Density of work piece in gm/cc

Table 4.1: Results for MRR

Trial no.	Work piece	Dielectric fluid	Pulse-on Time (µs)	Pulse-off Time (µs)	Current (Amps)	Powder	Tool	MRR mm^3/min	S/N ratio
1.	Tungsten carbide	Kerosene	15	10	3	Gr	Cu	0.941	-0.523
2.	Tungsten carbide	Kerosene	15	10	3	Al_2O_3	Al	0.463	-6.686

3.	Tungsten carbide	Kerosene	15	10	3	Mix	Br	0.672	-3.446
4.	Tungsten carbide	Kerosene	50	50	6	Gr	Cu	1.015	0.135
5.	Tungsten carbide	Kerosene	50	50	6	Al_2O_3	Al	0.655	-3.665
6.	Tungsten carbide	Kerosene	50	50	6	Mix	Br	1.202	1.598
7.	Tungsten carbide	Kerosene	100	75	9	Gr	Cu	1.443	3.190
8.	Tungsten carbide	Kerosene	100	75	9	Al_2O_3	Al	1.126	1.032
9.	Tungsten carbide	Kerosene	100	75	9	Mix	Br	0.886	-1.050
10.	Tungsten carbide	Kerosene	15	50	9	Gr	Al	1.286	2.185
11.	Tungsten carbide	Kerosene	15	50	9	Al_2O_3	Br	0.665	-3.538
12.	Tungsten carbide	Kerosene	15	50	9	Mix	Cu	1.107	0.886
13.	Tungsten carbide	Kerosene	50	75	3	Gr	Al	3.158	9.990
14.	Tungsten carbide	Kerosene	50	75	3	Al_2O_3	Br	1.631	4.250
15.	Tungsten carbide	Kerosene	50	75	3	Mix	Cu	1.425	3.076
16.	Tungsten carbide	Kerosene	100	10	6	Gr	Al	1.145	1.180
17.	Tungsten carbide	Kerosene	100	10	6	Al_2O_3	Br	0.553	-5.142
18.	Tungsten	Kerosene	100	10	6	Mix	Cu	1.012	0.106

	carbide								
19.	Tungsten carbide	Kerosene	15	75	6	Gr	Br	1.287	2.192
20.	Tungsten carbide	Kerosene	15	75	6	Al_2O_3	Cu	1.107	0.886
21.	Tungsten carbide	Kerosene	15	75	6	Mix	Al	1.341	2.549
22.	Tungsten carbide	Kerosene	50	10	9	Gr	Br	0.842	-1.492
23.	Tungsten carbide	Kerosene	50	10	9	Al_2O_3	Cu	0.521	-5.656
24.	Tungsten carbide	Kerosene	50	10	9	Mix	Al	0.661	-3.593
25.	Tungsten carbide	Kerosene	100	50	3	Gr	Br	2.497	7.949
26.	Tungsten carbide	Kerosene	100	50	3	Al_2O_3	Cu	1.242	1.886
27.	Tungsten carbide	Kerosene	100	50	3	Mix	Al	1.448	3.218

4.3 ANALYSIS OF VARIANCE – MRR

The Analysis of Variance (ANOVA) for the mean MRR at 95% confidence interval is given in Table 4.2.The results for MRR were analyzed using ANOVA for identifying the significant factors affecting the performance measures. The variance data for each factor were F tested to find the significance of each. The principle of the *F* test is that the larger the *F* value for a particular parameter, the greater the effect on the performance characteristic, due to the change in that process parameter. ANOVA Table 4.2 shows that Pulse-off (F-33.19), Current (F-20.88), Powder (F-24.7) and Pulse-on (F-5.55) are factors that significantly affect the MRR. Acc. to ANOVAs Table 4.2 shown below, there are two interactions Current × Powder (F-6.42) and Powder × Tool (F-5.87) are significant and affect the MRR, where other factors like Tool and one interaction Current × Tool are are insignificant to affect the MRR. Table 4.3 ANOVAs Response Table shows the Rank of

various parameters and shows that Pulse-off and Powder are most significant factors which affect the MRR. MRR increases with increase in Pulse-On (15-100µs) and Pulse-Off (10-75µs).MRR decreases with addition of mixed powder and increases with Graphite powder. Figure 4.1 which show the variation of MRR with the input parameters.

Table 4.2: ANOVA for MRR

	SS	**v**	**V**	**F**	**F(Critical)**	**P**	**SS'**	**% contribution**	**Status**
Pulse-on ,A	0.4167	2	0.2083	5.55	5.14	0.07	0.2857	3.24	Significant
Pulse-off, B	2.4915	2	1.2457	33.19	5.14	0.003	2.3605	26.72	Significant
Current, C	1.5676	2	0.7838	20.88	5.14	0.008	1.4366	16.26	Significant
Powder, D	1.8541	2	0.9270	24.7	5.14	0.006	1.7231	19.5	Significant
Tool, E	0.1273	2	0.0636	1.7		0.293		0.041	Insignificant
Current × Powder	0.9636	4	0.2409	6.42	5.14	0.05	0.7004	7.92	Significant
Current × Tool	0.3807	4	0.0951	2.54		0.195		1.33	Insignificant
Powder × Tool	0.8821	4	0.2205	5.87	5.14	0.057	0.6189	6.95	Significant
Residual Error	0.1502	4	0.0375						
Total	8.8338	26	0.339						

e-pooled	0.6582	10	0.0658				0.1212	19.41	

Table 4.3: Response table for means of MRR

Level	**Pulse-on, A**	**Pulse-off, B**	**Current, C**	**Powder, D**	**Tool, E**
1	0.9858	0.757	1.4978	1.5131	1.0908
2	1.2348	1.2357	1.0356	0.8851	1.2541
3	1.2617	1.4897	0.9489	1.0841	1.1374
Delta	0.276	0.7327	0.549	0.628	0.1632
Rank	**4**	**1**	**3**	**2**	**5**

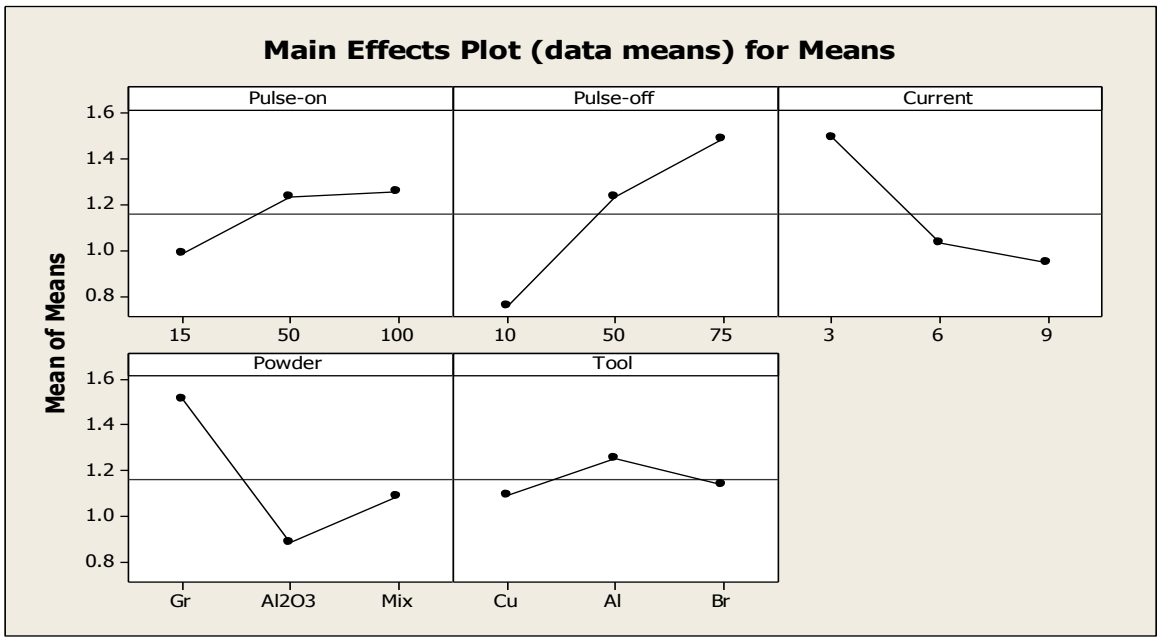

Figure 4.1: Main effects plot of MRR for Means

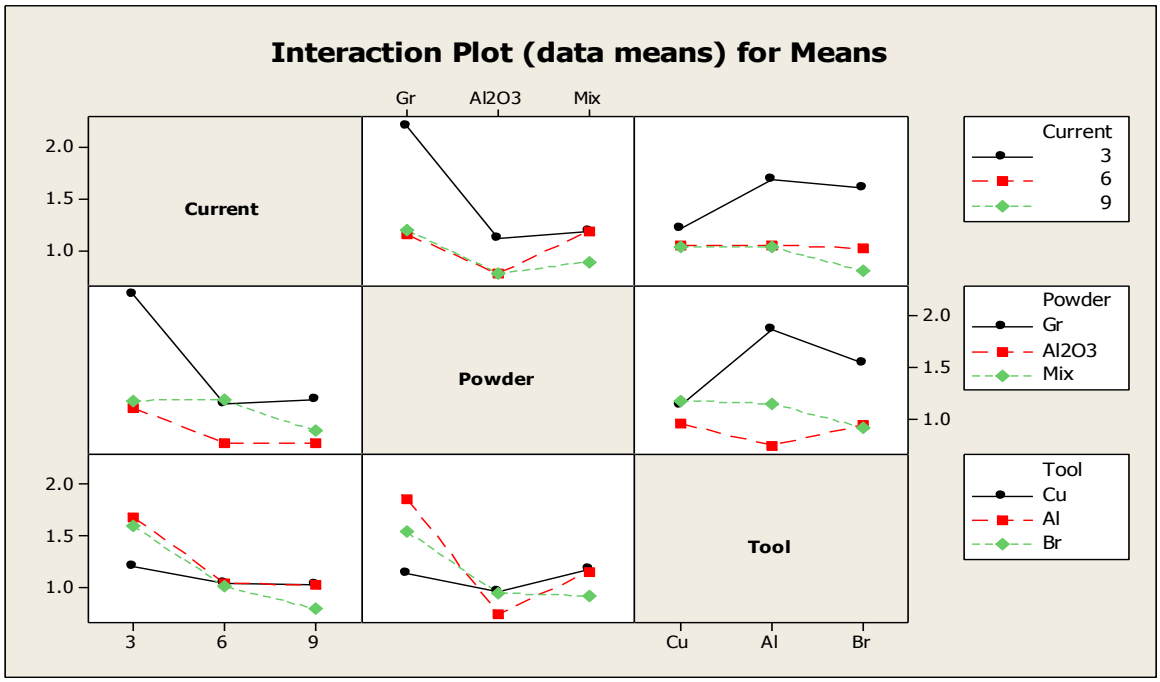

Figure 4.2: Interaction plot for MRR

4.4 RESULTS FOR S/N RATIO OF MRR

The S/N ratio consolidates several repetitions into one value and is an indication of the amount of variation present. The S/N ratios have been calculated to identify the major contributing factors and interactions that cause variation in the MRR. MRR is "Higher is better" type response which is given by:

$$(S/N)HB = -10 \log (MSDHB) \qquad \text{(Equation ....4.2)}$$

$$\text{Where } MSD_{HB} = \frac{1}{r}\sum_{j=1}^{r}\frac{1}{y_j^2} \qquad \text{(Equation ....4.3)}$$

MSDHB = Mean Square Deviation for higher-the-better response.

Table 4.4 shows the ANOVA results for S/N ratio of MRR at 95% confidence interval. According to F-test Pulse-Off, Powder and Current are the main parameters which affect the MRR and the left all other parameters are insignificant to MRR. Main effects plot of S/N ratio for MRR are shown in the figure 4.3 and 4.4 respectively.

Table 4.4: ANOVA for S/N ratio of MRR

	SS	v	V	F	F(Critical)	P	SS'	% of contribution	Status
Pulse-on ,A	17.837	2	8.918	2.95		0.163		2.15	Insignificant
Pulse-off, B	154.37	2	77.185	25.57	5.14	0.005	144.91	37.22	Significant
Current, C	45.45	2	22.725	7.53	5.14	0.044	35.99	9.24	Significant
Powder, D	95.455	2	47.727	15.81	5.14	0.013	85.995	22.08	Significant
Tool, E	1.333	2	0.6666	0.22		0.811		2.08	Insignificant
Current× Powder	21.088	4	5.272	1.75		0.301		0.55	Insignificant
Current × Tool	8.832	4	2.207	0.73		0.615		2.59	Insignificant
Powder ×Tool	33.483	4	8.3708	2.77		0.173		3.74	Insignificant
Residual Error	12.074	4	3.0185						
Total	389.293	26	14.972						
e-pooled	94.647	20	4.732				34.323	31.47	

Table 4.5: Response table for S/N ratio of MRR

Level	Pulse-on	pulse-off	Current	Powder	Tool
1	-0.6102	-2.806	2.1906	2.7565	0.44319
2	0.5158	1.1841	-0.0175	-1.8481	0.69025
3	1.3746	2.9021	-0.8928	0.3719	0.14678
Delta	1.9894	5.7082	3.0835	4.6047	0.54347
Rank	**4**	**1**	**3**	**2**	**5**

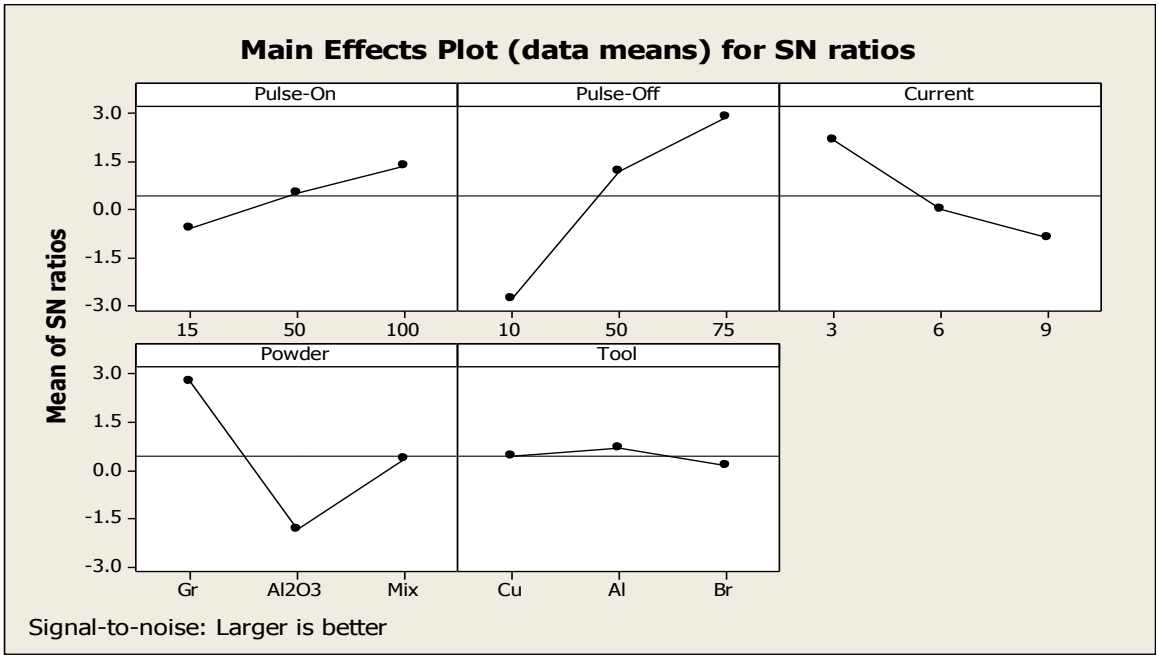

Figure 4.3: Main effects plot for MRR of S/N ratio

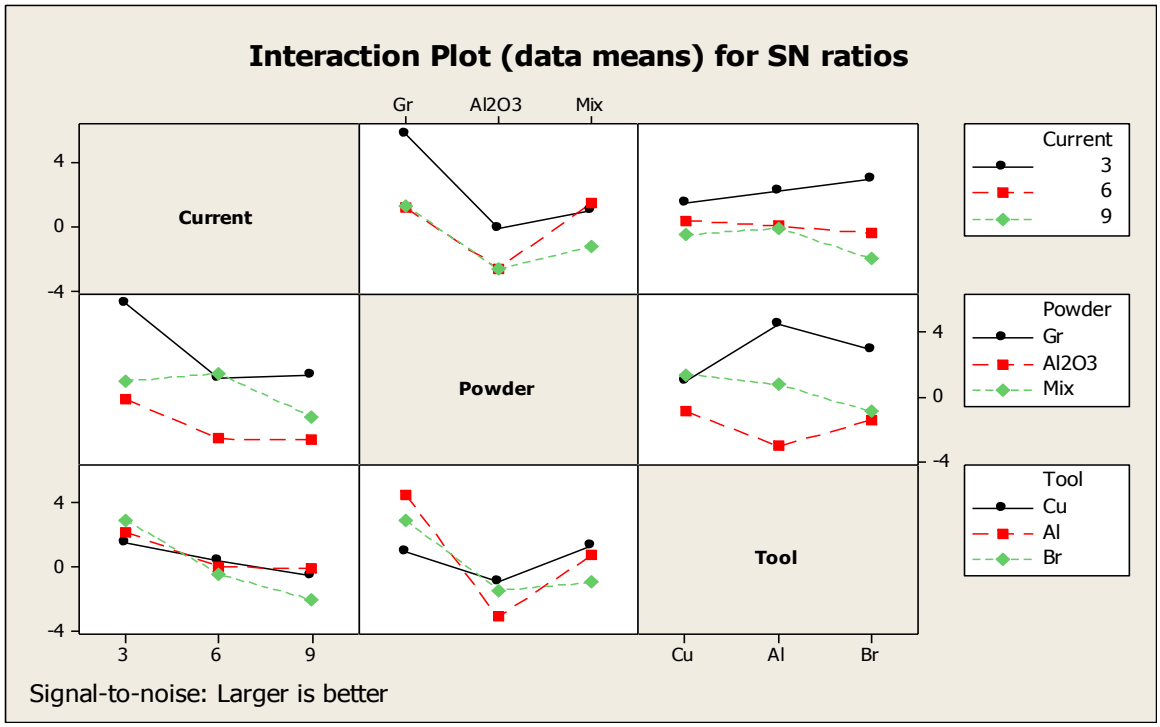

Figure 4.4: Interaction plot for SN Ratio of MRR

4.5 OPTIMAL DESIGN FOR MRR

In optimal design, level was chosen from which the best result is obtained, here there is some confliction between the results that at which level the best result is obtained so the optimal design is obtained.

In this experimental analysis, the main effect plot in Figure 4.1 used to estimate the mean MRR. From the, Table 4.6 it is concluded that highest MRR was observed when Tungsten Carbide was machined at Pulse-off (75µs), Pulse-on (100µs), 3 Amps Current with mixing of Graphite powder in the dielectric. There are also two interactions **Current × Powder** and **Powder × Tool** are also significant and affecting the MRR whereas in SN Ratio, MRR is observed at Pulse-off (75µs), 3 Amps Current with Mixed powder. Another factors are not so much affective here, we got maximum MRR in these two conditions but we have to select the best condition where we got maximum MRR, so this study shows that we got maximum MRR at Pulse-off (75µs), Pulse-on (100µs), 3 Amps Current with mixing of Graphite powder in the dielectric.

Table 4.6: Significant factors and interactions

Factor	Affecting mean		Affecting variation	
	Contribution Best level	**Best level**	**Contribution Best level**	**Best level**
Electrode, E	Insignificant	-	Insignificant	-
Pulse off, B	Significant	Level-3(75µs)	Significant	Level-3(75µs)
Pulse on, A	Significant	Level-3(100µs)	Insignificant	-
Current, C	Significant	Level-1(3 Amps.)	Significant	Level-1(3 Amps.)
Powder, D	Significant	Level-1(Gr)	Significant	Level-1(Gr)
Current × Powder	Significant	C_1D_1	Insignificant	-
Current × Tool	Insignificant	-	Insignificant	-
Powder × Tool	Significant	D_1E_2	Insignificant	-

Estimating the mean:

The different results were obtained from the different combinations of the parameters. After conducting the experiments, the optimum treatment condition within the experiment is determined on the basis of prescribed combination of factor levels is determined to one of those in the experiment

Mean value for MRR

$$\mu\, c_{1B_3A_3C_1D_1\,D_1E_2} = C_1D_1+D_1E_2+B_3+A_3+C_1+D_1-5\bar{T}$$

$$= 1.5131 + 1.2541 + 1.4897 + 1.2617 + 1.4978 + 1.5131 – 5 \times 1.208$$

$$= 2.488 mm^3/min$$

Here, $\bar{T}$ = sum of means/ 27

Confidence Interval around the Estimated Mean

The confidence interval is a maximum and minimum value between which the true average should fall at some stated percentage of confidence. Confidence Interval around the estimated MRR mean

$$CI_1 = \sqrt{\frac{F_{\propto,v1,v2}\ Ve}{\eta_{eff}}}$$

Where $F_{\alpha v1,v2}$ =F ratio

α = risk (0.01) confidence= 1-α

v_1 = DOF for mean which is always =1

v_2 = DOF for error= V_e

V_e = Variance of e-pooled

n_{eff}= Number of tests under that condition using the participating factors

$$n_{eff} = \frac{N}{1+dof_{C1\ B3\ A3\ C1D1\ D1E2}} = \frac{27}{1+2+2+2+2+4+4} = 1.588$$

$$CI_1 = \sqrt{\frac{F_{\propto,v1,v2}\ Ve}{\eta_{eff}}} = \sqrt{\frac{4.96 \times 0.0658}{1.588}} = 0.453$$

So the confidence interval around the MRR is given by 2.48 ± 0.453 mm^3/min

Chapter 5

RESULTS AND ANALYSIS OF TWR

5.1 INTRODUCTION

The effects of parameters i.e. electrode, pulse on time, pulse off time, current and powder was evaluated using ANOVA and factorial design analysis. A confidence interval of 95% has been used for the analysis. Total 27 experiments were performed and each experiment performs only at once.

5.2 RESULTS FOR TWR

The results for TWR for each of the 27 treatment conditions are given in Table 4.1. TWR of each sample is calculated from weight difference of work piece before and after the performance trial, which is given by:

TWR = $\frac{(Wi-Wf)}{\rho \times t} \times 1000$ mm^3/min (Equation…….....5.1)

Where, W_i = Initial weight of workpiece material (gm)

W_f= Final weight of workpiece material (gm)

t = Time period of trails in minutes

ρ = Density of workpiece in gm/cc

Table 5.1: Results for TWR

Trial no.	Workpiece	Dielectric	Pulse-on Time (µs)	Pulse-off Time (µs)	Current (Amps)	Powder	Tool	TWR mm^3/min.	S/N ratio
1.	Tungsten carbide	Kerosene	15	10	3	Gr	Cu	0.644	3.822
2.	Tungsten carbide	Kerosene	15	10	3	Al_2O_3	Al	0.343	9.29
3.	Tungsten carbide	Kerosene	15	10	3	Mix	Br	8.076	-18.14
4.	Tungsten	Kerosene	50	50	6	Gr	Cu	0.654	3.688

	carbide								
5.	Tungsten carbide	Kerosene	50	50	6	Al_2O_3	Al	1.678	-4.495
6.	Tungsten carbide	Kerosene	50	50	6	Mix	Br	9.415	-19.47
7.	Tungsten carbide	Kerosene	100	75	9	Gr	Cu	1.023	-0.197
8.	Tungsten carbide	Kerosene	100	75	9	Al_2O_3	Al	1.648	-4.339
9.	Tungsten carbide	Kerosene	100	75	9	Mix	Br	11.133	-20.93
10.	Tungsten carbide	Kerosene	15	50	9	Gr	Al	1.120	-0.984
11.	Tungsten carbide	Kerosene	15	50	9	Al_2O_3	Br	6.984	-16.88
12.	Tungsten carbide	Kerosene	15	50	9	Mix	Cu	1.673	-4.469
13.	Tungsten carbide	Kerosene	50	75	3	Gr	Al	0.598	4.466
14.	Tungsten carbide	Kerosene	50	75	3	Al_2O_3	Br	4.872	-13.75
15.	Tungsten carbide	Kerosene	50	75	3	Mix	Cu	0.470	6.558
16.	Tungsten carbide	Kerosene	100	10	6	Gr	Al	1.156	-1.259
17.	Tungsten carbide	Kerosene	100	10	6	Al_2O_3	Br	3.086	-9.787
18.	Tungsten carbide	Kerosene	100	10	6	Mix	Cu	0.587	4.627
19.	Tungsten carbide	Kerosene	15	75	6	Gr	Br	2.091	-6.407

20.	Tungsten carbide	Kerosene	15	75	6	Al_2O_3	Cu	1.829	-5.244
21.	Tungsten carbide	Kerosene	15	75	6	Mix	Al	0.815	1.776
22.	Tungsten carbide	Kerosene	50	10	9	Gr	Br	7.458	-17.45
23.	Tungsten carbide	Kerosene	50	10	9	Al_2O_3	Cu	1.251	-1.945
24.	Tungsten carbide	Kerosene	50	10	9	Mix	Al	1.665	-4.428
25.	Tungsten carbide	Kerosene	100	50	3	Gr	Br	4.154	-12.36
26.	Tungsten carbide	Kerosene	100	50	3	Al_2O_3	Cu	0.791	2.036
27.	Tungsten carbide	Kerosene	100	50	3	Mix	Al	1.214	-1.684

5.3 ANALYSIS OF VARIANCE – TWR

The Analysis of Variance (ANOVA) for the mean TWR at 95% confidence interval is given in Table 4.2.The results for TWR were analyzed using ANOVA for identifying the significant factors affecting the performance measures. The variance data for each factor were F tested to find the significance of each. The principle of the *F* test is that the larger the *F* value for a particular parameter, the greater the effect on the performance characteristic, due to the change in that process parameter. ANOVA Table 5.2 shows that Tool (F-91.19), Powder (F-8.65) and Current (F-6.48) are the factors that affect the TWR. There is one interaction **Powder × Tool** (F-8.20) is also significant and the remaining factors like Pulse-on, Pulse-off and the other interactions are insignificant. According to ANOVAs Table 5.2 Tool is the most significant factor which affects the TWR. TWR increases with increase in current from 3 Amps to 9 Amps and by changing the Tools. From Response Table, by using mixed powder we get higher TWR and minimum TWR is coming when we use Cu tool and

Graphite powder. Table 5.3 shows ranks to various factors like Tool and Powder are most significant and Pulse-on , Pulse-off are most insignificant factors.

Table 5.2: ANOVA for TWR

Sources	SS	V	V	F	F(Critical)	P	SS'	% of contribution	Status
Pulse-on ,A	1.196	2	0.598	0.65		0.571		0.75	Insignificant
Pulse-off, B	0.814	2	0.407	0.44		0.672		0.90	Insignificant
Current, C	11.983	2	5.991	6.48	5.14	0.056	8.94	3.65	Significant
Powder, D	15.984	2	7.992	8.65	5.14	0.035	12.94	5.28	Significant
Tool, E	168.562	2	84.280	91.19	5.14	0.001	165.52	67.54	Significant
Current × Powder	0.824	4	0.206	0.22		0.912		2.13	Insignificant
Current × Tool	11.689	4	2.922	3.16		0.145		2.29	Insignificant
Powder × Tool	30.299	4	7.574	8.20	5.14	0.033	24.22	9.88	Significant
Residual Error	3.697	4	0.924						
Total	245.048	26	9.424						
e-pooled	18.22	12	1.518				14.91	13.64	

Table 5.3: Response table for Means of TWR

Level	Pulse-on ,A	pulse-off, B	Current, C	Powder, D	Tool, E
1	2.6194	2.6962	2.3513	2.0998	0.9913
2	3.1179	3.0759	2.3679	2.4980	1.1374
3	2.7547	2.7199	3.7728	3.8942	6.3632
Delta	0.4984	0.3797	1.4214	1.7944	5.3719
Rank	**4**	**5**	**3**	**2**	**1**

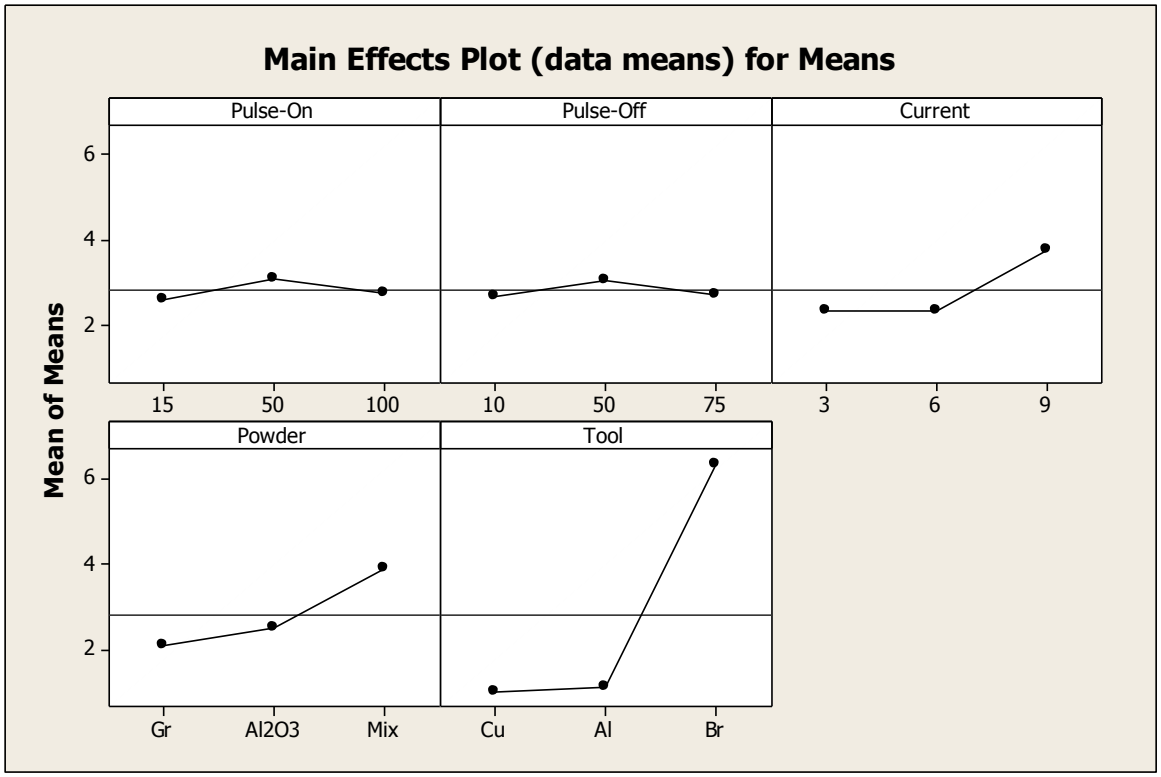

Figure 5.1: Main effects plot for TWR

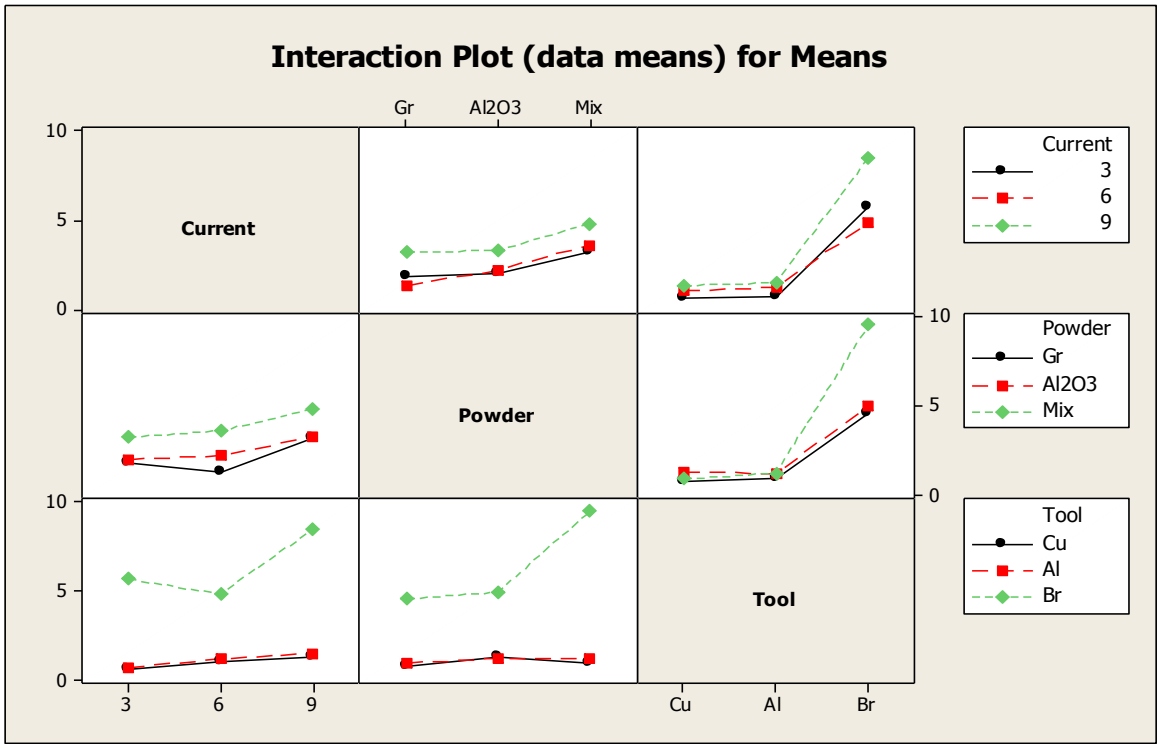

Figure 5.2: Interaction plot for TWR

5.4 ANOVA FOR S/N RATIO FOR TWR

The S/N ratio consolidates several repetitions into one value and is an indication of the amount of variation present. The S/N ratios have been calculated to identify the major contributing factors and interactions that cause variation in the TWR. TWR is 'Lower is better' type response which is given by:

$$S/N_{LB} = -10 \log (MSD) = -10 \log [(\frac{1}{r} \sum_{i=1}^{r} y^2 i) \quad \text{(Equation 5.2)}$$

$$\text{Where } MSD_{LB} = \frac{1}{r} \sum_{i=1}^{r} (y_j^2) \quad \text{(Equation 5.3)}$$

Table 5.4 shows the ANOVA for S/N ratio for TWR at 95% confidence interval and it shows that there are mainly two factors Tool [F-32.87] and Current [F-6.57] are significantly affect the TWR and the remaining all factors and interactions are insignificant. The main effects are shown in the following tables and figures:

Table 5.4: ANOVA for S/N of TWR

Sources	SS	V	V	F	F(Critical)	P	SS'	% contribution	Status
Pulse-on ,A	5.38	2	2.690	0.12		0.887		1.22	Insignificant
Pulse-off, B	24.34	2	12.170	0.56		0.611		0.31	Insignificant
Current, C	315.56	2	150.780	6.57	5.14	0.059	284.55	13.61	Significant
Powder, D	49.29	2	24.643	1.13		0.408		0.87	Insignificant
Tool, E	1433.56	2	716.782	32.87	5.14	0.003	1402.55	67.09	Significant
Current × Powder	35.31	4	8.827	0.40		0.799		1.27	Insignificant
Current × Tool	54.39	4	13.599	0.62		0.671		o.36	Insignificant
Powder × Tool	85.19	4	21.298	0.98		0.509		1.10	Insignificant
Residual Error	87.24	4	21.809						
Total	2090.26	26	80.394						
e-pooled	341.14	22	15.506				108.09	19.29	

Table 5.5 Response table for S/N ratio of TWR

Level	Pulse-on	pulse-off	Current	Powder	Tool
1	-4.1376	-3.9192	-2.1972	-2.9659	0.9862
2	-5.2044	-6.0708	-4.0642	-5.0131	-0.1838
3	-4.8784	-4.2304	-7.9590	-6.2414	-15.0228
Delta	1.0668	2.1516	5.7618	3.2755	16.0090
Rank	**5**	**4**	**2**	**3**	**1**

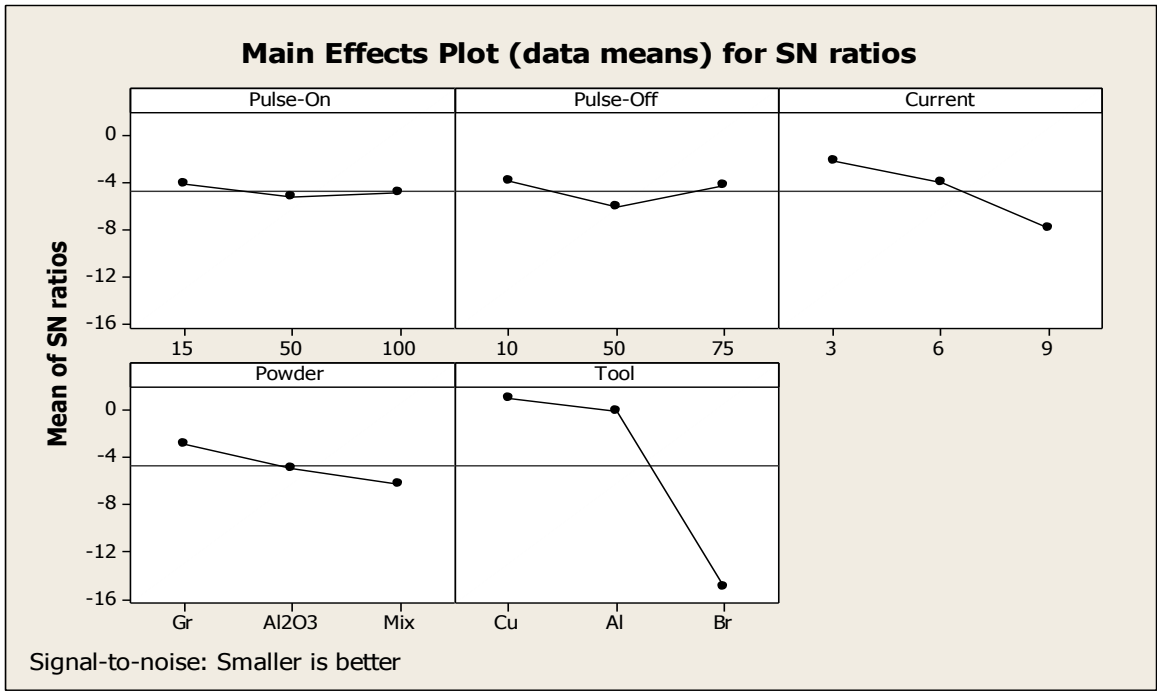

Figure 5.3 Main effects plot of TWR for S/N ratio

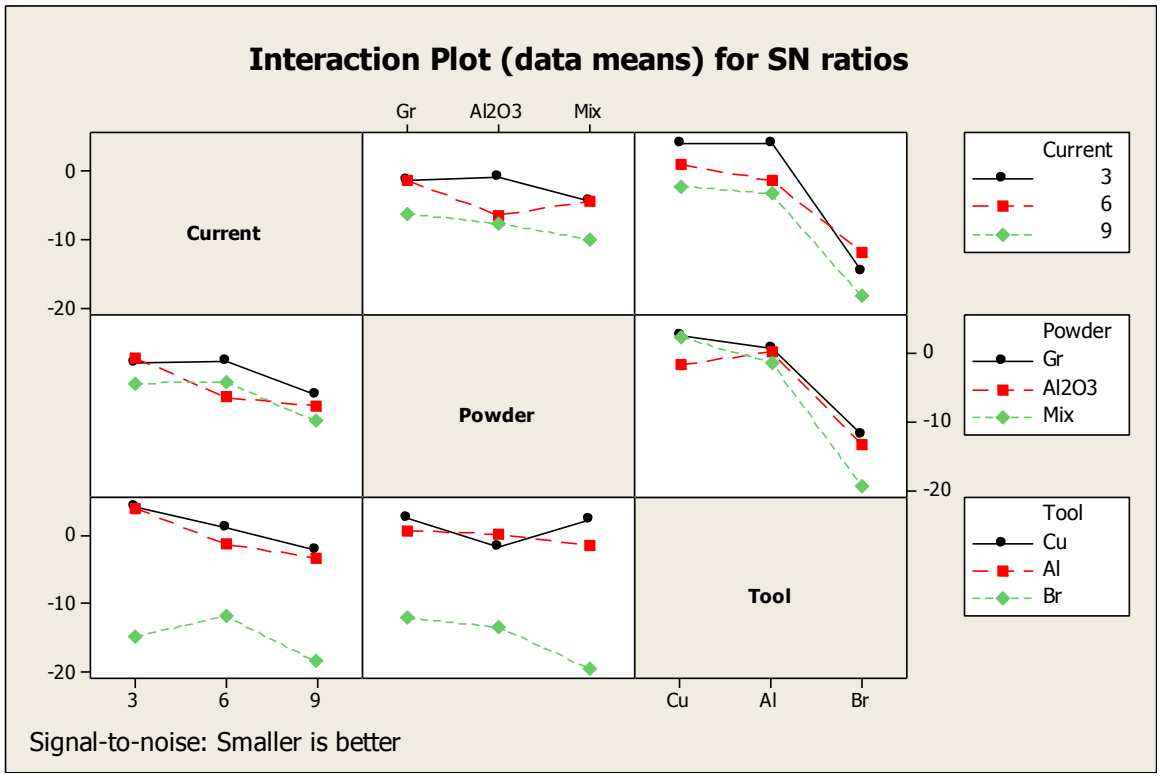

Figure 5.4 Interaction plot of TWR for S/N ratio

5.5 OPTIMAL DESIGN FOR TWR

In optimal design we have to choose a level from which the best result is obtained, here there is some confliction between the results that at which level the best result is obtained so the optimal design is obtained.

In this experimental analysis, the main effect plot in Figure 5.1 used to estimate the mean TWR. From the, Table 5.6 it is concluded that lowest TWR was observed when Tungsten carbide is machined by using Cu as a electrode, 3 Amps current with Gr powder mixed in the dielectric. One interaction **Powder × Tool** is also significant and give minimum TWR. In S/N ratio highest TWR was to be observed when workpiece is machined with Cu as a tool and at 3 Amps current. So by studying this table it is suggested that the best value of TWR is obtained when Tungsten carbide is machined at 3 Amps current with Cu as electrode and graphite powder mixed in the dielectric.

Table 5.6 Significant factors and interactions

Factor	Affecting mean		Affecting variation	
	Contribution Best level	**Best level**	**Contribution Best level**	**Best level**
Electrode, E	Significant	Level-1, Cu	Significant	Level-1, Cu
Pulse off, B	Insignificant		Insignificant	
Pulse on, A	Insignificant		Insignificant	
Current, C	Significant	Level-1, 3 Amps	Significant	Level-1, 3 Amps
Powder, D	Significant	Level-1, Gr	Insignificant	
Current × Powder	Insignificant		Insignificant	
Current × Tool	Insignificant		Insignificant	
Powder × Tool	Significant	D_1E_1	Insignificant	

Estimating the mean for TWR

The TWR is a lower average response is better (LB) characteristic. Depending on the characteristic, different treatment combinations has chosen to obtain satisfactory results. We get different results from the different combinations of the parameters. After conducting the experiments the optimum treatment condition within the experiments determined on the basis of prescribed combination of factor levels is determined to one of those in the experiment

Mean value for TWR

$$\mu_{D_1E_1E_1C_1D_1} = E_1D_1+E_1+C_1+D_1-3\bar{T}$$

$$= 6.363 + 0.9913 + 2.3513 + 2.0998 – 3\times3.214$$

$$= 6.363 + 0.9913 + 2.3513 + 2.0998 – 9.642$$

$$= 2.163 mm^3/min$$

Here, $\bar{T}$ = sum of means/ 27

Confidence Interval around the Estimated Mean

The confidence interval is a maximum and minimum value between which the true average should fall at some stated percentage of confidence. Confidence Interval around the estimated TWR mean

$$CI_1 = \sqrt{\frac{F_{\propto,v1,v2}\ Ve}{\eta_{eff}}}$$

Where $F_{\alpha v1,v2}$ =F ratio

α = risk (0.01) confidence= 1-α

v_1 = DOF for mean which is always =1

v_2 = DOF for error= V_e

V_e = Variance of e-pooled

n_{eff}= Number of tests under that condition using the participating factors

$$n_{eff} = \frac{N}{1+dof\ \ D1E1\ \ E1\ C1\ D1} = \frac{27}{1+2+2+2+4} = 2.45$$

$$CI_1 = \sqrt{\frac{F_{\propto,v1,v2}\ Ve}{\eta_{eff}}} = \sqrt{\frac{4.75\times 1.518}{2.45}} = 1.715$$

So the confidence interval around the TWR is given by 2.163 ± 1.715mm^3/min.

Chapter 6

RESULTS AND ANALYSIS OF MICRO HARDNESS

6.1 INTRODUCTION

The effects of parameters i.e. electrode, pulse on time, pulse off time, current and powder was evaluated using ANOVA and factorial design analysis. A confidence interval of 95% has been used for the analysis. Total 27 experiments were performed and each experiment performs only at once.

6.2 RESULTS FOR MICRO HARDNESS

The micro hardness measurement is dependent on the diameter of indentation on the samples. The indents formed in the pyramid shaped indenter were measured with Quantimet software using a load of 1 kg for 25 seconds. The results for micro hardness for each of the 27 treatment conditions with repetition are shown in Table 6.1.

Table 6.1: Results for micro hardness

Trial no.	Pulse-on Time, µs	Pulse-off Time, µs	Current Amps	Powder	Tool	Micro-Hardness-1	Micro-Hardness-2	MEAN	S/N ratio
1.	15	10	3	Gr	Cu	247.018	237.978	242.498	47.694
2.	15	10	3	Al_2O_3	Al	265.163	263.973	264.568	48.450
3.	15	10	3	Mix	Br	233.896	239.576	236.736	47.485
4.	50	50	6	Gr	Cu	274.486	336.720	305.603	49.703
5.	50	50	6	Al_2O_3	Al	341.631	341.141	341.386	50.668
6.	50	50	6	Mix	Br	346.758	393.315	370.037	51.364
7.	100	75	9	Gr	Cu	473.891	259.227	366.559	51.282
8.	100	75	9	Al_2O_3	Al	390.628	413.901	402.265	52.090
9.	100	75	9	Mix	Br	327.724	424.624	376.174	51.507
10.	15	50	9	Gr	Al	290.759	355.525	323.142	50.187

11.	15	50	9	Al_2O_3	Br	411.483	327.836	369.660	51.356
12.	15	50	9	Mix	Cu	211.441	237.712	224.475	47.023
13.	50	75	3	Gr	Al	170.425	260.039	232.618	47.332
14.	50	75	3	Al_2O_3	Br	165.427	252.638	195.128	44.461
15.	50	75	3	Mix	Cu	240.543	225.107	232.825	47.340
16.	100	10	6	Gr	Al	347.246	294.839	320.644	50.120
17.	100	10	6	Al_2O_3	Br	375.442	345.214	360.385	51.135
18.	100	10	6	Mix	Cu	315.674	505.334	410.487	52.266
19.	15	75	6	Gr	Br	250.961	237.788	244.367	47.760
20.	15	75	6	Al_2O_3	Cu	305.912	340.548	323.232	50.190
21.	15	75	6	Mix	Al	246.133	270.548	258.340	48.243
22.	50	10	9	Gr	Br	490.447	360.868	425.654	52.581
23.	50	10	9	Al_2O_3	Cu	372.676	252.825	312.760	49.904
24.	50	10	9	Mix	Al	355.897	240.537	298.217	49.490
25.	100	50	3	Gr	Br	306.991	327.857	317.207	50.026
26.	100	50	3	Al_2O_3	Cu	253.949	394.842	323.922	50.208
27.	100	50	3	Mix	Al	529.892	460.220	495.056	53.893

6.3 ANALYSIS OF VARIANCE - MICRO HARDNESS

In ANOVAs' table 6.2 shows that Pulse-on [F-24.22], Current [F-10.26], Pulse-off [F-6.17] are significantly affect the micro-hardness. Two interactions **Current × Powder** [F-5.65] **and Current × Tool** [F-6.36] are also significant. The other factors powder and tool are insignificant. Pulse-on is a most significant factor which affects the Micro-hardness. According to ANOVAs' response table, various ranks of parameters are shown in the table 6.3.Acc. to response table; powder and tool are the least significant factors.

Table 6.2: ANOVA for mean of Micro hardness

Sources	SS	V	V	F	F(Critical)	P	SS'	% of contribution	Status
Pulse-on ,A	47972	2	23985.9	24.22	5.14	0.006	45505.5	31.85	Significant
Pulse-off, B	12211	2	6105.7	6.17	5.14	0.060	9744.5	6.82	Significant
Current, C	20330	2	10165.2	10.26	5.14	0.027	17863.5	12.50	Significant
Powder, D	902	2	450.8	0.46		0.664		1.09	Insignificant
Tool, E	2149	2	1074.4	1.08		0.420		1.99	Insignificant
Current × Powder	22367	4	5591.8	5.65	5.14	0.061	17434	12.20	Significant
Current × Tool	25185	4	6296.4	6.36	5.14	0.050	20252	14.17	Significant
Powder × Tool	7787	4	1946.7	1.97		0.264			Insignificant
Residual Error	3961	4	990.3						
Total	142865	26	5494.807						
e-pooled	14799	12	1233.25				4736	22.46	

Table 6.3: Response table for means of micro hardness

Level	Pulse-on	pulse-off	Current	Powder	Tool
1	276.3	319.1	279.2	308.7	304.7
2	298.5	341.2	326.1	318.4	326.3
3	374.7	289.3	344.3	322.5	318.6
Delta	98.4	51.9	65.1	13.8	21.6
Rank	**1**	**3**	**2**	**5**	**4**

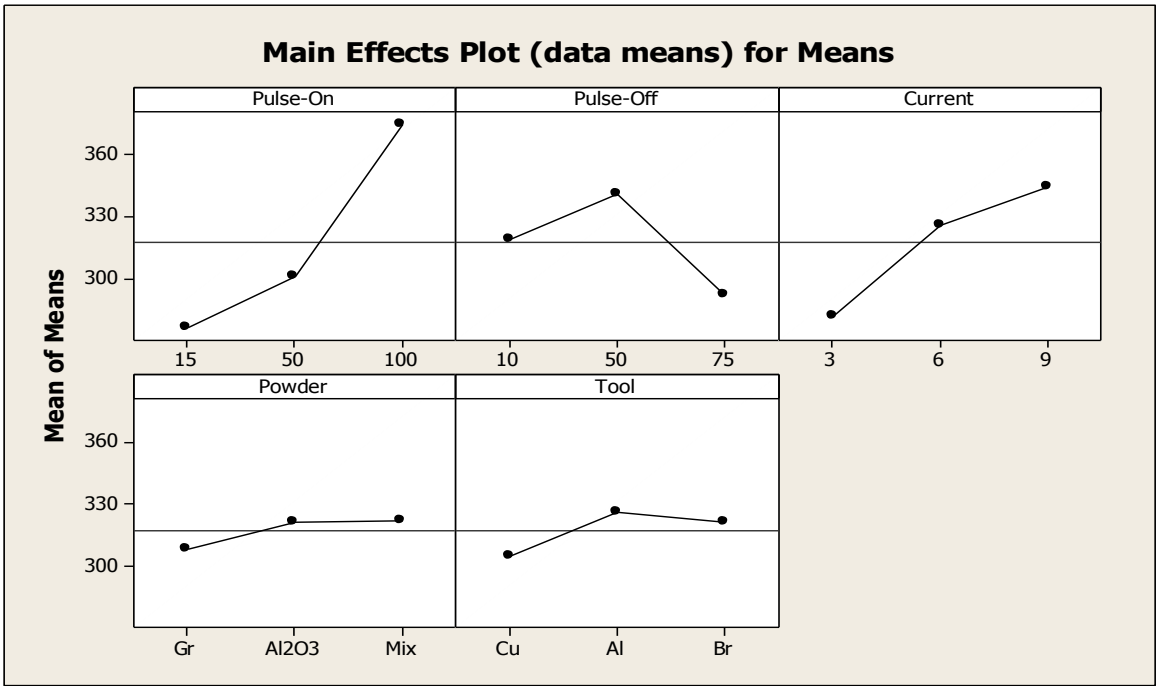

Figure 6.1: Main effect plot for micro hardness for mean

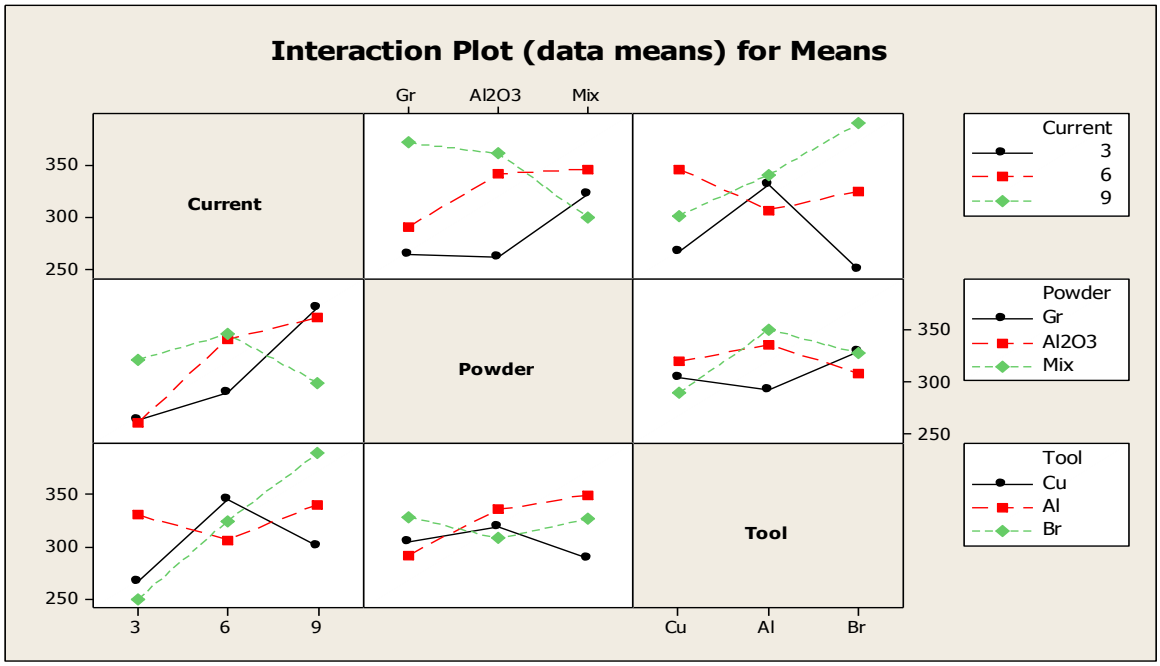

Figure 6.2: Interaction plot of means micro hardness

6.4 ANOVA FOR S/N RATIO OF MICROHARDNESS

MRR is "Higher is better" type response which is given by:

$$(S/N)HB = -10 \log (MSDHB) \qquad \text{(Equation ....6.1)}$$

$$\text{Where } MSD_{HB} = \frac{1}{r}\sum_{j=1}^{r}\frac{1}{y_j^2} \qquad \text{(Equation ....6.2)}$$

MSDHB = Mean Square Deviation for higher-the-better response.

Table 6.4 shows the ANOVA for S/N ratio for micro hardness at 95% confidence interval. In S/N Ratio's ANOVAs table, it has same result as above in mean ANOVAs table. But in S/N Ratios ANOVAs table all the three interactions are significant. Here also pulse-on is most affecting significant factor. Powder and Tool are least significant factors. Main effect plot and interaction plot of S/N ratio for micro hardness shown in the Figure 6.3 and Figure 6.4

Table 6.4: ANOVA of S/N ratio for micro hardness

Sources	SS	V	V	F	F(Critical)	P	SS'	% of contribution	Status
Pulse-on ,A	36.668	2	18.3338	55.82	5.14	0.001	35.946	31.09	Significant
Pulse-off, B	11.478	2	5.7392	17.47	5.14	0.011	10.756	9.30	Significant
Current, C	21.153	2	10.5766	32.20	5.14	0.003	20.431	17.67	Significant
Powder, D	0.255	2	0.1274	0.39		0.702		0.40	Insignificant
Tool, E	1.324	2	1.3245	2.02		0.248		0.52	Insignificant
Current × Powder	16.592	4	16.5923	12.63	5.14	0.015	15.148	13.10	Significant
Current × Tool	19.020	4	19.0199	14.48	5.14	0.012	17.576	15.20	Significant
Powder × Tool	7.789	4	7.7895	5.93	5.14	0.056	6.345	5.48	Significant
Residual Error	1.314	4	1.3137						
Total	115.594	26	4.445						
e-pooled	2.893	8	0.361				1.069	8.16	

Table 6.5: Response table for S/N ratios of micro hardness

Level	Pulse-on	pulse-off	Current	Powder	Tool
1	48.71	49.90	48.54	49.63	49.51
2	49.21	50.49	50.16	49.83	50.05
3	51.39	48.91	50.60	49.85	49.74
Delta	2.68	1.58	2.06	0.21	0.54
Rank	**1**	**3**	**2**	**5**	**4**

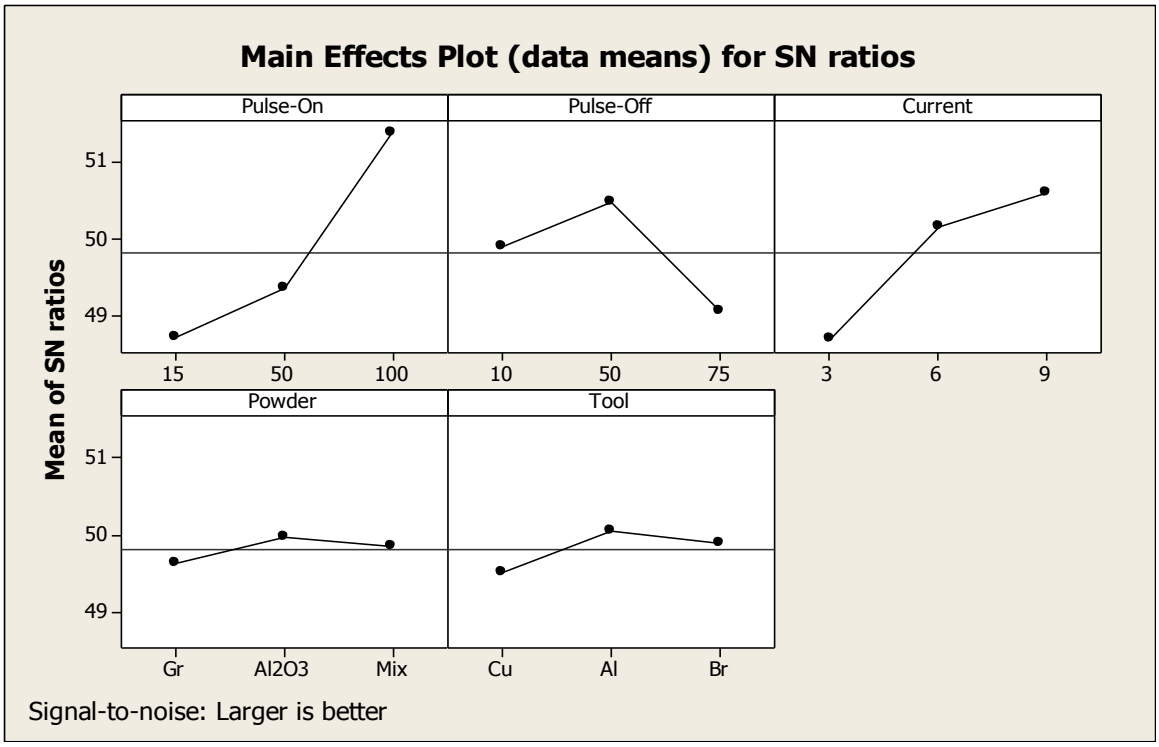

Figure 6.3: Main effects plot for S/N ratio of micro hardness

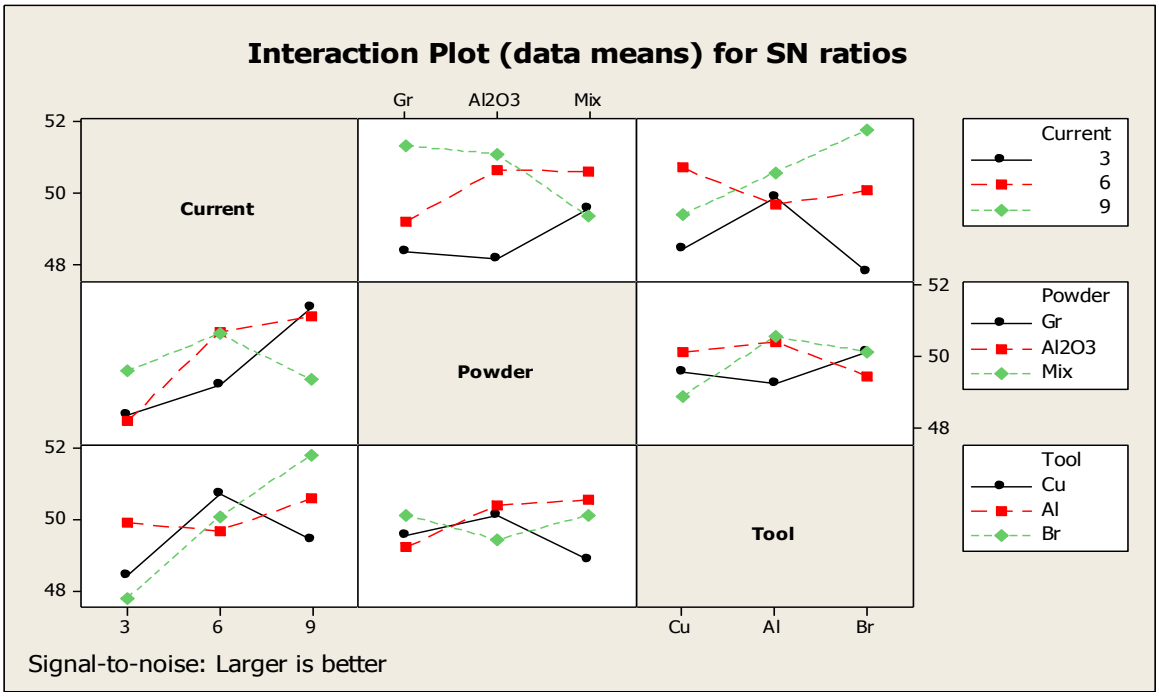

Figure 6.4: Interaction plot of S/N ratio for micro hardness

6.5 OPTIMAL DESIGN FOR MICRO HARDNESS

In this experimental analysis, the main effect plot and interaction plot in Figure 6.1 and Figure 6.2 used to estimate the mean micro hardness. From Table 6.6 it is concluded that highest micro hardness was observed that when the workpiece was machined at 9 Amps current, 50µs Pulse-off and at 100µs Pulse-on. In S/N ratio highest micro hardness was to be observed when workpiece material was machined with the same condition as in Means condition, 9 Amps current, 50µs Pulse-off and at 100µs Pulse-on and in this only one more interaction is significant than means. Table 6.6 shows the optimal design for micro-hardness.

Table 6.6: significant factors and their interactions

Factor	**Affecting mean**		**Affecting variation**	
	Contribution Best level	**Best level**	**Contribution Best level**	**Best level**
Electrode, E	Insignificant	-	Insignificant	-
Pulse off, B	Significant	Level-2, 50µs	Significant	Level-2, 50µs
Pulse on, A	Significant	Level-3, 100µs	Significant	Level-3, 100µs

Current, C	Significant	Level-3, 9 Amps	Significant	Level-3, 9 Amps
Powder, D	Insignificant	-	Insignificant	-
Current × Powder	Significant	C_3D_3	Significant	C_3D_3
Current × Tool	Significant	C_3E_2	Significant	C_3E_2
Powder × Tool	Insignificant	-	Significant	D_3E_2

Estimating the mean for Micro hardness

The micro hardness is a higher average response is better (HB) characteristic. Depending on the characteristic, different treatment combinations has chosen to obtain satisfactory results. We get different results from the different combinations of the parameters. After conducting the experiments the optimum treatment condition within the experiments determined on the basis of prescribed combination of factor levels is determined to one of those in the experiment

Mean value for Micro hardness

$$\mu_{C_3D_3\,C_3E_2\,D_3E_2\,A_3\,C_3\,B_2} = A_3 + B_2 + C_3 + C_3D_3 + C_3E_2 + D_3E_2 - 5\bar{T}$$

$$= 374.7 + 341.2 + 344.3 + 344.3 + 318.6 + 326.3 - 5\times 317.55$$

$$= 464.7 \text{ HVN}$$

Here, $\bar{T}$ = sum of means/ 27

Confidence Interval around the Estimated Mean

The confidence interval is a maximum and minimum value between which the true average should fall at some stated percentage of confidence. Confidence Interval around the estimated Micro hardness mean

$$CI_1 = \sqrt{\frac{F_{\propto,v1,v2}\ Ve}{\eta_{eff}}}$$

Where $F_{\alpha v1,v2}$ =F ratio

α = risk (0.01) confidence= 1-α

v_1 = DOF for mean which is always =1

v_2 = DOF for error= V_e

V_e = Variance of e-pooled

n_{eff}= Number of tests under that condition using the participating factors

$$n_{eff} = \frac{N}{1+dof_{C3D3\ C3E2\ D3E2\ A3\ C3\ B2}} = \frac{27}{1+2+2+2+4+4+4} = 1.42$$

$$CI_1 = \sqrt{\frac{F_{\propto,v1,v2}\ Ve}{\eta_{eff}}} = \sqrt{\frac{4.75 \times 1233.25}{1.42}} = 64.22$$

So the confidence interval around the Micro hardness is given by 464.7 ± 64.22 HVN

Chapter 7

RESULTS AND ANALYSIS OF SURFACE ROUGNESS

7.1 INTRODUCTION

The effects of parameters i.e. electrode, pulse on time, pulse off time, current and powder was evaluated using ANOVA and factorial design analysis. A confidence interval of 95% has been used for the analysis. Total 27 experiments were performed and each experiment performs only at once.

7.2 RESULTS FOR SURFACE ROUGNESS

Surface Roughness is measured from the centre of every sample and total 27 experiments are performed to measure the surface roughness of every sample and the following results are obtained:

Table 7.1: Results for surface roughness

Trial no.	Pulse-on Time, µs	Pulse-off Time, µs	Current (Amps)	Powder	Tool material	Roughness	S/N ratio
1.	15	10	3	Gr	Cu	1.65	-4.349
2.	15	10	3	Al_2O_3	Al	1.47	-3.346
3.	15	10	3	Mix	Br	2.58	-8.232
4.	50	50	6	Gr	Cu	2.24	-7.005
5.	50	50	6	Al_2O_3	Al	1.84	-5.296
6.	50	50	6	Mix	Br	2.89	-9.218
7.	100	75	9	Gr	Cu	6.42	-16.150
8.	100	75	9	Al_2O_3	Al	3.35	-10.500
9.	100	75	9	Mix	Br	5.24	-14.386
10.	15	50	9	Gr	Al	2.98	-9.484
11.	15	50	9	Al_2O_3	Br	1.97	-5.889
12.	15	50	9	Mix	Cu	3.14	-9.938
13.	50	75	3	Gr	Al	1.85	-5.343

14.	50	75	3	Al_2O_3	Br	3.09	-9.799
15.	50	75	3	Mix	Cu	2.25	-7.043
16.	100	10	6	Gr	Al	2.18	-6.769
17.	100	10	6	Al_2O_3	Br	3.27	-10.290
18.	100	10	6	Mix	Cu	2.97	-9.455
19.	15	75	6	Gr	Br	3.29	-10.343
20.	15	75	6	Al_2O_3	Cu	3.11	-9.855
21.	15	75	6	Mix	Al	2.91	-9.277
22.	50	10	9	Gr	Br	2.42	-7.676
23.	50	10	9	Al_2O_3	Cu	1.86	-5.390
24.	50	10	9	Mix	Al	2.84	-9.066
25.	100	50	3	Gr	Br	2.63	-8.399
26.	100	50	3	Al_2O_3	Cu	1.75	-4.860
27.	100	50	3	Mix	Al	3.94	-11.909

7.3 ANALYSIS OF VARIANCE - SURFACE ROUGHNESS

Results of Surface roughness's were analyzed by using ANOVA for identifying the factors which affect the performance and we can check that which factor is significant or not. ANOVA for the mean surface roughness at 95% confidence interval is given in Table 7.2.In this ANOVAs' table Pulse-on [F-19.93], Pulse-off [F-18.69], Current [F-13.14] and Powder [F-7.95] are significant factors and affect the surface roughness. Remaining all factors and interactions are insignificant in nature. According to Response table Table 7.3 for means pulse-on is the most significant factor. Tool is least significant factor which affects the surface roughness. Surface roughness increases with increase in Pulse-off [10µs-75µs] and Current [3amps-9amps].

Table 7.2 ANOVA for Means of the Roughness

	SS	V	V	F	F(Critical)	P	SS'	% of contribution	Status
Pulse-on ,A	6.9539	2	3.4770	19.93	5.14	0.008	5.903	19.48	Significant
Pulse-off, B	6.5241	2	3.2620	18.69	5.14	0.009	5.474	18.06	Significant
Current, C	4.5863	2	2.2932	13.14	5.14	0.017	3.536	11.67	Significant
Powder, D	2.7746	2	1.3873	7.95	5.14	0.040	1.724	5.69	Significant
Tool, E	0.8978	2	0.4489	2.57		0.191		0.50	Insignificant
Current × Powder	3.1088	4	0.7772	4.45		0.089		3.32	Insignificant
Current × Tool	2.2948	4	0.5737	3.29		0.138		0.64	Insignificant
Powder × Tool	2.4640	4	0.6160	3.53		0.125		1.20	Insignificant
Residual Error	0.6979	4	0.1745						
Total	30.3023	26	1.1654						
e-pooled	9.4633	18	0.525				1.719	44.56	

Table 7.3 Response table for means for Roughness

Level	Pulse-on	pulse-off	Current	Powder	Tool
1	2.567	2.360	2.357	2.851	2.821
2	2.364	2.598	2.744	2.412	2.596
3	3.528	3.501	3.358	3.196	3.042
Delta	1.163	1.141	1.001	0.783	0.447
Rank	**1**	**2**	**3**	**4**	**5**

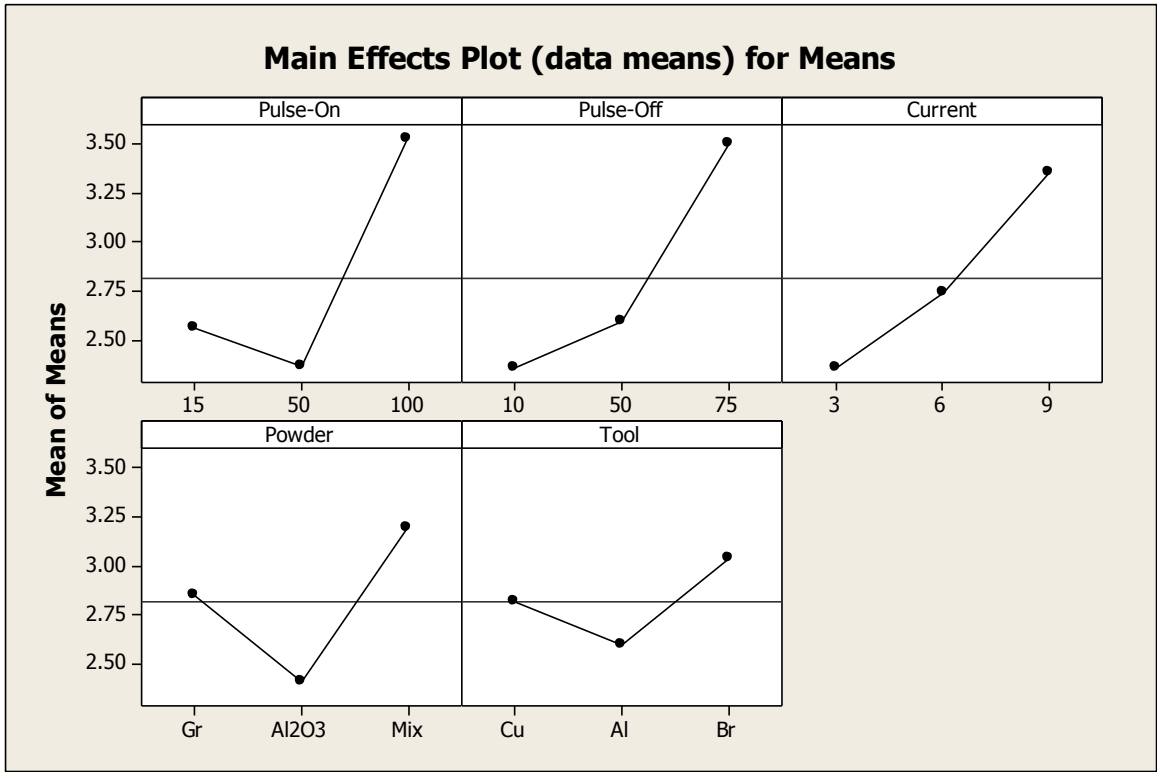

Figure 7.1: Main effects plot for surface roughness

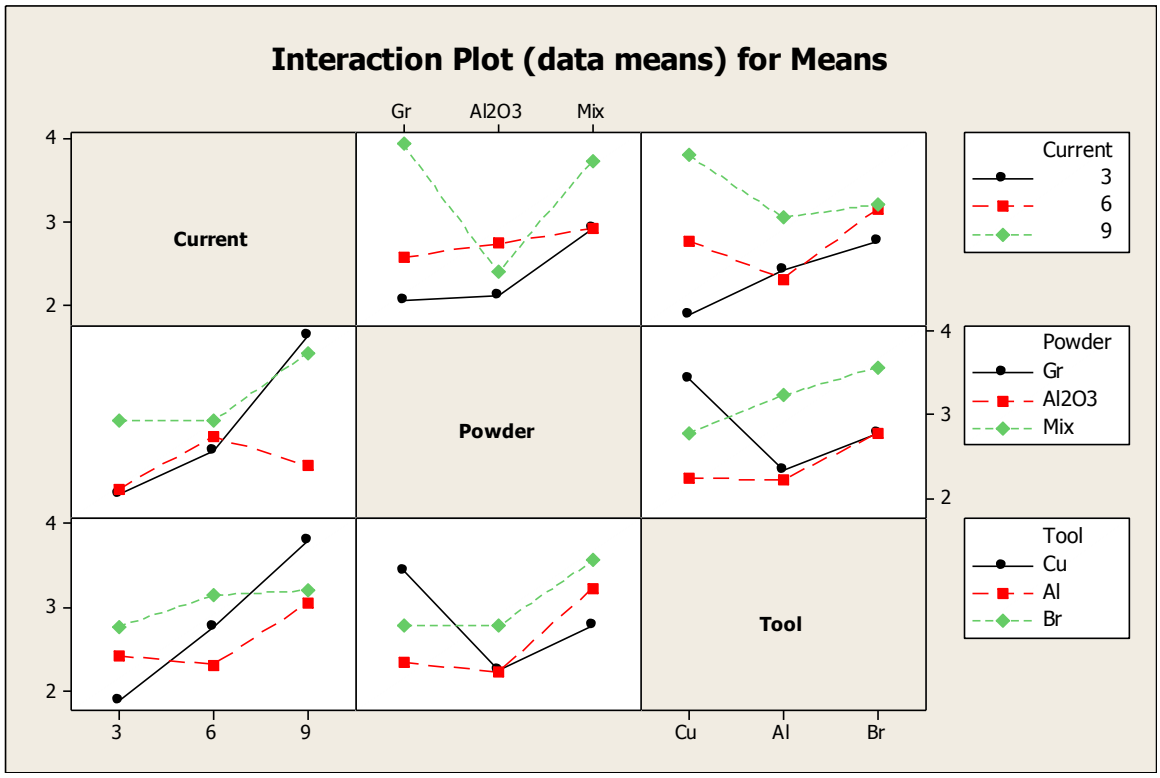

Figure 7.2: Interaction plot surface roughness

7.4 ANOVA FOR S/N RATIO FOR ROUGHNESS

The S/N ratio consolidates several repetitions into one value and is an indication of the amount of variation present. The S/N ratios have been calculated to identify the major contributing factors and interactions that cause variation in the Surface roughness. Surface roughness is 'Lower is better' type response which is given by:

$$S/N_{LB} = -10 \log (MSD) = -10 \log [(\frac{1}{r} \sum_{i=1}^{r} y^2 i) \quad \text{(Equation 7.1)}$$

$$\text{Where } MSD_{LB} = \frac{1}{r} \sum_{i=1}^{r} (y_j^2) \quad \text{(Equation 7.2)}$$

Table 5.4 shows the ANOVA for S/N ratio for roughness at 95% confidence interval and it shows that there are mainly 4 factors, pulse-off, pulse-on, current and powder are significantly affect the roughness whereas tools and all interactions are insignificant.

Table 7.4 ANOVA for S/N ratio of Roughness

	SS	V	V	F	F(Critical)	P	SS'	% of contribution	Status
Pulse-on ,A	45.587	2	22.793	17.60	5.14	0.010	39.073	17.27	Significant
Pulse-off, B	47.209	2	23.604	18.23	5.14	0.010	40.69	17.99	Significant
Current, C	35.473	2	17.737	13.70	5.14	0.016	28.95	12.80	Significant
Powder, D	30.295	2	15.148	11.70	5.14	0.021	23.78	10.51	Significant
Tool, E	10.683	2	5.341	4.13		0.107		1.84	Insignificant
Current × Powder	20.538	4	5.134	3.97		0.105		3.32	Insignificant
Current × Tool	21.055	4	5.264	4.07		0.102		3.55	Insignificant
Powder × Tool	10.176	4	2.544	1.96		0.265		0.94	Insignificant
Residual Error	5.179	4	1.295						
Total	226.194	26	8.699						
e-pooled	58.628	18	3.257				21.855	41.43	

Table 7.5 Response table for S/N ratio of Roughness

Level	Pulse-on	pulse-off	Current	Powder	Tool
1	-7.858	-7.175	-7.032	-8.391	-8.228
2	-7.315	-8.000	-8.612	-7.248	-7.888
3	-10.303	-10.300	-9.831	-9.837	-9.360
Delta	2.987	3.125	2.800	2.589	1.471
Rank	**2**	**1**	**3**	**4**	**5**

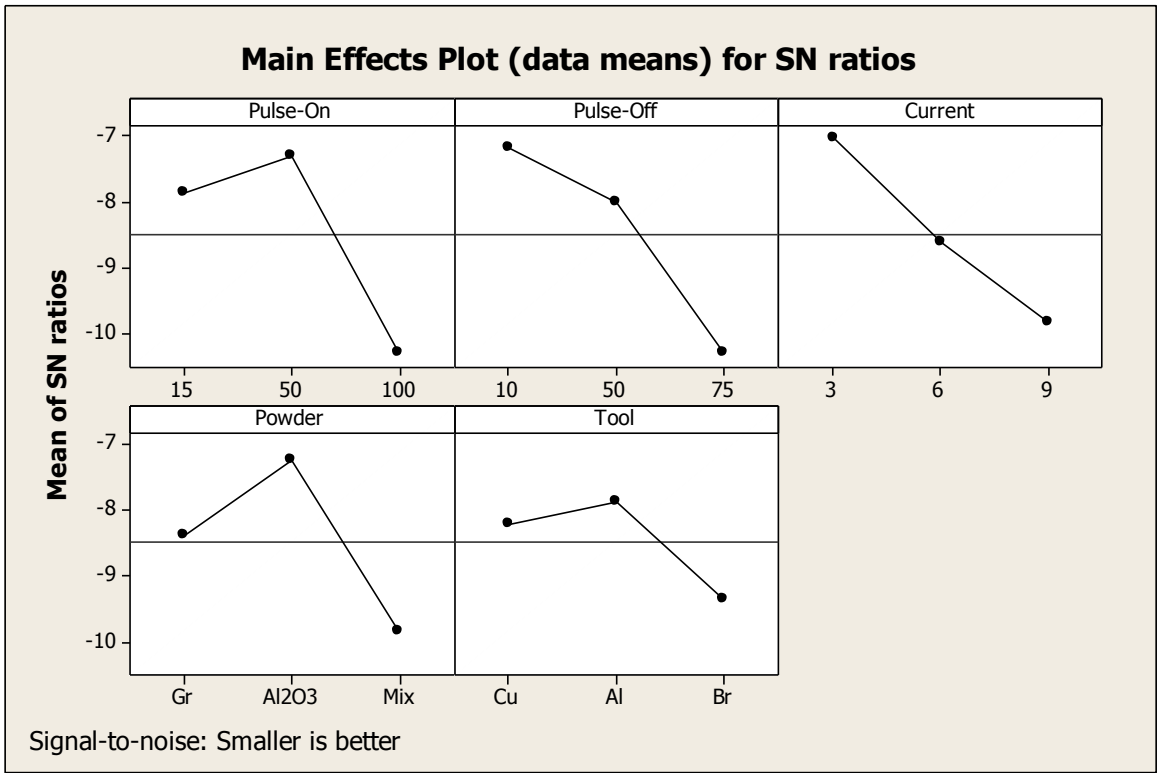

Figure 7.3 Main effects plot for S/N ratio of surface roughness

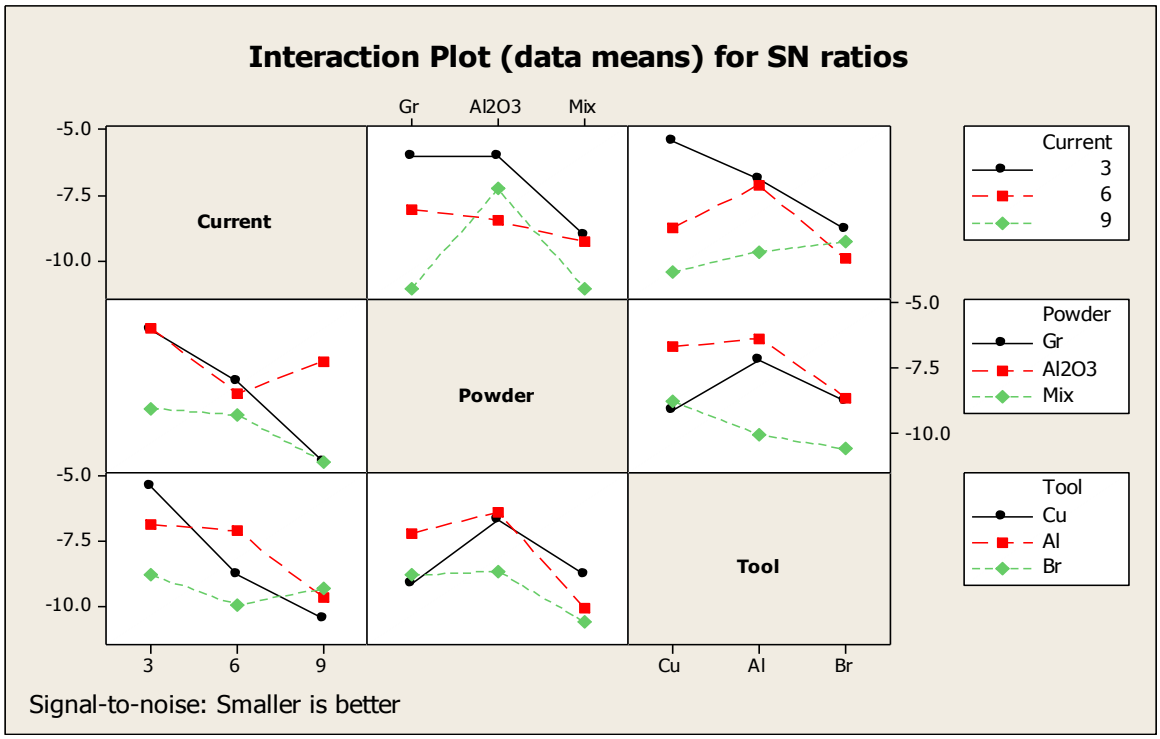

Figure 7.4 Interaction plot for of S/N ratio for roughness

7.5 OPTIMAL DESIGN FOR SURFACE ROUGHNESS

In this experimental analysis, the main effect plot and interaction plot in Figure 7.1 and Figure 7.2 used to estimate the mean surface roughness. From the, Table 7.6, It was concluded that lowest roughness value was to be observed when Tungsten carbide was machined at 3 Amps current, 50µs Pulse-off, 10µs Pulse-on and with addition of aluminium oxide powder mixed in the dielectric. In case of SN ratio, design is same as in case of means. So the best design was to be suggested that when Tungsten carbide was machined at 3 Amps current, 50µs Pulse-off, 10µs Pulse-on and with addition of aluminium oxide powder mixed in the dielectric.

Table 7.6: Significant factors and interactions

Factor	**Affecting mean**		**Affecting variation**	
	Contribution Best level	**Best level**	**Contribution Best level**	**Best level**
Electrode, E	Insignificant	-	Insignificant	-
Pulse off, B	Significant	Level-1, 50µs	Significant	Level-1, 50µs

Pulse on, A	Significant	Level-2, 10µs	Significant	Level-2, 10µs
Current, C	Significant	Level-1, 3 Amps	Significant	Level-1, 3 Amps
Powder, D	Significant	Level-2, Al_2O_3	Significant	Level-2, Al_2O_3
Current × Powder	Insignificant	-	Insignificant	-
Current × Tool	Insignificant	-	Insignificant	-
Powder × Tool	Insignificant	-	Insignificant	-

Estimating the mean for Surface Roughness

The surface roughness is a lower average response is best (LB) characteristic. Depending on the characteristic, different treatment combinations has chosen to obtain satisfactory results. We get different results from the different combinations of the parameters. After conducting the experiments the optimum treatment condition within the experiments determined on the basis of prescribed combination of factor levels is determined to one of those in the experiment

Mean value for roughness

$$\mu_{B_2 A_1 C_1 D_2} = B_2 + A_1 + C_1 + D_2 - 3\bar{T}$$

$$= 2.360 + 2.364 + 2.357 + 2.412 - 3\times 2.819$$

$$= 9.493 - 8.458$$

$$= 1.035 \text{ micron}$$

Here, $\bar{T}$ = sum of means/ 27

Confidence Interval around the Estimated Mean

The confidence interval is a maximum and minimum value between which the true average should fall at some stated percentage of confidence. Confidence Interval around the estimated roughness mean

$$CI_1 = \sqrt{\frac{F_{\propto,v1,v2}\ Ve}{\eta_{eff}}}$$

Where $F_{\alpha v1,v2}$ =F ratio

α = risk (0.01) confidence= 1-α

v_1 = dof for mean which is always =1

v_2 = dof for error= V_e

V_e = Variance of e-pooled

n_{eff}= Number of tests under that condition using the participating factors

$$n_{eff} = \frac{N}{1+dof_{B2\ A1\ C1\ D2}} = \frac{27}{1+2+2+2+2} = 3$$

$$CI_1 = \sqrt{\frac{F_{\propto,v1,v2}\ Ve}{\eta_{eff}}} = \sqrt{\frac{4.41 \times 0.525}{3}} = 0.878$$

So the confidence interval around the Surface Roughness is given by 1.035 ± 0.878 Microns

CHAPTER 8

REGRESSION ANALYSIS

8.1. Introduction

In **regression analysis** includes many techniques for modelling and analyzing several variables, when the focus is on the relationship between a dependent variable and one or more independent variables. More specifically, regression analysis helps one understand how the typical value of the dependent variable changes when any one of the independent variables is varied, while the other independent variables are held fixed. Most commonly, regression analysis estimates the conditional expectation of the dependent variable given the independent variables — that is, the average value of the dependent variable when the independent variables are fixed. Less commonly, the focus is on a quantile, or other location parameter of the conditional distribution of the dependent variable given the independent variables. In all cases, the estimation target is a function of the independent variables called the **regression function**. In regression analysis, it is also of interest to characterize the variation of the dependent variable around the regression function, which can be described by a probability distribution.

Regression analysis is widely used for prediction and forecasting, where its use has substantial overlap with the field of machine learning. Regression analysis is also used to understand which among the independent variables are related to the dependent variable, and to explore the forms of these relationships. In restricted circumstances, regression analysis can be used to infer causal relationships between the independent and dependent variables. However this can lead to illusions or false relationships, so caution is advisable. A large body of techniques for carrying out regression analysis has been developed. Familiar methods such as linear regression and ordinary least squares regression are parametric, in that the regression function is defined in terms of a finite number of unknown parameters that are estimated from the data. Nonparametric regression refers to techniques that allow the regression function to lie in a specified set of functions, which may be infinite-dimensional.

The performance of regression analysis methods in practice depends on the form of the data generating process, and how it relates to the regression approach being used. Since the true form of the data-generating process is generally not known, regression analysis often depends to some extent on making assumptions about this process. These assumptions are sometimes testable if a large amount of data is available. Regression models for prediction are often useful even when the assumptions are moderately violated, although they may not perform optimally. However, in many applications, especially with small effects or questions of causality based on observational data, regression methods give misleading results.

A statistical technique used to explain or predict the behaviour of a dependent variable. Generally, a regression equation takes the form of

$$Y= a + bx +c \qquad \text{(Equation no..... 8.1)}$$

Where Y is the dependent variable that the equation tries to predict, X is the independent variable that is being used to predict Y, a is the Y-intercept of the line, and c is a value called the regression residual. The values of a and b are selected so that the square of the regression residuals is minimized.

8.2. Results by Regression of Analysis

8.2.1. Results of Regression of Analysis for the MRR

The equation comes through regression analysis for MRR is:

The regression equation is

MRR = 0.414 - 0.0141 A + 0.158 B - 0.0499 C - 0.0401 D - 0.0156 E (Equation no.....8.2)

The value of R-Sq = 64.3%

8.2.2. Results of Regression of Analysis for the TWR

The equation comes through regression analysis for TWR is:

The regression equation is

TWR = - 9.13 - 0.122 A + 1.28 B + 1.08 C + 3.87 D + 0.203 E (Equation no.....8.3)

The value of R-Sq = 73.9%

8.2.3. Results of Regression of Analysis for the Micro hardness

The equation comes through regression analysis for Micro hardness is:

The regression equation is:

Micro hardness = - 1.30 + 0.284 A + 0.901 B + 0.571 C - 0.085 D + 0.315 E (Equation no.....8.4)

The value of R-Sq = 51.3%

8.2.4. Results of Regression of Analysis for the Surface roughness

The equation comes through regression analysis for Surface roughness is:

The regression equation is:

R = - 1.15 + 0.355 A + 0.816 B + 0.744 C - 0.143 D + 0.228 E (Equation no.....8.5)

The value of R-Sq = 59.3%

Chapter 9

MICROSTRUCTURE AND COMPOSITION ANALYSIS

9.1 Introduction

The effect of various input parameters i.e. current, pulse on time, pulse off time, electrode material, powder on the surface properties of the workpiece material has been discussed in this chapter. In the EDM process, the estimated discharge point temperature is thousands degrees (◦C) in order to rapidly melt machined material at this charge point. The locally generated high-temperature sparks cause the surrounding dielectric fluid to evaporate rapidly and its volume to expand. The high pressure generated by this inertial enclosure effect quickly removes molten metal from the surface of machined material. But, the molten metal on the surface of machined materials are not completely flushed away with the surrounding dielectric fluid during this process. The residual molten material re-solidifies on the machined surface to form a rapidly solidified layer. Thus the rapidly solidified layer produces a huge change in both the surface topography and surface metallurgy of machined material. The state of sub surface characteristics occurs in the rapidly solidified layer and is generally in the form of micro cracks, spalling, change in hardness, residual stress, metallurgical transformations, and heat affected zones (HAZ). The rapidly solidified layer also has different micro-structural and metallographic characteristic than the base material [38]. Therefore in this chapter change in micro-structure is studied with the help of Scanning Electron Microscope (SEM) and composition is checked by Energy Dispersion Spectroscopy (EDS).The 4 samples of Tungsten carbide, 3 samples are get machined from out of 4 samples and 1 sample is of parent metal and on these samples both Scanning Electron Microscope (SEM) and Energy Dispersion Spectroscopy (EDS) are analysed.

9.2 Microstructure Analysis

Microstructure analysis was carried out on some selected samples using Scanning Electron Microscope to study the change in the microstructure after machining. The 4 samples of Tungsten carbide, 3 samples are get machined from out of 4 samples and 1 sample is of parent metal and on these samples both Scanning Electron Microscope (SEM). The samples

were prepared as per standard before SEM analysis on three different magnifications, namely, 50×, 100×, 250× and 500×

9.3.1 Method of Sample Preparation for SEM

The steps for the sample preparation for SEM are given below:

1) Cut out the samples in 19×20 mm on wire cut EDM.

2) Clean the surface with wire brush.

3) Clean the samples with acetone.

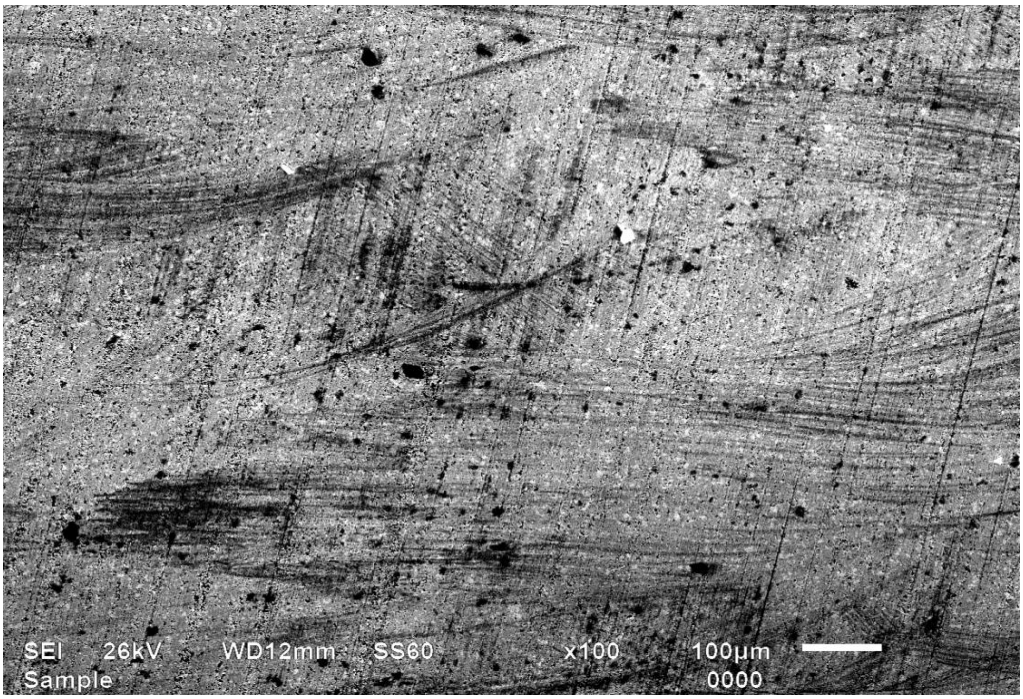

Figure9.1 Tungsten Carbide before Machining

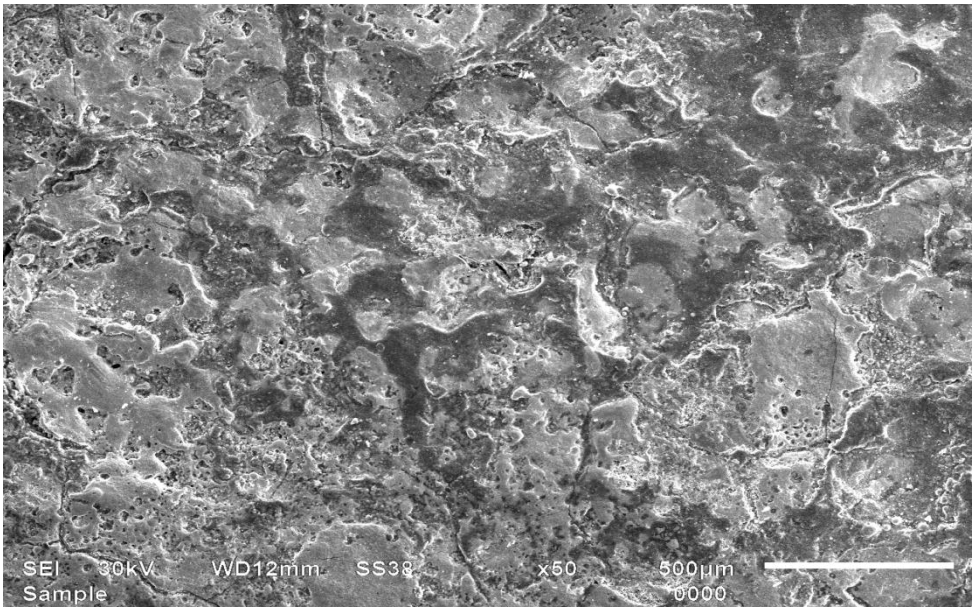

Figure 9.2: SEM micrograph at 50× of Tungsten Carbide machined with Cu electrode with Graphite mixing in kerosene oil (I 6Amp, pulse on time 50µs, pulse off time 50µs)

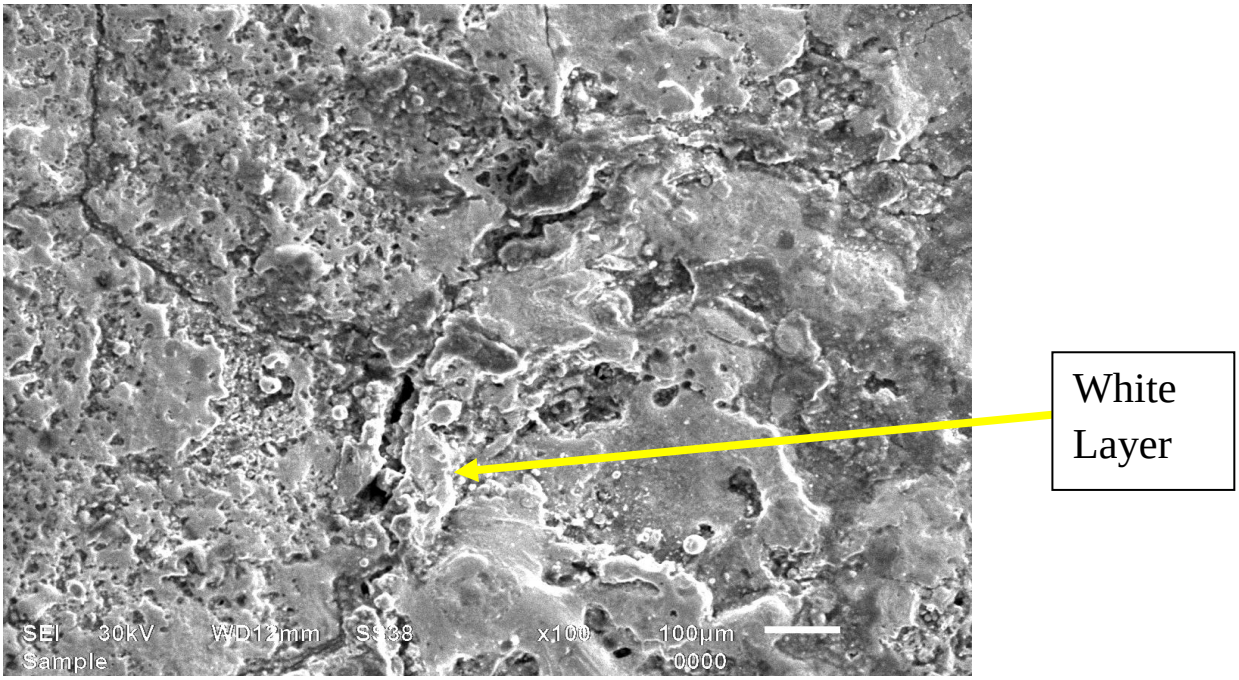

Figure 9.3: SEM micrograph at 100× of Tungsten Carbide machined with Cu electrode with Graphite mixing in kerosene oil (I 6Amp, pulse on time 50µs, pulse off time 50µs)

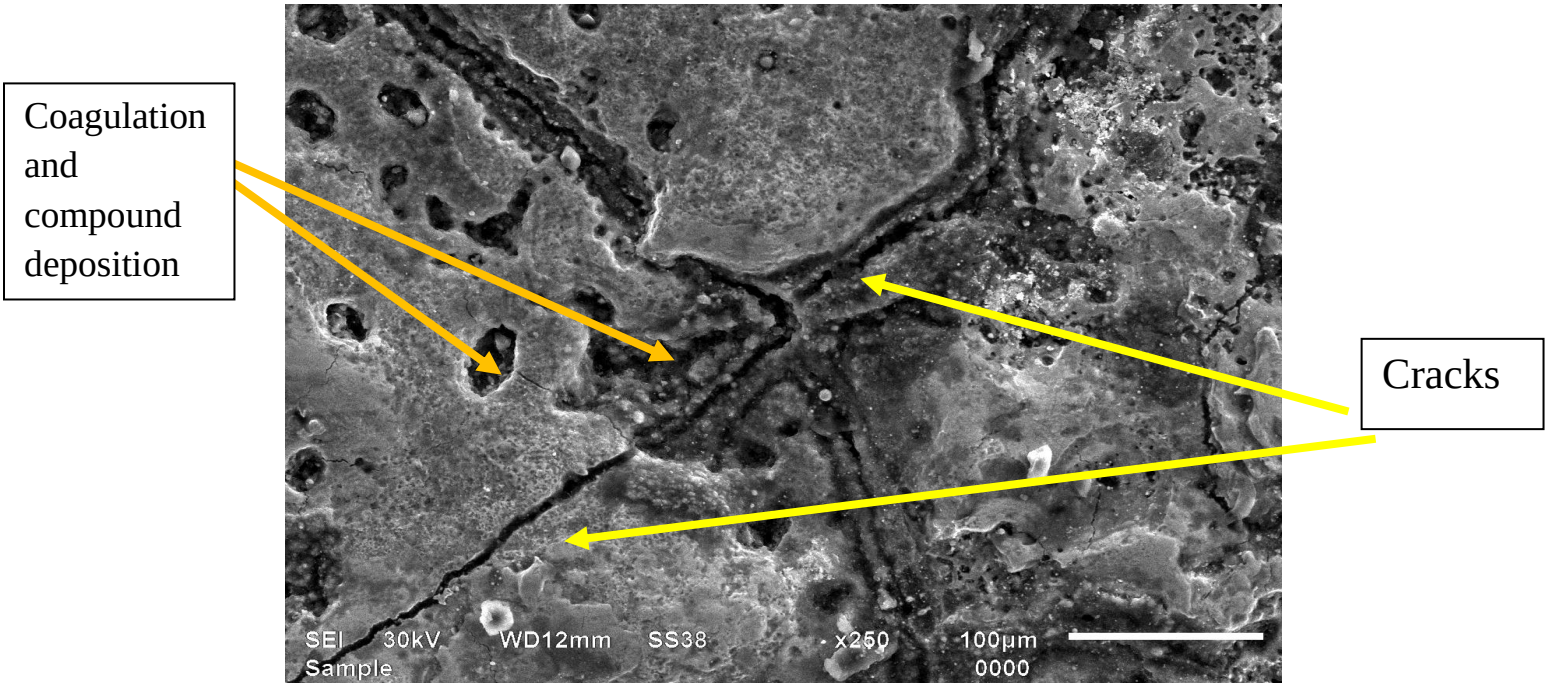

Figure 9.4: SEM micrograph at 250× of Tungsten Carbide machined with Cu electrode with Graphite mixing in kerosene oil (I 6Amp, pulse on time 50µs, pulse off time 50µs)

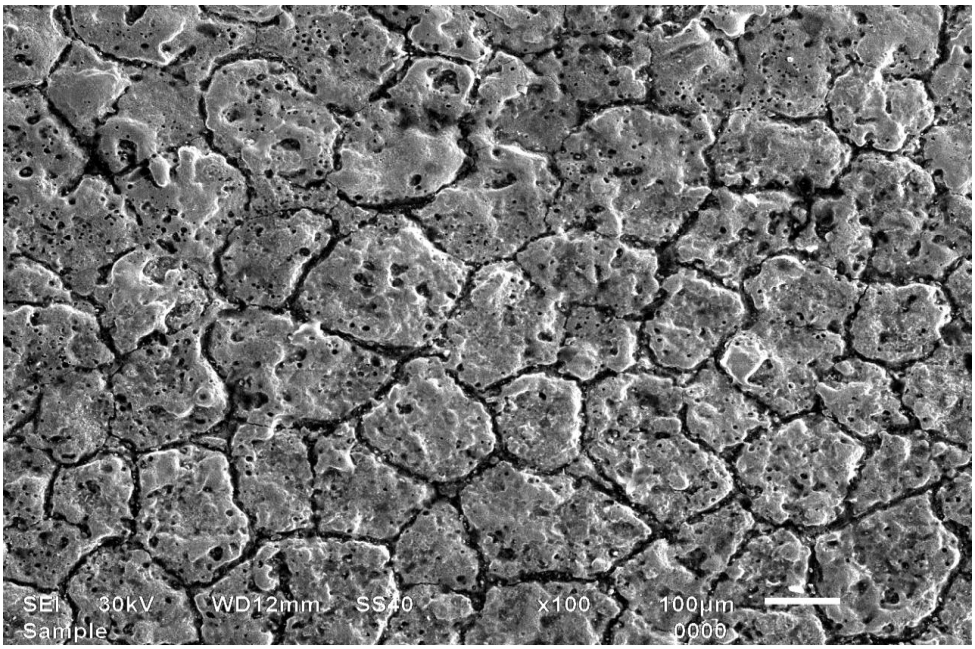

Figure 9.5: SEM micrograph at 100× of Tungsten Carbide machined with Br electrode with mixed powder mixing in kerosene oil (I 6Amp, pulse on time 100µs, pulse off time 10µs)

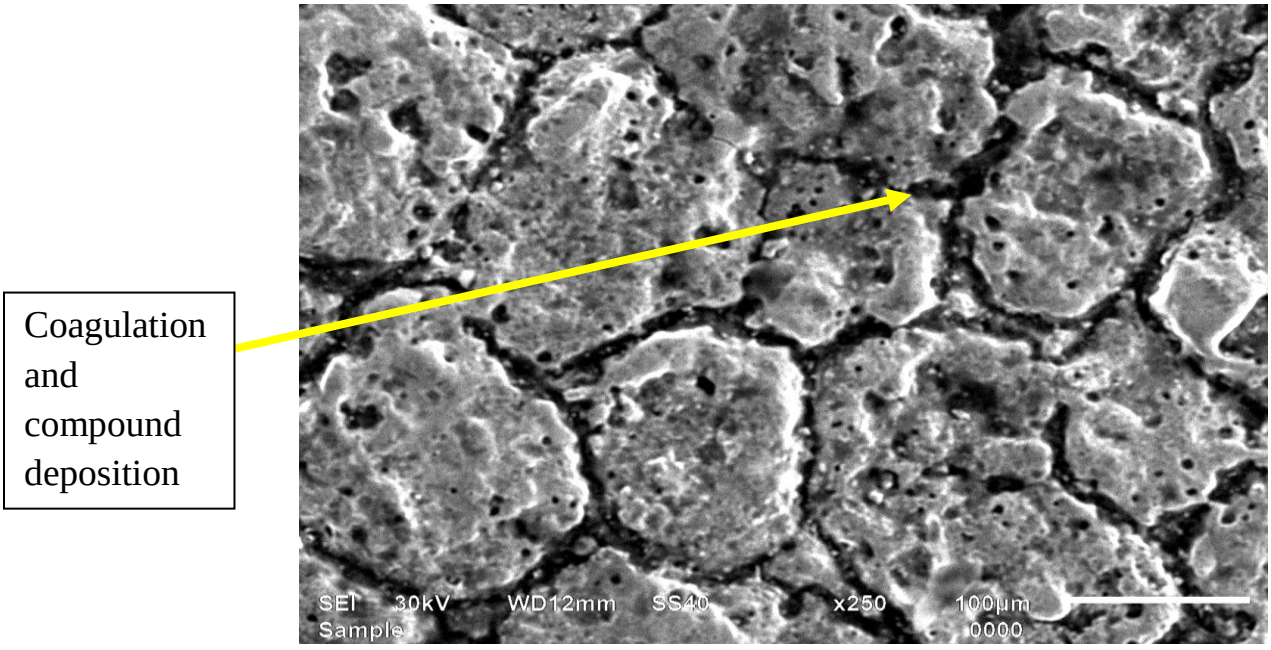

Figure 9.6: SEM micrograph at 250× of Tungsten Carbide machined with Br electrode with mixed powder mixing in kerosene oil (I 6Amp, pulse on time 100µs, pulse off time 10µs)

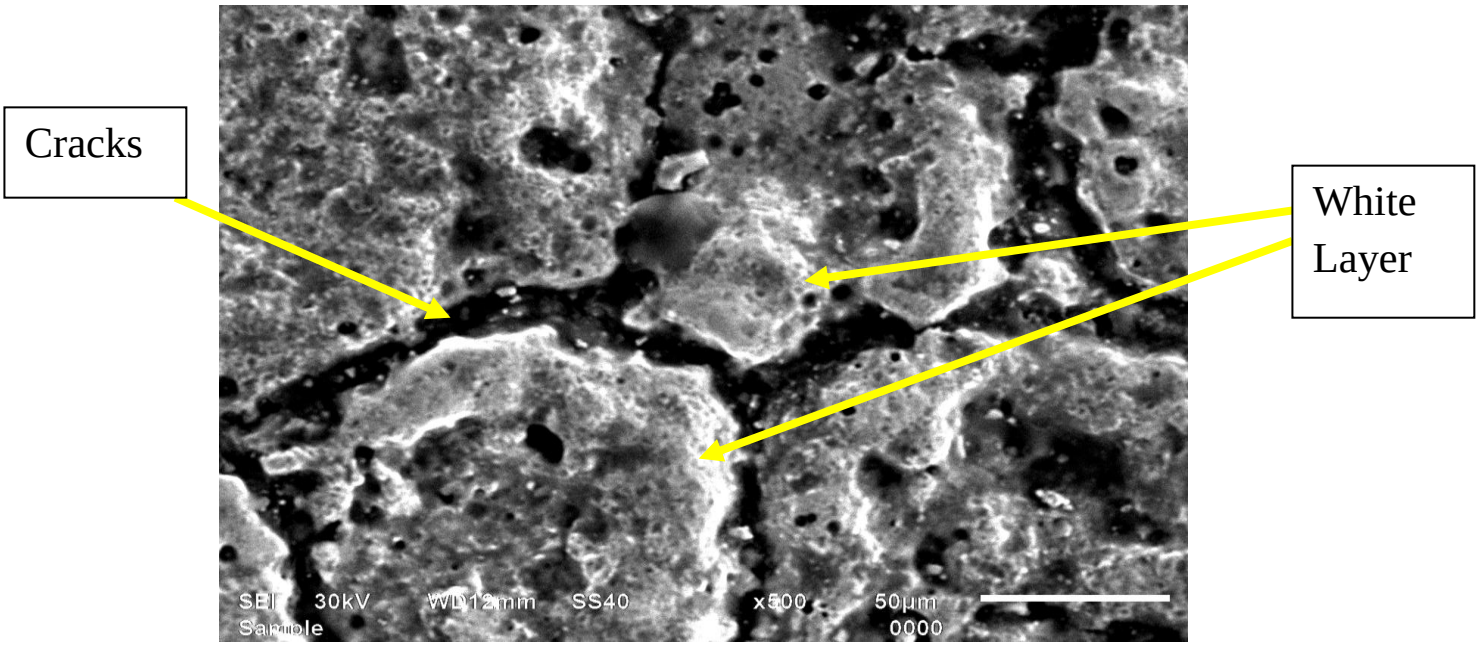

Figure 9.7: SEM micrograph at 500× of Tungsten Carbide machined with Br electrode with Mixed powder mixing in kerosene oil (I 6Amp, pulse on time 100µs, pulse off time 10µs)

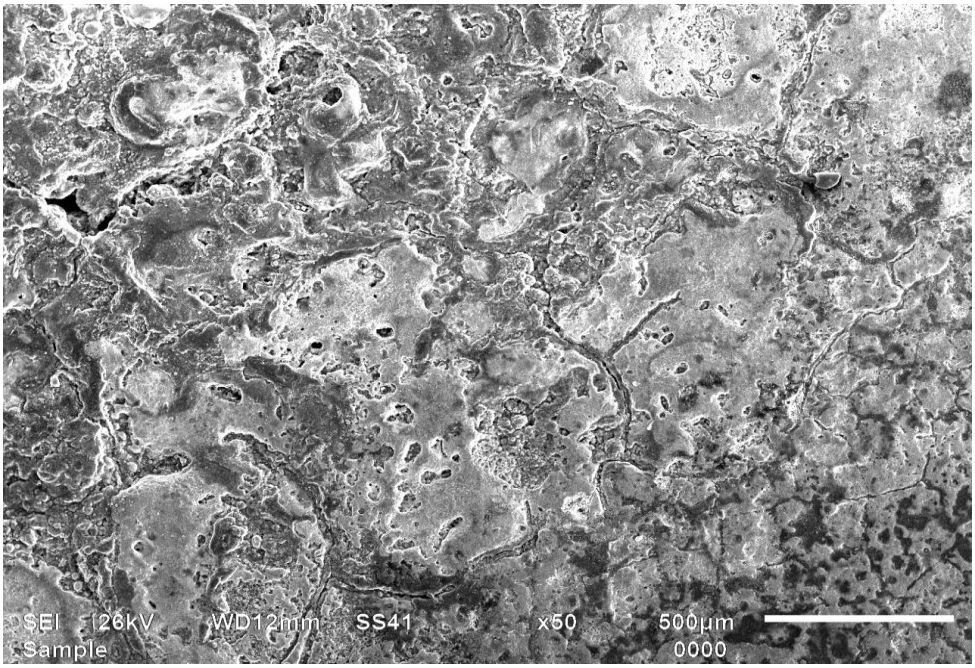

Figure 9.8: SEM micrograph at 50× of Tungsten Carbide machined with Al electrode with Aluminium oxide powder mixing in kerosene oil (I 9Amp, pulse on time 100µs, pulse off time 10µs)

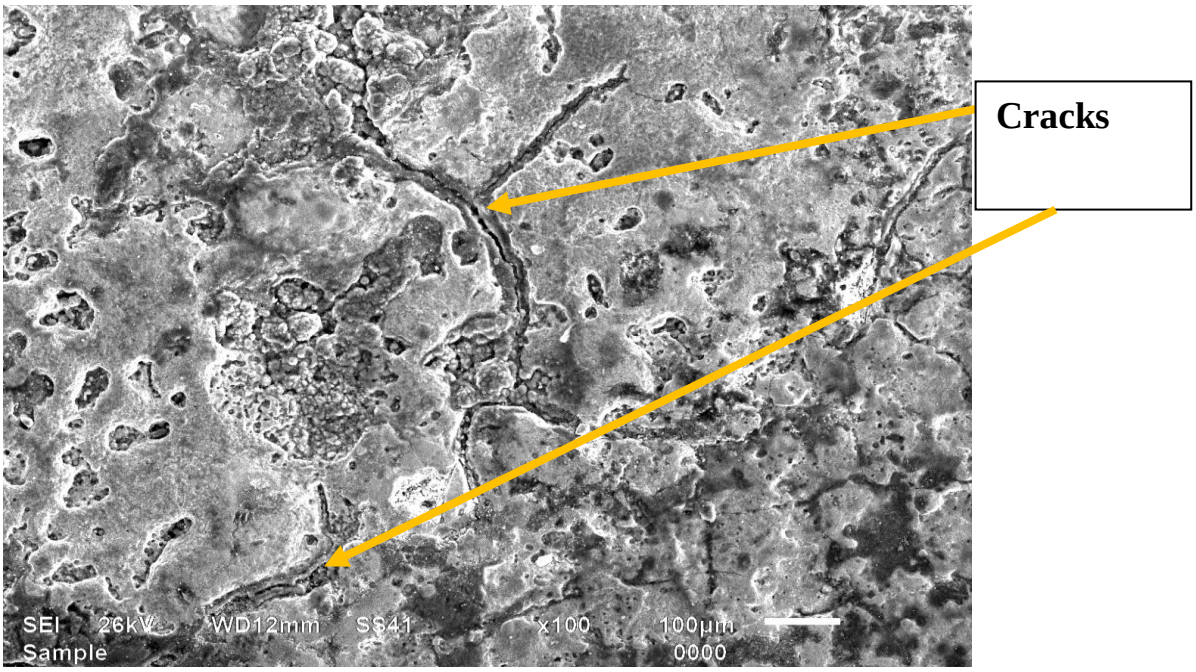

9.9: SEM micrograph at 100× of Tungsten Carbide machined with Al electrode with Aluminium oxide powder mixing in kerosene oil (I 9Amp, pulse on time 100µs, pulse off time 10µs)

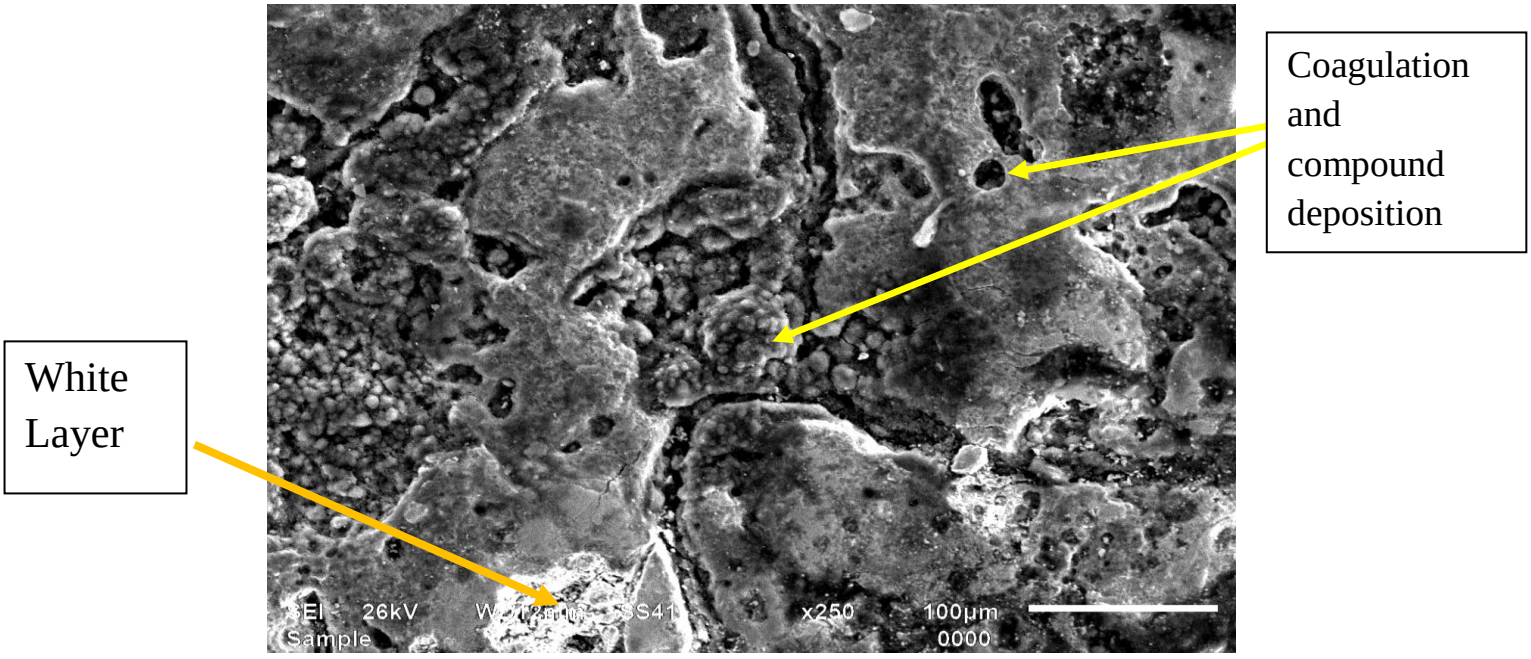

Figure 9.10: SEM micrograph at 250× of Tungsten Carbide machined with Al electrode with Aluminium oxide powder mixing in kerosene oil (I 3Amp, pulse on time 50µs, pulse off time 50µs)

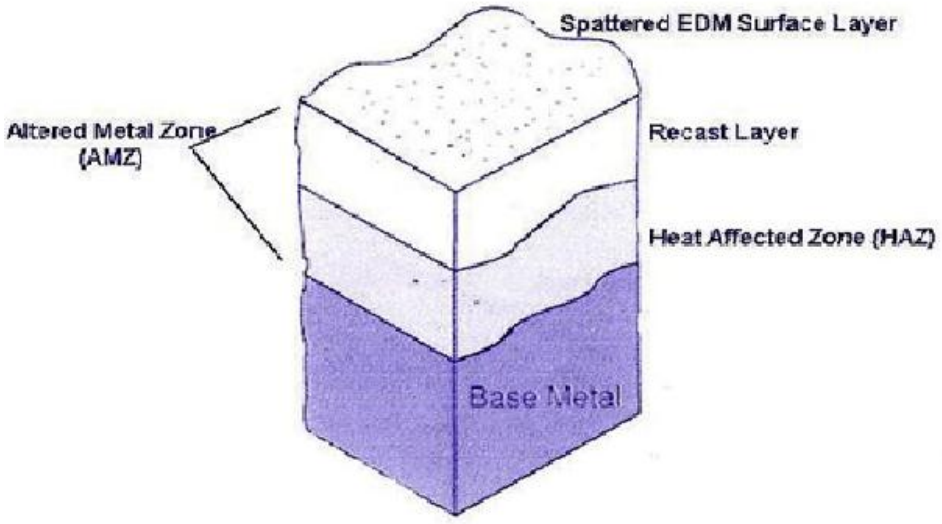

Figure 9.11 Different layers formed on EDM machined surface [37]

Microstructure shown in above figures, it was observed that no. of cracks increases as the value of current increases. As current increases there are more cracks, coagulation and compound deposition on the surface shown in the Micro-structure. There is recast layer is formed on the machined surface and increases as the current increases. The surface is rough

because of debris which are not flashed away completely from the machining zone. Different layers which were formed in the machined are shown in the Figure 8.11. With the temperature of the discharges reaching 8000˚C to 12,000˚C, metallurgical changes occur in the surface layer of the workpiece. Additionally a thin recast layer at high powers is formed. Some annealing of the workpiece can be expected in a zone just below the machined surface. In addition, not all the workpiece material melted by the discharge is expelled into the dielectric. The remaining melted material is quickly chilled, primarily by heat conduction into the bulk of the workpiece, resulting in an exceedingly hard surface. The depth of the annealed layer is proportional to the amount of power used in the machining operation. The amount of annealing is usually about two points of hardness below the parent metal for finish cutting. In the roughing cuts, the annealing effect is approximately five points of hardness below the parent metal. Choosing electrodes that produce more stable machining can reduce the annealing effect. A finish cut removes the annealed material left by the previous high-speed roughing. The altered surface layer, which is produced during EDM, significantly lowers the fatigue strength of alloys. The altered layer consists of a recast layer with or without micro-cracks, some of which may extend into the base metal, plus metallurgical alterations such as re-hardened and tempered layers, heat-affected zones, and inter granular precipitates [36]. Generally, during EDM roughing, the layer showing micro structural changes, including a melted and re-solidified layer. The action of EDM altered the metallurgical structure and characteristics in recast layer. The recast layer is formed by the un-expelled molten metal solidifying in the craters. The white layer is densely infiltrated with carbon to the point that its structure is different than that of the base material.

9.3 Analysis of Energy Dispersion Spectroscopy (EDS)

In this Analysis, Energy Dispersion Spectroscopy is used to determine and analyse the composition of the samples. Through this technique we can see that what amount of changes come after the machining of our samples at the different conditions. We take 4 samples of Tungsten carbide, 3 samples are get machined from out of 4 samples and 1 sample is of parent metal and on these samples both Energy Dispersion Spectroscopy (EDS). The samples were prepared as per standard before EDS analysis.

9.3.1 For Tungsten carbide before machining

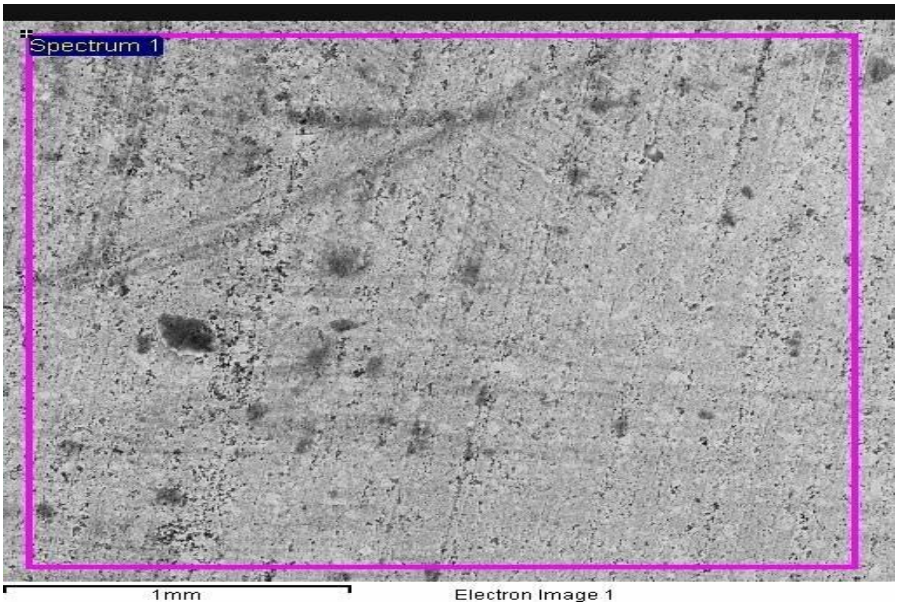

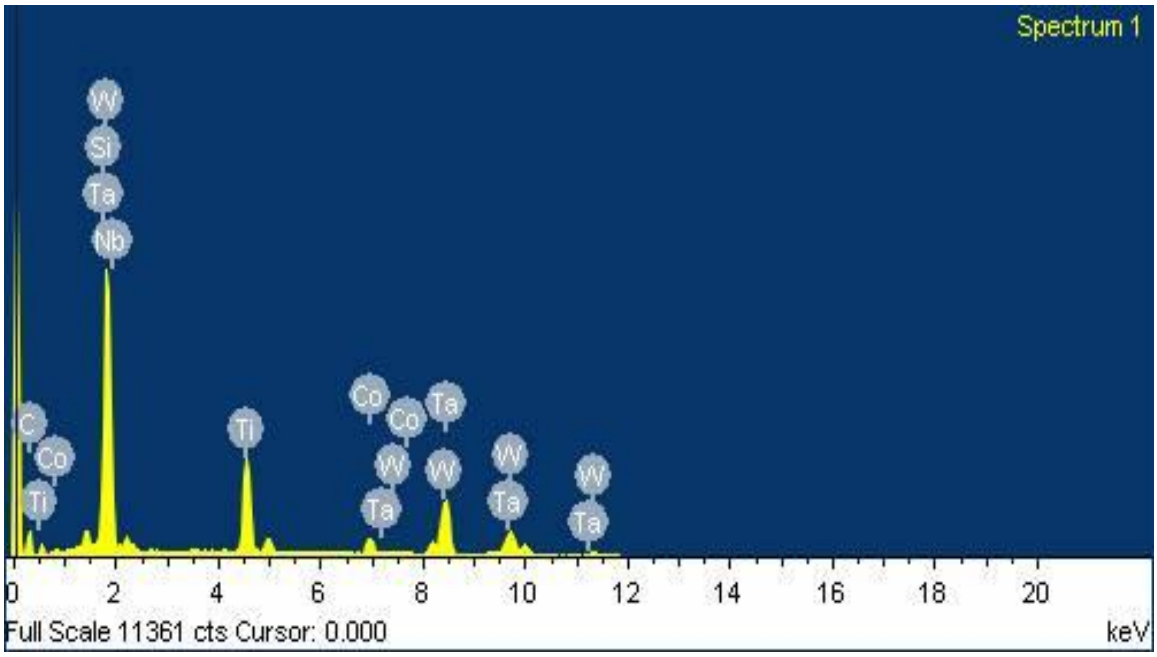

Figure 9.12: EDS spectrum of Tungsten Carbide of sample-1

Table-9.3.1 Composition of Tungsten Carbide of sample-1

Sr. no.	Element	Weight%	Atomic%
1.	C K	15.31	61.39
2.	Si K	0.19	0.33
3.	Ti K	16.36	16.45
4.	Co K	5.24	4.28
5.	Nb L	4.05	2.10
6.	Ta M	8.35	2.22
7.	W M	50.50	13.23
	Totals	100.00	

9.3.2 : EDS of Tungsten Carbide machined with Cu electrode with Graphite powder mixing in kerosene oil (I 3Amp, pulse on time 50µs, pulse off time 50µs)

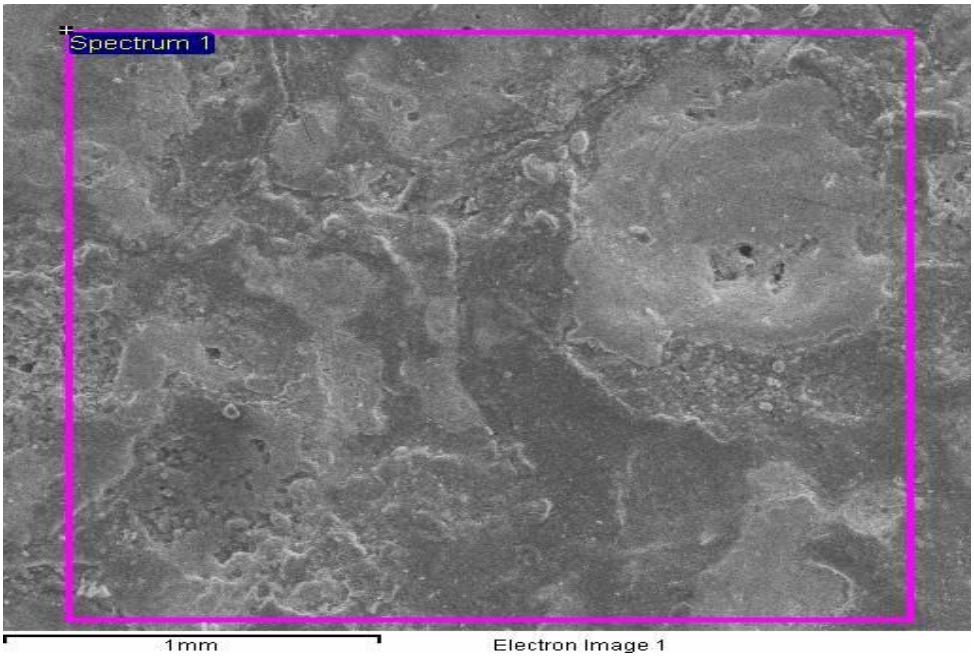

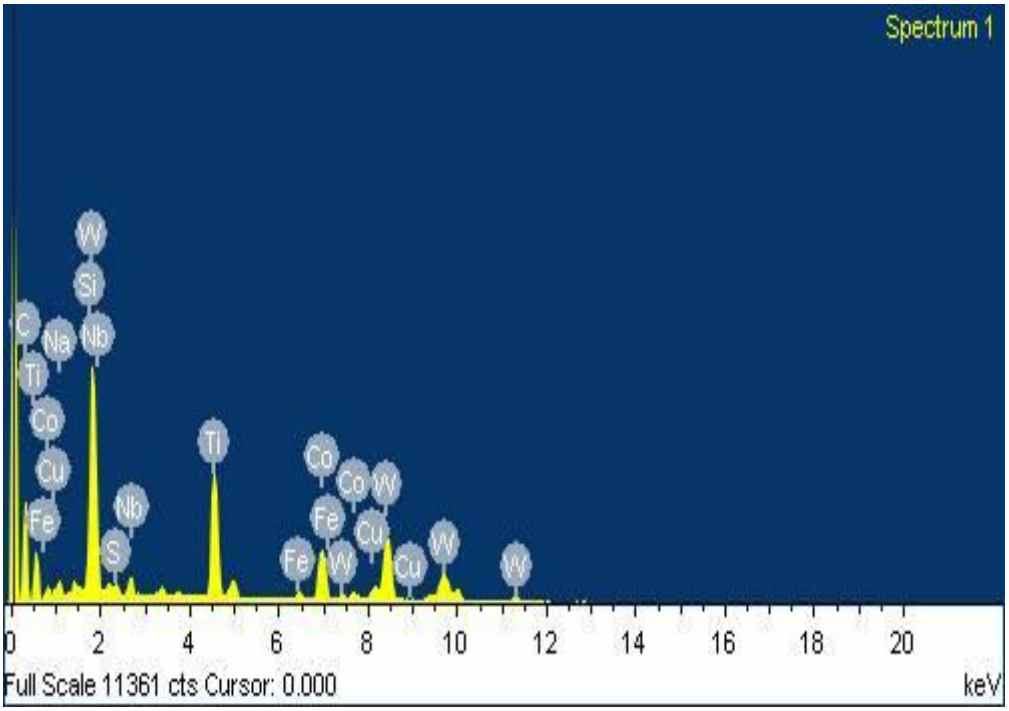

Figure 9.13: EDS spectrum of the Tungsten Carbide of sample-2

Table-9.3.2 Composition of Tungsten Carbide of sample-2

Sr. no.	Element	Weight%	Atomic%
1.	C K	37.85	78.49
2.	Na K	1.14	1.24
3.	Si K	2.00	1.77
4.	S K	0.42	0.32
5.	Ti K	14.17	7.37
6.	Fe K	1.20	0.54
7.	Co K	12.79	5.40
8.	Cu K	1.85	0.73
9.	Nb L	2.04	0.55
10.	W M	26.54	3.60
	Totals	100.00	

9.3.3 EDS of Tungsten Carbide machined with Br electrode with Mixed powder mixing in kerosene oil (I 6Amp, pulse on time 100µs, pulse off time 10µs)

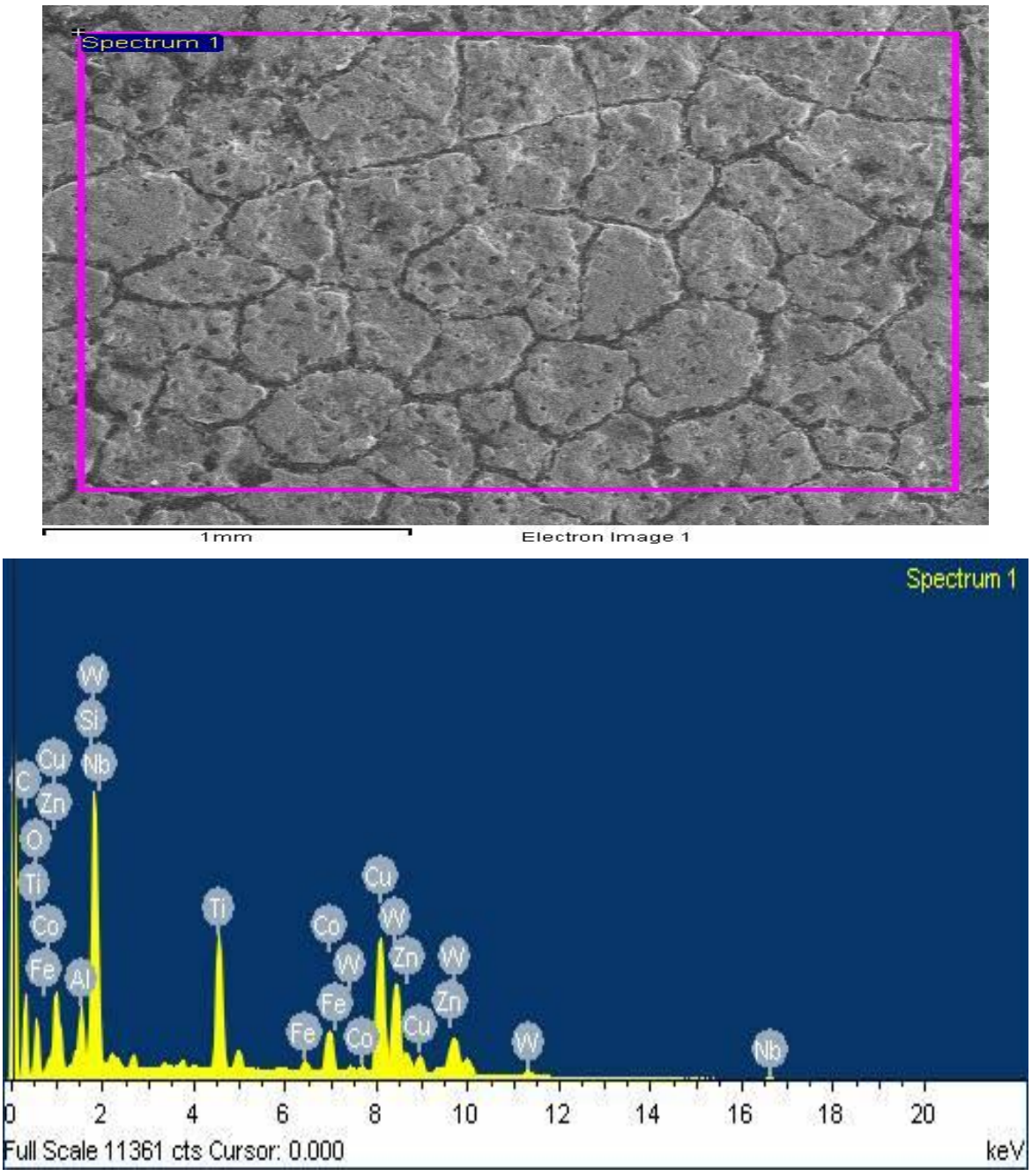

Figure 9.14: EDS spectrum of the Tungsten Carbide of sample-3

Table-9.3.3 Composition of Tungsten Carbide of sample-3

Sr. no.	Element	Weight%	Atomic%
1.	C K	21.07	52.29
2.	O K	9.51	17.71
3.	Al K	2.00	2.21
4.	Si K	1.93	2.05
5.	Ti K	7.77	4.83
6.	Fe K	0.99	0.53
7.	Co K	5.08	2.57
8.	Cu K	25.50	11.96
9.	Zn K	4.82	2.20
10.	Nb L	1.25	0.40
11.	W M	20.07	3.25
	Totals	100.00	

9.3.4 EDS of Tungsten Carbide machined with Al electrode with Aluminium oxide powder mixing in kerosene oil (I 9Amp, pulse on time 100µs, pulse off time 10µs)

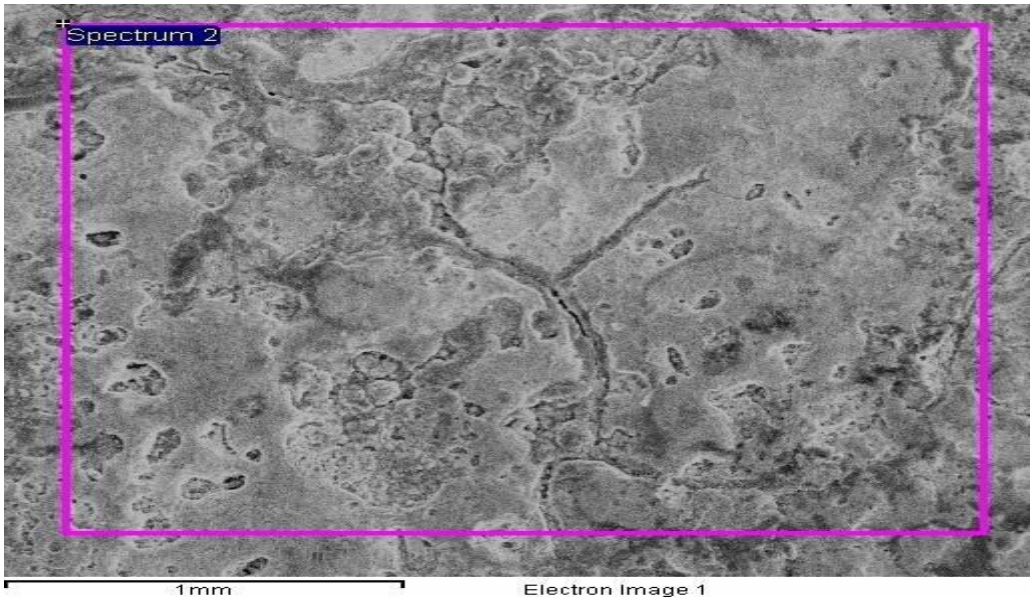

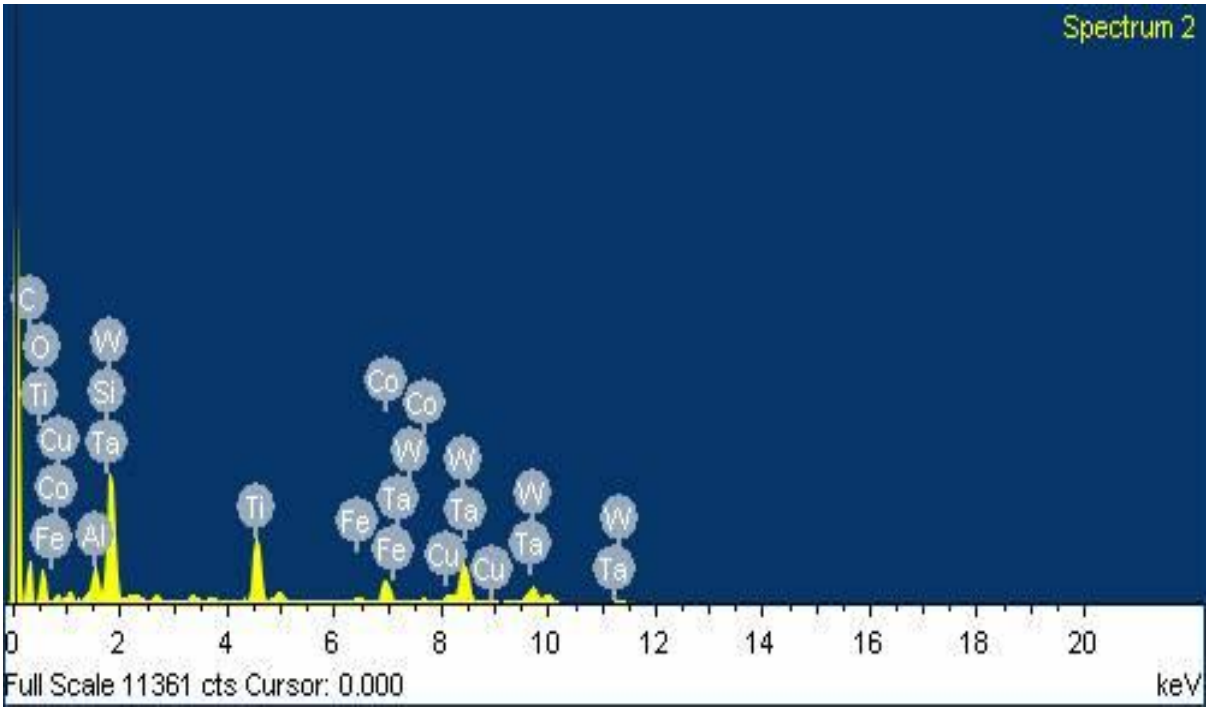

Figure 9.15: EDS spectrum of Tungsten Carbide of sample-4

Table-9.3.4 Composition of Tungsten Carbide of sample-4

Sr. no.	Element	Weight%	Atomic%
1.	C K	25.16	53.25
2.	O K	18.31	29.09
3.	Al K	2.42	2.28
4.	Si K	0.14	0.12
5.	Ti K	11.54	6.12
6.	Fe K	1.31	0.60
7.	Co K	8.48	3.66
8.	Cu K	1.36	0.55
9.	Ta K	4.62	0.65
10.	W M	26.66	3.69
	Totals	100.00	

Energy-dispersive X-ray spectroscopy (EDS or EDX) is an analytical technique used for the elemental analysis or chemical characterization of a sample. It relies on the investigation of an interaction of some source of X-ray excitation and a sample. From above analysis, it seems very clear that the composition of material is very different from the before and after machining because of presence of various materials in powders and tools. Composition of all samples is also different from each other because conditions of experiments are also different from each other. In parent metal or in sample-1, W is 50% and C is 15.13%, in sample-2, W is 26.54% and C is 37.85% but here some addition of extra material from parent metal are Cu, Fe and S. In sample-3, W is 20.07% and C is 21.07% with addition of some extra metals like Al and Zn. In sample-4, W is 26.66% and C is 25.16% with addition of O and Ta. In sample-4 due to presence of aluminium oxide powder in the dielectric, Aluminium layer present in the sample-4.

Chapter 10

Results and Conclusions

10.1 RESULTS

ANOVA is used to study the effect of various parameters like pulse-on, pulse-off, current, powder and tool. Some of these factors and their interactions found significant in some cases and some of them found insignificant in some cases. The purpose of the ANOVA was to identify the important parameters in prediction of MRR, TWR, micro hardness, surface roughness. The major results which we get out from this study are given below:

10.1.1 MRR

ANOVA Table 4.2 shows that Pulse-off (F-33.19), Current (F-20.88), Powder (F-24.7) and Pulse-on (F-5.55) are factors that significantly affect the MRR. Acc. to ANOVAs Table 4.2 shown below, there are two interactions Current × Powder (F-6.42) and Powder × Tool (F-5.87) are significant and affect the MRR, where other factors like Tool and one interaction Current × Tool are are insignificant to affect the MRR. Pulse-off and Powder are most significant factors which affect the MRR. MRR increases with increase in Pulse-On (15-100µs) and Pulse-Off (10-75µs).MRR decreases with addition of mixed powder and increases with the addition of Graphite powder

In SN ratio, According to F-test Pulse-Off [F-25.57], Powder [F-15.81], and Current [F-7.53], are the main parameters which affect the MRR and the left all other parameters are insignificant to MRR. The maximum MRR was obtained at Pulse-off (75µs), Pulse-on (100µs), and 3 Amps Current with mixing of Graphite powder in the dielectric.

So the confidence interval around the MRR is given by 2.48 ± 0.453 mm^3/min.

10.1.2 TWR

ANOVA table 5.2 shows that Tool (F-91.19), Powder (F-8.65) and Current (F-6.48) are the factors that affect the TWR. There is one interaction **Powder × Tool** (F-8.20) is also significant and the remaining factors like Pulse-on, Pulse-off and the other interactions are insignificant. According to ANOVAs table 5.2 Tool is the most significant factor which

affects the TWR. TWR increases with increase in current from 3 Amps to 9 Amps and by changing the Tools. By using mixed powder we get higher TWR and minimum TWR is coming when we use Cu tool and Graphite powder. Tool and Powder are most significant and Pulse-on, Pulse-off are most insignificant factors.

In SN ratio, there are mainly two factors Tool [F-32.87] and Current [F-6.57] are significantly affect the TWR and the remaining all factors and interactions are insignificant.

The best result of TWR is obtained when Tungsten carbide is machined at 3 Amps current with Cu as electrode and graphite powder mixed in the dielectric. So the confidence interval around the TWR is given by 2.163 ± 1.715mm^3/min.

10.1.3 MICRO HARDNESS

In ANOVAs' table 6.2 shows that Pulse-on [F-24.22], Current [F-10.26], Pulse-off [F-6.17] are significantly affect the micro-hardness. Two interactions **Current × Powder** [F-5.65] **and Current × Tool** [F-6.36] are also significant. The other factors powder and tool are insignificant. Pulse-on is a most significant factor which affects the Micro-hardness. Here we notice that mainly two factors are affecting the micro hardness one is pulse-on which is most significant and other is Current who has also 12 % contribution.

In SN Ratio, all the three interactions are significant. Here also pulse-on is most affecting significant factor following by Current and Pulse-off. Powder and Tool are least significant factors. The best result for micro hardness is when Tungsten carbide machined at 9 Amps current, 50µs Pulse-off and at 100µs Pulse-on.

The confidence interval around the Micro hardness is given by 464.7 ± 64.22 HVN.

10.1.4 SURFACE ROUGHNESS (Ra)

In surface roughness, Table 7.2 shows Pulse-on [F-19.93], Pulse-off [F-18.69], Current [F-13.14] and Powder [F-7.95] are significant factors and affect the surface roughness. Remaining all factors and interactions are insignificant in nature. According to Response table 7.3 for means pulse-on is the most significant factor. Tool is least significant factor which affects the surface roughness. Surface roughness increases with increase in Pulse-off [10µs-75µs] and Current [3amps-9amps].

In SN Ratio, all the factors are significant leaving only tool is insignificant here; here all the interactions are insignificant. Acc. to ANOVAs table 7.2, **Pulse-off** [F-18.23]**, Pulse-on** [F-

17.60]**, Current** [F-13.70] **and Powder** [F-11.70]**,** therefore Pulse-off and current are most significant to decrease the surface roughness.

So the best design was to be suggested that when Tungsten carbide was machined at 3 Amps current, 50µs Pulse-off, 10µs Pulse-on and with addition of aluminium oxide powder mixed in the dielectric

The confidence interval around the Surface Roughness is given by 1.035 ± 0.878 Microns

10.1.5. MICROSTRUCTURE ANALYSIS

During machining due to very high temperature metal melts and vaporizes in the dielectric. This phenomena causes re-crystallization of the metal grains takes place and after that further cooling takes place due to which micro-structure of metal, therefore change in micro-structure is studied with the help of Scanning Electron Microscope (SEM).Microstructure shown in above figures 9.1-9.10, it was analyzed that no. of cracks increases as the value of current increases. As current increases there are more cracks, coagulation and compound deposition on the surface shown in the Micro-structure. The crater size is more when machined at 8Amp without powder in dielectric. Crater size increased with increase in current. There is recast layer is formed on the machined surface and increases as the current increases.. The surface is rough because of debris which are not flashed away completely from the machining zone. Different layers which were formed in the machined surface, with the temperature of the discharges reaching 8000˚C to 12,000˚C, metallurgical changes occur in the surface layer of the workpiece. Additionally a thin recast layer at high powers is formed. All these things are getting clear in the micro structures shown in the above figures and shows how the cracks are formed on the machined surface with increase in current.

10.1.6 Analysis of Energy Dispersion Spectroscopy (EDS)

In this Analysis, Energy Dispersion Spectroscopy is used to determine and analyse the composition of the samples. Through this technique we can see that what amount of changes come after the machining of our samples at the different conditions. Energy-dispersive X-ray spectroscopy (EDS or EDX) is an analytical technique used for the elemental analysis or chemical characterization of a sample. It relies on the investigation of an interaction of some source of X-ray excitation and a sample. From above analysis, it seems very clear that the composition of material is very different from the before and after machining because of

presence of various materials in powders and tools. Composition of all samples is also different from each other because conditions of experiments are also different from each other. In parent metal or in sample-1, W is 50% and C is 15.13%, in sample-2, W is 26.54% and C is 37.85% but here some addition of extra material from parent metal are Cu, Fe and S. In sample-3, W is 20.07% and C is 21.07% with addition of some extra metals like Al and Zn. In sample-4, W is 26.66% and C is 25.16% with addition of O and Ta. In sample-4 due to presence of aluminium oxide powder in the dielectric, Aluminium layer present in the sample-4.

10.2 CONCLUSIONS

In this study, it is studied that the effect of various input parameters of MRR, TWR, Micro hardness and Surface roughness. According to this study the following conclusions are made:

1. MRR increases with the addition of graphite powder and with increase in the pulse-on.

2. MRR decreases with the addition of mixed powder in the dielectric
3. Cu tool gives us minimum TWR.
4. TWR increases with the increase in current from 3 to 9 Amps.
5. The optimum Micro hardness was observed at high currents and Micro hardness; it also increases with increase in pulse-on.
6. Aluminium tool is most significant among the other tools in Micro hardness
7. Surface roughness decreases at low current and it also get decreases with the addition of aluminium oxide powder.
8. No. of cracks and thickness of white layer increases with increase in current.

APPENDIX-A

TECHNICAL SPECIFICATIONS OF EDM MACHINE

The experiment has been conducted on Electrical Discharge Machine model T-3822M, Victory Electromech, Kolhapur, India. Technical data of machine is as under:

1. Electrical Data

Supply voltage	415V, 3Ø, 50 Hz
Connected load	3 KVA
Open gap voltage output	135±5% V
Max. Machine current	12Amp
Current range	3 ranges of 4Amp each
Current adjustment	0-4Amp in each current range

2. Machine Tool

Height	1300mm
Width	730mm
Depth	840mm
Net weight	325 kg
Quill travel	150mm

3. Work Tank

Length	132.3mm
Width	211.48mm
Height	132.3mm
Thickness	12mm

APPENDIX-B

SPECIFICATIONS OF MEASURING INSTRUMENTS

1. PERTHOMETER

Make and model	Mitutoyo, Japan
Measurement method	Stylus
Cut-off wavelength	0.08mm
Evaluation length	0.24mm

2. MICRO HARDNESS TESTER

Make and model	Metatech, MVH-2, Pune, India,
Software used	Quantimet
Load	1 kg
Dwell time	25 sec

3. SCANNING ELETRON MICROSCOPE

Make and model	JSM-840A Joel, Japan
Magnification range	10× to 3, 00,000×

APPENDIX –C

TECHNICAL SPECIFICATIONS OF DIELECTRIC MEDIUM

KEROSENE OIL

Appearance	Clear, transparent, light
Density (kg/m3)	817.15
Flash Point (˚C)	40
Boiling Point (˚C)	600
G.C.V. (Kcal/kg)	11200
Viscosity (centistokes)	2.71

REFERENCES

[1] Panday P.C., Shan H.S. (2007), "Modern Machining Processes", Tata McGraw-Hill, New Delhi, India, ISBN -07-096553-6.

[2] `Ross Phillip J., (1990), "Taguchi Techniques for Quality Engineering", McGraw-Hill, ISBN 0-07-053866-2

[3] Hocheng H, Lei W.T, Hsu H.S (1997), Preliminary study of material removal in electrical-discharge machining of SiC/Al , Journal of Materials Processing Technology, Volume 63, Issues 1-3, Pages 813-818

[4] Lee. H. T., Tai. T. Y. (2003), Relationship between EDM parameters and surface crack formation , Journal of Materials Processing Technology, Volume 142, Issue 3, Pages 676-683

[5] Kanagarajan D, Karthikeyan R, kumar P.K, and Sivaraj P (2008), Influence of process parameters on electric discharge machining of WC/30%Co composites, Proc. IMechE Vol. 222 Part B: J. Engineering Manufacture

[6] Bhaduri D , Kuar A.S , Sarkar S , Biswas S.K & Mitra S (2009), Electro Discharge Machining of Titanium Nitride- Aluminium Oxide Composite for Optimum Process Criterial Yield, Materials and Manufacturing Processes, 24: 1312–1320

[7] Abdulkareem S, Khan A.A and Konneh M (2010), Cooling Effect on Electrode and Process Parameters in EDM, Materials and Manufacturing Processes, 25: 462–466

[8] Lin Y.C, Chen Y.F, Lin C.T and Tzeng H.J (2008), Electrical Discharge Machining (EDM) Characteristics Associated with Electrical Discharge Energy on Machining of Cemented Tungsten Carbide, Materials and Manufacturing Processes, 23: 391–399

[9] Battacharya S.K, Elmenshawy M.F, Garber S and Wallbank J (1981), A correlation between machining parameters and mach inability in EDM, INT. J PROD. RES., 1981, VOL. 19, NO.2 111-122

[10] Puertas I & Luis C. J (2004), A Study of Optimization of Machining Parameters for Electrical Discharge Machining of Boron Carbide, Material and manufacturing processes Vol. 19, No. 6, pp. 1041–1070, 2004

[11] Lin Y.C ,Cheng C.H , Su B.L & Hwang L.R (2006), Machining Characteristics and Optimization of Machining Parameters of SKH 57 High-Speed Steel Using Electrical-

Discharge Machining Based on Taguchi Method, Materials and Manufacturing Processes, 21: 922–929, 2006

[12] Kucukturk G & Cogun C (2010), A new method for machining of electrically non-conductive workpiece using EDM Technique, Machining Science and Technology, 14:189–207

[13] Singh P. N, Raghukandan K, Pai B.C (2004), Optimization by Grey relational analysis of EDM parameters on machining Al–10%SiCP composites, Journal of Materials Processing Technology 155–156 (2004) 1658–1661

[14] George P.M, Raghunath B.K, Manocha L.M, Warrier A. M (2003), EDM machining of carbon–carbon composite—a Taguchi approach, Journal of Materials Processing Technology 145 (2004) 66–71

[15] Lin Y.C, Wang A.C, Wang D.A and Chen C.C (2009), Machining Performance and Optimizing Machining Parameters of Al2O3–TiC Ceramics Using EDM Based on the Taguchi Method, Materials and Manufacturing Processes, 24: 667–674, 2009

[16] Singh H, Shukla D.K. (2012), Optimizing electric discharge machining parameters for tungsten-carbide utilizing thermo-mathematical modelling, International Journal of Thermal Sciences (2012) 1-15

[17] Singh S, Maheshwari S, Pandey P.C (2003), Some investigations into the electric discharge machining of hardened tool steel using different electrode materials, Journal of Materials Processing Technology 149 (2004) 272–277

[18] Jahan M.P ,Rahman M,Wong Y.S (2011), A review on the conventional and micro-electrodischarge machining of tungsten carbide, International Journal of Machine Tools & Manufacture 51 (2011) 837–858

[19] Luis C.J, Puertas I, Villa G (2005), Material removal rate and electrode wear study on the EDM of silicon carbide, Journal of Materials Processing Technology 164–165 (2005) 889–896

[20] Tzeng Yih-fong, Chen Fu-chen (2006), Multi-objective optimisation of high-speed electrical discharge machining process using a Taguchi fuzzy-based approach, Materials and Design 28 (2007) 1159–1168

[21] Bu¨lent Ekmekci (2007), Residual stresses and white layer in electric discharge machining (EDM), Applied Surface Science 253 (2007) 9234–9240

[22] Guu Y. H. , Chou C. Y. & Chiou S.T (2005), Study of the effect of machining parameters of machining Characteristics of Fe-Mn-Al alloy, Materials and Manufacturing Processes, 20: 905–916, 2005

[23] Pradhan D and Jayaswal S.C (2011), Behaviour of copper and aluminium electrodes on EDM of EN-8 alloy steel, International Journal of Engineering Science and Technology (IJEST), Vol. 3 No. 7 July 2011

[24] Wong Y.S, Lim L.C, Rahuman I, Tee W.M. (1997), Near-mirror-finish phenomenon in EDM using powder-mixed dielectric, Journal of Materials Processing Technology 79 (1998) 30–40

[25] Tzeng Y.F and Lee C.Y (2001), Effects of Powder Characteristics on Electro discharge Machining Efficiency, Int J Adv Manuf Technol (2001) 17:586–592

[26] Kansal H.K, Singh S, Kumar P (2005), Parametric optimization of powder mixed electrical discharge machining by response surface methodology, Journal of Materials Processing Technology 169 (2005) 427–436

[27] Cogun C, Ozerkan B and Karacay T (2006), An experimental investigation on the effect of powder mixed dielectric on machining performance in electric discharge machining, Proc. IMechE Vol. 220 Part B: J. Engineering Manufacture

[28] Kumar A, Maheshwari S, Sharma C. & Beri N (2010), A Study of Multi objective Parametric Optimization of Silicon Abrasive Mixed Electrical Discharge Machining of Tool Steel, Materials and Manufacturing Processes, 25: 1041–1047, 2010

[29] Kansal H.K, Singh S, Kumar P (2005), Technology and research developments in powder mixed electric discharge machining (PMEDM), Journal of Materials Processing Technology 184 (2007) 32–41

[30] Kumar S, Batra U (2011), Surface modification of die steel materials by EDM method using tungsten powder-mixed dielectric, Journal of Manufacturing Processes 14 (2012) 35–40

[31] Kansal H.K, Singh S, Kumar P (2007), Effect of Silicon Powder Mixed EDM on Machining Rate of AISI D2 Die Steel, Journal of Manufacturing Processes Vol. 9/No. 1

[32] Pecas P, Henriques E (2007), Electrical discharge machining using simple and powder-mixed dielectric: The effect of the electrode area in the surface roughness and topography, journal of materials processing technology 2 0 0 (2 0 0 8) 250–258

[33] Klocke F, Lung D, Antonoglou G, Thomaidis D (2003), The effects of powder suspended dielectrics on the thermal influenced zone by electro discharge machining with small discharge energies, Journal of Materials Processing Technology 149 (2004) 191–197

[34] Han M.S, Min B.K, Lee S.J (2007), Improvement of surface integrity of electro-chemical discharge machining process using powder-mixed electrolyte, Journal of Materials Processing Technology 191 (2007) 224–227

[35] Wu K.L, Yan B.H, Huang F.Y, Chen S.C (2005), Improvement of surface finish on SKD steel using electro-discharge machining with aluminium and surfactant added dielectric, International Journal of Machine Tools & Manufacture 45 (2005) 1195–1201

[36] Hassan El-Hofy, Advance non-traditional machining process by McGraw-Hill

[37] www.google.Com

[38] Chiang K.T, Chang F.P, Tsai D.C (2007), Modelling and analysis of the rapidly re-solidified layer of SG cast iron in the EDM process through the response surface methodology, Journal of Materials Processing Technology 182 (2007) 525–533